

A Study on Network Survivability Analysis for Ad Hoc Networks

(アドホックネットワークにおけるネットワーク生存性評価に関する研究)

Dissertation submitted in partial fulfillment for the
degree of Doctor of Engineering

Zhipeng Yi

Under the supervision of
Professor Tadashi Dohi

Dependable Systems Laboratory,
Department of Information Engineering,
Graduate School of Engineering,
Hiroshima University, Higashi-Hiroshima, Japan

March 2016

A Study on Network Survivability Analysis for Ad Hoc Networks

Dissertation submitted in partial fulfillment for the
degree of Doctor of Engineering

Zhipeng Yi

Under the supervision of
Professor Tadashi Dohi

Dependable Systems Laboratory,
Department of Information Engineering,
Graduate School of Engineering,
Hiroshima University, Higashi-Hiroshima, Japan

March 2016

Abstract

Network survivability is an attribute that network is continually available even if a communication failure occurs, and is an emerging requirement for highly reliable communication services in wireless ad hoc networks (WAHNs) and mobile ad hoc networks (MANETs). Moreover, quantitative network survivability is defined as the probability that the network can keep to be connected even under node failures and DoS attacks, and known as one of the most important measures to design dependable computer networks. Markov modeling is a typical method to quantifying network survivability. On the other hand, border effect in communication network area is also one of the most troublesome problems to quantify accurately the performance/dependability of WAHNs/MANETs, because the assumption on uniformity of network node density is often unrealistic to describe the actual communication area. This problem appears in modeling the node behavior of WAHNs/MANETs and in quantification of their network survivability. This fact motivates us to reformulate the existing network survivability models for WAHNs/MANETs by taking account of border effects.

In this thesis, we propose three node behavior models and consider two types network communication areas. We analysis these network survivability models by semi-Markov process (SMP) and Markov regenerative process (MRGP). Also, we develop a simulation model to validate our analytical models.

In Chapter 1, we introduce the definition of network survivability, importance of network survivability quantification and motivation of our study.

In Chapter 2, we propose two stochastic models; binomial model and negative binomial model to quantify the network survivability and compare them with the existing Poisson model. Then, we focus on the border effects, and reformulate the network survivability models based on a SMP, where two kinds of communication network areas are considered; square area and circular area. Based on some geometric ideas, we improve the quantitative network survivability measures for three stochastic models (Poisson, binomial and negative binomial) taking account of border effects.

In Chapter 3, we concern the fact that the continuous-time Markov chain (CTMC) modeling is not sufficient to analyze the relationship between battery state and node behavior in MANETs. In particular, such a problem seriously

arises when we treat the transient behavior of the power-aware MANET. Here, we present the quantitative network survivability analysis for a power-aware MANET based on MRGP, and calculate the network survivability through both stationary and transient analyses for the SMP-based models.

In Chapter 4, we derive analytically the upper and lower bounds of network survivability as well as an approximate form based on the expected number of active nodes in both square and circular areas, under a general assumption that the battery life in each node is non-exponentially distributed. We perform the transient analysis as well as the steady-state analysis of network survivability based on a SMP, and complement the results in Chapter 3.

We propose some analytical formulas on the quantitative network survivability in Chapter 2, Chapter 3 and Chapter 4, but need to validate them by comparing with the exact value of network survivability in a comprehensive way. In Chapter 5, we revisit the lower and upper bounds of network survivability by taking account of border effects in network communication areas, and develop a refined simulation model in two kinds of communication areas; square area and circular area. We compare the analytical bounds of network survivability with the simulation solution. It is shown through simulation experiments that the analytical solutions often fail the exact network survivability measurement.

Finally, some conclusions and remarks are given in Chapter 6.

Acknowledgements

First and foremost, I would like to extend my sincere gratitude to Professor Tadashi Dohi, the supervisor of my study, for his constant guidance, kind advice and continuous encouragement throughout the progress of this work.

Also, my thanks go to Associate Professor Hiroyuki Okamura and Professor Kazufumi Kaneda, for their useful suggestions and checking the manuscript.

Finally, it is my special pleasure to acknowledge the hospitality and encouragement of the past and present members of the Dependable Systems Theory Laboratory, Department of Information Engineering, Hiroshima University.

Contents

Abstract	iii
Acknowledgements	vii
1 Introduction	1
1.1 Survivability Analysis with Border Effects	1
1.2 Survivability Analysis for MANETs	3
1.3 Survivability Analysis with Battery Charge	4
1.4 A Simulation Approach to Quantify Survivability	5
1.5 Organization of Dissertation	6
2 Survivability Analysis with Border Effects for MANETs	7
2.1 Preliminary	7
2.1.1 State of Node	7
2.1.2 Semi-Markov Node Model	9
2.2 Quantitative Network Survivability Measure	11
2.2.1 Node Isolation and Connectivity	11
2.2.2 Network Survivability	13
2.3 Border Effects of Communication Network Area	17
2.3.1 Square Border Effect	17
2.3.2 Circular Border Effect	20
2.4 Numerical Examples	21
2.4.1 Comparison of Steady-state Network Survivability	21
2.4.2 Transient Analysis of Network Survivability	26
3 Survivability Analysis for Power-Aware MANETs	31
3.1 Model Description	31

3.1.1	State of Node	31
3.1.2	MRGP modeling	33
3.2	Survivability Analysis	35
3.2.1	Definition	35
3.3	MRGP Analysis	38
3.3.1	Stationary Analysis	38
3.3.2	Transient Analysis	42
3.4	Numerical Examples	45
3.4.1	Stationary Analysis	45
3.4.2	Transient Analysis	50
3.5	APPENDIX 1	54
3.6	APPENDIX 2	55
4	Survivability Analysis for Power-Aware MANETs with Battery Charge	57
4.1	Model Description	57
4.1.1	Node Classification	57
4.1.2	Semi-Markov Node Model	59
4.2	Quantitative Network Survivability	61
4.2.1	Network Survivability Measures	61
4.3	Border Effects of Network Communication Area	67
4.4	Numerical Examples	68
4.4.1	Comparison of Network Survivability	68
4.4.2	Transient Analysis of Network Survivability	72
4.5	Appendix	74
5	A Simulation Approach to Quantify Network Survivability for MANETs	83
5.1	Simulation Algorithms	83
5.2	Numerical Examples	87
6	Conclusions	95
6.1	Summary and Remarks	95
6.2	Future Works	96

<i>CONTENTS</i>	xi
Bibliography	97
Publication List of the Author	102

Chapter 1

Introduction

Network survivability is an attribute that network is continually available even if a communication failure occurs, and is an emerging requirement for highly reliable communication services in WAHNs and MANETs. Moreover, it has been defined as the probability that the network can keep to be connected even under node failures and DoS attacks, and known as one of the most important concepts to design dependable computer networks. Markov modeling is a typical method for the network survivability performance evaluation.

On the other hand, border effect in communication network area is one of the most important problems to quantify accurately the performance/dependability of WAHNs/MANETs, because the assumption on uniformity of network node density is often unrealistic to describe the actual communication area. This problem appears in modeling the node behavior of WAHNs/MANETs and in quantification of their network survivability. In this thesis, we evaluate network survivability in three steps; formulation of border effects, node behavior analysis and simulation experiments.

1.1 Survivability Analysis with Border Effects

Network survivability is regarded as the most fundamental issue to design resilient networks. Since unstructured networks such as P2P network and MANET can change dynamically their configurations, the survivability requirement for unstructured networks is becoming much more popular than static networks. Network survivability is defined by various authors [1, 2, 3, 4]. Chen et al. [5], Cloth and Haverkort [6], Heegaard and Trivedi [7], Liu et al. [8], Liu and Trivedi

[9] consider the survivability of virtual connections in telecommunication networks and define the quantitative survivability measures related to performance metrics like the loss probability and the delay distribution of non-lost packets. Their survivability measures are analytically tractable and depend on the performance modeling under consideration, where the transition behavior has to be described by a CTMC or a stochastic Petri net. More recently, Zheng et al. [10] conduct a survivability analysis for virtual machine-based intrusion tolerant systems, and take the similar approach to the works [1, 2, 3, 4].

On the other hand, Xing and Wang [11, 12] perceive the survivability of a MANET as the probabilistic k -connectivity, and provide a quantitative analysis on impacts of both node misbehavior and failure. They approximately derive the lower and upper bounds of network survivability based on k -connectivity, which implies that every node pair in a network can communicate with at least k neighbors. On the probabilistic k -connectivity, significant research works are done in [13, 14] to build the node degree distribution models. Unfortunately, the resulting upper and lower bounds are not always tight to characterize the connectivity-based network survivability, so that a refined measure of network survivability should be defined for analysis. Roughly speaking, the connectivity-based network survivability analysis in [11, 12] focuses on the path behavior and can be regarded as a myopic approach to quantify the survivability attribute. The performance-based network survivability analysis in [1, 2, 3, 4] is, on the other hand, a black-box approach to describe the whole state changes. Although both approaches possess advantage and disadvantage, in this thesis we concern only the former case.

We develop somewhat different stochastic models from Xing and Wang [11, 12] by introducing different degree distributions. More specifically, they propose binomial and negative binomial models in addition to the familiar Poisson model, under the assumption that mobile nodes are uniformly distributed. We also extend the semi-Markov model to a Markov regenerative process model and deal with a generalized stochastic model to describe a power-ware MANET. However, it should be noted that the above network survivability models are based on multiple unrealistic assumptions to treat an ideal communication network environment. One of them is ignorance of border effects arising to represent

network connectivity. In typical MANETs such as sensor networks, it is common to assume that each node is uniformly distributed in a given communication network area. Since the shape of communication network area is arbitrary in real world, it is not always guaranteed that the node degree is identical even in the border of network area. In other words, border effects in communication network area tend to decrease both the communication coverage and the node degree, which reflect the whole network availability. Laranjeira and Rodrigues [17] show that the relative average node degree for nodes in borders is independent of the node transmission range and of the overall network node density in a square communication network area. Bettsetetter [18] also gives a mathematical formula to calculate the average node degree for nodes in borders for a circular communication network area. However, these works just concern to investigate the connectivity of a wireless sensor network, but not the quantitative survivability evaluation for MANETs. This fact motivates us to reformulate the existing network survivability models [11, 12] for MANETs with border effects.

1.2 Survivability Analysis for MANETs

Since unstructured networks such as P2P and MANETs dynamically change their configuration, they require the higher network survivability than static networks. One important problem on mobile network is to reduce the energy consumption of mobile nodes. As we know, in the power-aware wireless ad hoc network, the energy consumption problem of a node can cause the communication barrier which reflects the whole network dependability and performance. We investigate the relationship between energy consumption and security based on a CTMC. More specifically we suppose that two power consumption levels (high and low) alternate randomly, and that its transition behavior is described by a simple CTMC where all state transitions follow exponential distributions. In addition to the energy consumption level, our model represent the behavior of malicious attacks such as DoS attacks, and analyze the dynamic behavior of power-aware wireless ad hoc network to quantify the network survivability as the probabilistic k -connectivity. However, in general, the battery life distribution cannot be represented by an exponential distribution [20]. In other words, the CTMC model is too simple to investigate the effect of battery life on the

network survivability. This motivates us to revisit the network survivability analysis for power-aware MANETs.

1.3 Survivability Analysis with Battery Charge

There exist a number of challenging issues to provide big data services in ubiquitous circumstance. The drastic improvement of network performance is definitely needed to process a large amount of data, especially, in the system level. On the other hand, it is important to keep the high service level on the big data stream and evaluate the network dependability in the design phase to develop highly dependable ubiquitous network systems. Network survivability is defined as an attribute that network is continually available even though a communication failure occurs, and is regarded as the most fundamental issue to design resilient communication networks. Since unstructured networks, such as P2P network and MANET, can change dynamically their configurations, the survivability requirement for unstructured networks is becoming much more popular than static networks. In the near future, it is expected that this trend may be accelerated even in the big data service. Although quantitative network survivability is defined by various authors [1, 2, 5], it is still a challenging issue from the complex and autonomous properties of unstructured networks. Xing and Wang [12] perceive the survivability of a wireless ad hoc network as the probabilistic k -connectivity [13, 14, 18], and provide a quantitative analysis on impacts of both node misbehavior and failure. They approximately derive the lower and upper bounds of network survivability based on k -connectivity, which implies that every node pair in the network can communicate with at least k neighbors. Unfortunately, the upper and lower bounds of network survivability in [12] are not always tight to quantify the network survivability. We are motivated by the above fact and extend the seminal model [12] by introducing the compound distributions of Poisson model.

We evaluate a power-aware MANET by using a MRGP and investigate an effect of variability in power level, which is caused by the low-battery state in each node, but does not consider the possible case where the battery in each mobile node can be re-charged at the lower battery state in their MRGP modeling framework. In addition, We implicitly assume that the so-called border

effects can be ignored in their modeling. It is well known that the shape of communication area with border effects strongly depends on the network properties. Laranjeira and Rodrigues [17] develop a geometry analysis to quantify the network connectivity, and refine the reliability assurance of wireless sensor networks. More specifically, it is common to assume in the network analysis that the communication node is uniformly distributed in an ideal communication area. Since the border effects in network communication areas tend to decrease both the communication coverage and the node degree, they must reflect the whole network survivability including availability and reliability. Laranjeira and Rodrigues [17] show that the relative average node degree for nodes in borders is independent of the node transmission range and of the overall network node density in a square communication area.

Most recently, We revisit a power-aware MANET model in Xing and Wang [12] taking account of both border effects and the possibility of re-charge, and quantify the network survivability more accurately. We suppose that each node state is modulated by a semi-Markov process and that the node density in an arbitrary communication area is given by a simple Poisson model, where two types of communication areas are considered; square area [17] and circular area [18].

1.4 A Simulation Approach to Qunatify Survivability

Finally, we develop a simulation model to quantify the network survivability accurately. In past, several simulation models have been proposed in the literature to quantify network connectivity or to detect survival routes in MANETs (see Caro et al. [21] and Guo [22]). To our best knowledge, an exact simulation model to quantify the network survivability based on connectivity [11, 12] has not been proposed yet. It is definitely needed to check the resulting quantitative survivability based on the analytical approaches by comparing with the simulation solution. It is indeed significant to point out that the analytical solutions in the literature [11, 12] have not been validated in comparison with the simulation solution because of its complexity.

1.5 Organization of Dissertation

This thesis is organized as follows:

Firstly, in Chapter 2, we propose two stochastic models; binomial model and negative binomial model to quantify the network survivability and compare them with the existing Poisson model, and propose refined measures for network survivability taking account of the expected number of active nodes and border effects in MANETs. More specifically, we represent an approximate form of connectivity-based network survivability with the expected number of active nodes, instead of its upper and lower bounds [11, 12], and consider border effects in both two types of communication network areas; square area [17] and circular area [18].

In Chapter 3, we consider MRGP for the node behavior. The MRGP consists of several discrete states and time sequence of state transition, and is an extension from CTMC and renewal process. When the transition of power states follow general distributions, the model should be described by an MRGP. Particularly, this chapter focuses on both stationary and transient analysis of network survivability based on our MRGP model for power-aware MANETs.

In Chapter 4, we further extend the result of Chapter 3 for the other stochastic models including a binomial model and a negative binomial model. We derive analytically the upper and lower bounds of network survivability [12] as well as an approximate form based on the expected number of active nodes in both square [17] and circular [18] areas, under a general assumption that the battery life in each node is non-exponentially distributed. Also, we perform the transient analysis as well as the steady-state analysis of network survivability, and complements our early paper.

In Chapter 5, we propose a simulation algorithm to calculate the exact network survivability in two types communication areas. Numerical examples are also given, where we conduct a Monte Carlo simulation on the node degree and investigate the impact of border effects.

Finally, the thesis is concluded with some remarks and future directions in Chapter 6.

Chapter 2

Survivability Analysis with Border Effects for MANETs

Taking account of border effects in communication network areas is one of the most important problems to quantify accurately the performance/dependability of MANETs, because the assumption on uniformity of network node density is often unrealistic to describe the actual communication areas. This problem appears in both modeling the node behavior of MANETs and quantitation of their network survivability. In this chapter, we focus on the border effects in MANETs and reformulate the network survivability models based on a SMP, where two kinds of communication network areas are considered; square area and circular area. Based on some geometric ideas, we improve the quantitative network survivability measures for three stochastic models by taking account of the border effects, and revisit the existing lower and upper bounds of connectivity-based network survivability.

2.1 Preliminary

2.1.1 State of Node

Since nodes in MANETs cooperate with the routing processes to maintain network connectivity, each of node is designed as it behaves autonomously, but its discipline to require, send and receive the route information, is defined as a strict protocol. At the same time, it is also important to decide the protocol in order to prevent propagation of the erroneous route information caused by malicious attacks. Xing and Wang [11, 12] consider a MANET that suffers such

a malicious attack, whose node states are defined as follows:

- *Cooperative state (C)*: Initialized state of a node, which responds to route discoveries and forwards data packets to others.
- *Selfish state (S)*: State of a node, which may not forward control packets or data packets to others, but responds to only route discoveries for its own purpose from the reason of low power.
- *Jellyfish state (J)*: State of a node, which launches Jellyfish DoS attack.
- *Black hole state (B)*: State of a node, which launches Black hole DoS attack.
- *Failed state (F)*: State of a node, which can no longer perform basic functions such as initiation or response of route discoveries.

For common DoS attacks, the node in Jellyfish attack receives route requests and route replies. The main mechanism of Jellyfish state is to delay packets without any reason. On the other hand, the node in Black hole attack can respond a node with a fake message immediately by declaring as it is in the optimal path or as it is only one-hop away to other nodes.

Based on the node classification above, we consider a semi-Markov model to describe the stochastic behavior of a node by combining states with respect to the wellness. Suppose that a node may change its behavior under the following assumptions:

- A cooperative node may become a failed node due to energy exhaustion or misconfiguration. It is apt to become a malicious node when it launches DoS attack.
- A malicious node cannot become a cooperative node again, but may become a failed node.
- A node in failed state may become a cooperative node again after it is repaired and responds to routing requests to others.
- A failed node can become cooperative again if it is recovered and responds to routing operations.

2.1.2 Semi-Markov Node Model

Similar to [11, 12], let $S = \{C, S, J, B, F\}$ be a state space, and describe the node behavior transition by a stochastic process, $\{Z(t), t \geq 0\}$, associated with space S . Let X_n denote the state at transition time t_n . Define

$$\begin{aligned} \Pr(X_{n+1} = x_{n+1} | X_0 = x_0, \dots, X_n = x_n) \\ = \Pr(X_{n+1} = x_{n+1} | X_n = x_n), \end{aligned} \quad (2.1)$$

where $x_i \in S$ for $0 \leq i \leq n + 1$. From Eq. (2.1), the stochastic process $\{X_n, n = 0, 1, 2, \dots\}$ constitutes a CTMC with state space S , if all the transition times are exponentially distributed. However, since the transition time from one state to another state is subject to random behavior of a node, it is not realistic to characterize all the transition times by only exponentially distributed random variables. For instance, if a node is more inclined to fail due to energy consumption as time passes, and the less residual energy is left, then the more likely a node changes its behavior to selfish. This implies that the future action of a node may depend on how long it has been in the current state and that transition intervals may have arbitrary probability distributions.

From the above reason it is common to assume a SMP for $\{Z(t), t \geq 0\}$ to describe the node behavior transitions, which is defined by

$$Z(t) = X_n, \forall t_n \leq t \leq t_{n+1}. \quad (2.2)$$

Letting $T_n = t_{n+1} - t_n$ be the sojourn time between the n -th and $(n + 1)$ -st transitions, we define the associated semi-Markov kernel $\mathbf{Q} = (Q_{ij}(t))$ by

$$Q_{ij}(t) = \Pr(X_{n+1} = j, T_n \leq t | X_n = i) = p_{ij} F_{ij}(t), \quad (2.3)$$

where $p_{ij} = \lim_{t \rightarrow \infty} Q_{ij}(t) = \Pr(X_{n+1} = j | X_n = i)$ is the transition probability between state i and j ($i, j = c, s, j, b, f$) corresponding to $S = \{C, S, J, B, F\}$, and $F_{ij}(t) = \Pr(T_n < t | X_{n+1} = j, X_n = i)$ is the transition time distribution from state i to j .

Figure 2.1 illustrates the transition diagram of the homogeneous SMP, $\{Z(t), t \geq 0\}$, under consideration, which is somewhat different from the SMP in [11, 12], because it is somewhat simplified by eliminating redundant states. Let $1/\lambda_{ij}$ denote the mean transition time from state i to state j , and define the

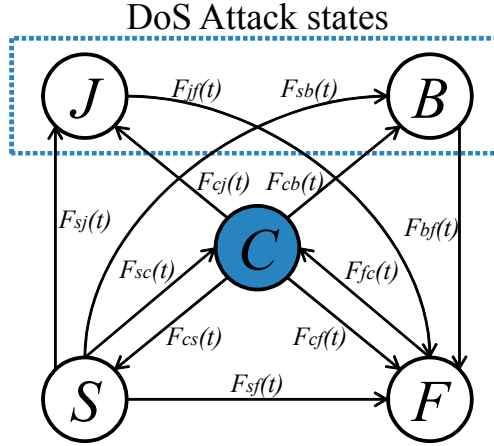


Figure 2.1: Semi-Markov transition diagram for node behavior.

Laplace-Stieltjes transform (LST) by $q_{ij}(s) = \int_0^\infty \exp\{-st\} dQ_{ij}(t)$. From the familiar SMP analysis technique, it is immediate to see that

$$q_{cs}(s) = \int_0^\infty \exp\{-st\} \bar{F}_{cj}(t) \bar{F}_{cb}(t) \bar{F}_{cf}(t) dF_{cs}(t) \quad (2.4)$$

$$q_{cj}(s) = \int_0^\infty \exp\{-st\} \bar{F}_{cs}(t) \bar{F}_{cb}(t) \bar{F}_{cf}(t) dF_{cj}(t) \quad (2.5)$$

$$q_{cb}(s) = \int_0^\infty \exp\{-st\} \bar{F}_{cs}(t) \bar{F}_{cj}(t) \bar{F}_{cf}(t) dF_{cb}(t) \quad (2.6)$$

$$q_{cf}(s) = \int_0^\infty \exp\{-st\} \bar{F}_{cs}(t) \bar{F}_{cj}(t) \bar{F}_{cb}(t) dF_{cf}(t) \quad (2.7)$$

$$q_{sc}(s) = \int_0^\infty \exp\{-st\} \bar{F}_{sj}(t) \bar{F}_{sb}(t) \bar{F}_{sf}(t) dF_{sc}(t) \quad (2.8)$$

$$q_{sj}(s) = \int_0^\infty \exp\{-st\} \bar{F}_{sc}(t) \bar{F}_{sb}(t) \bar{F}_{sf}(t) dF_{sj}(t) \quad (2.9)$$

$$q_{sb}(s) = \int_0^\infty \exp\{-st\} \bar{F}_{sc}(t) \bar{F}_{sj}(t) \bar{F}_{sf}(t) dF_{sb}(t) \quad (2.10)$$

$$q_{sf}(s) = \int_0^\infty \exp\{-st\} \bar{F}_{sc}(t) \bar{F}_{sj}(t) \bar{F}_{sb}(t) dF_{sf}(t) \quad (2.11)$$

$$q_{jf}(s) = \int_0^\infty \exp\{-st\} dF_{jf}(t) \quad (2.12)$$

$$q_{bf}(s) = \int_0^\infty \exp\{-st\} dF_{bf}(t) \quad (2.13)$$

$$q_{fc}(s) = \int_0^\infty \exp\{-st\} dF_{fc}(t), \quad (2.14)$$

where in general $\bar{\psi}(\cdot) = 1 - \psi(\cdot)$. Define the recurrent time distribution from state C to state C and its LST by $H_{cc}(t)$ and $h_{cc}(s)$, respectively. Then, from

the one-step transition probabilities from Eqs.(2.4)-(2.14), we have

$$\begin{aligned}
h_{cc}(s) &= \int_0^\infty \exp\{-st\} dH_{cc}(t) \\
&= q_{cs}(s)q_{sc}(s) + q_{cs}(s)q_{sj}(s)q_{jf}(s)q_{fc}(s) \\
&\quad + q_{cs}(s)q_{sb}(s)q_{bf}(s)q_{fc}(s) + q_{cs}(s)q_{sf}(s)q_{fc}(s) \\
&\quad + q_{cj}(s)q_{jf}(s)q_{fc}(s) + q_{cb}(s)q_{bf}(s)q_{fc}(s) \\
&\quad + q_{cf}(s)q_{fc}(s).
\end{aligned} \tag{2.15}$$

Let $P_{ci}(t)$ denote the transition probability from the initial state C to respective states $i \in \{c, s, j, b, f\}$ corresponding to $S = \{C, S, J, B, F\}$. Then, the LSTs of the transition probability, $p_{ci} = \int_0^\infty \exp\{-st\} dP_{ci}(t)$, are given by

$$p_{cc}(s) = \left\{ \bar{q}_{cs}(s) \quad q_{cj}(s) \quad q_{cb}(s) \quad q_{cf}(s) \right\} / \bar{h}_{cc}(s) \tag{2.16}$$

$$p_{cs}(s) = q_{cs}(s) \left\{ \bar{q}_{sc}(s) \quad q_{sj}(s) \quad q_{sb}(s) \quad q_{sf}(s) \right\} / \bar{h}_{cc}(s) \tag{2.17}$$

$$p_{cj}(s) = \{q_{cm}(s) + q_{cs}(s)q_{sj}(s)\} \bar{q}_{mf}(s) / \bar{h}_{cc}(s) \tag{2.18}$$

$$p_{cb}(s) = \{q_{cm}(s) + q_{cs}(s)q_{sb}(s)\} \bar{q}_{mf}(s) / \bar{h}_{cc}(s) \tag{2.19}$$

$$\begin{aligned}
p_{cf}(s) &= \{q_{cf}(s) + q_{cs}(s)q_{sf}(s) + q_{cs}(s)q_{sj}(s)q_{jf}(s) \\
&\quad + q_{cs}(s)q_{sb}(s)q_{bf}(s) + q_{cj}(s)q_{jf}(s) \\
&\quad + q_{cb}(s)q_{bf}(s)\} \bar{q}_{fc}(s) / \bar{h}_{cc}(s).
\end{aligned} \tag{2.20}$$

From Eqs.(2.16)-(2.20), the transient solutions, $P_{ci}(t)$, $i \in \{c, s, j, b, f\}$, which mean the probability that the state travels in another state i at time t , can be derived numerically, by means of the Laplace inversion technique (*e.g.* see [45]). As a special case, it is easy to derive the steady-state probability $P_i = \lim_{t \rightarrow \infty} P_{ci}(t)$, $i \in \{c, s, b, j, f\}$ corresponding to S . Based on the LSTs, $p_{cj}(s)$, we calculate $P_i = \lim_{t \rightarrow \infty} P_{ci}(t) = \lim_{s \rightarrow 0} p_{ci}(s)$ from Eqs.(2.16)-(2.20).

2.2 Quantitative Network Survivability Measure

2.2.1 Node Isolation and Connectivity

An immediate effect of node misbehaviors and failures in MANETs is the node isolation problem [12]. It is a direct cause for network partitioning, and eventually affects network survivability. The node isolation problem is caused by four types of neighbors; Failed, Selfish, Jellyfish and Blackhole nodes. For an example, we suppose in Fig. 2.2 that the node u has 4 neighbors when it initiates a

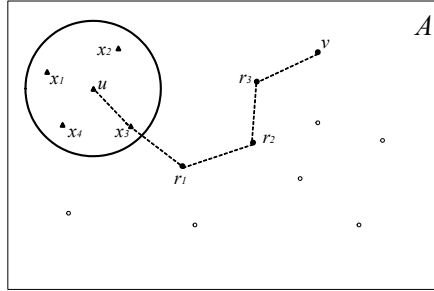


Figure 2.2: Isolation by Failed, Selfish or Jellyfish neighbors.

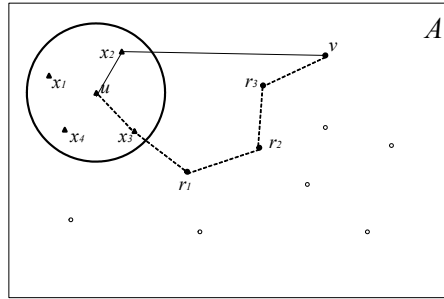


Figure 2.3: Isolation by Blackhole neighbors.

route discovery to another node v . Then it must go through by its neighbors x_i ($i = 1, 2, 3, 4$). If all neighbors of u are Failed, Selfish or Jellyfish nodes, then u can no longer communicate with the other nodes. In this case, we find that u is isolated by Failed and Selfish neighbors. On the other hand, if one of neighbors is Blackhole (*i.e.* x_2 in Fig. 2.3), it gives u a faked one-hope path, and makes u always choose it. In this case, we find that u is isolated by the Blackhole neighbor.

We define the node degree $D_{(u)}$ for node u by the maximum number of neighbors [13], and let $D_{(i,u)}$ be the number of node u 's neighbors at state $i \in \{c, s, j, b, f\}$. Then the isolation problem in our model can be formulated as follows: Given a node u with degree d , *i.e.*, $D_{(u)} = d$, if $D_{(s,u)} + D_{(f,u)} + D_{(j,u)} = d$ or $D_{(b,u)} \geq 1$, then the cooperative degree is zero, *i.e.*, $D_{(c,u)} = 0$,

and u is isolated from the network, so it holds that

$$\begin{aligned}
& \Pr(D_{(c,u)} = 0 | D_{(u)} = d) \\
&= \Pr(D_{(b,u)} \geq 1 | D_{(u)} = d) + \Pr(D_{(s,u)} + D_{(f,u)} + D_{(j,c)} = d | D_{(u)} = d) \\
&= 1 - (1 - P_b)^d + (1 - P_c - P_b)^d,
\end{aligned} \tag{2.21}$$

where P_c is the steady-state probability of a node in a cooperative state and P_b is the steady-state probability of a node launching Blackhole attacks. In the transient case, the steady-state probability P_c and P_b are replaced by $P_{cc}(t)$ and $P_{cb}(t)$, respectively.

In this paper, a node is said to be k -connected to a network if its associated cooperative degree is given by k (≥ 1). Given node u with degree d , *i.e.*, $D_{(u)} = d$, u is said to be k -connected to the network if the cooperative degree is k , *i.e.* $D_{(c,u)} = k$, which holds only if u has no Blackhole neighbor and has exactly k cooperative neighbors, *i.e.*, $D_{(b,u)} = 0$ and $D_{(c,u)} = k$, respectively. Then, from the statistical independence of all nodes, it is straightforward to see that

$$\begin{aligned}
& \Pr(D_{(c,u)} = k | D_{(u)} = d) \\
&= \Pr(D_{(c,u)} = k, D_{(b,u)} = 0 | D_{(u)} = d) \\
&= \Pr(D_{(c,u)} = k, D_{(b,c)} = 0, D_{(s,u)} + D_{(f,u)} + D_{(j,u)} = d - k) \\
&= \binom{d}{k} (P_c)^k (1 - P_c - P_b)^{d-k}.
\end{aligned} \tag{2.22}$$

2.2.2 Network Survivability

In the seminal paper [12], the network survivability is defined as the probability that MANET is a k -vertex-connected graph. Strictly speaking, it is difficult to validate the vertex-connectivity in the graph whose configuration dynamically changes such as MANETs. Therefore, Xing and Wang [12] derive approximately low and upper bounds of network survivability when the number of nodes is sufficiently large by considering the connectivity of a node in a MANET \mathcal{M} . The upper and lower bounds of connectivity-based network survivability are given by

$$NS_k(\mathcal{M})_U = (1 - \Pr(D_{(c,u)} < k))^{N_D}, \tag{2.23}$$

$$NS_k(\mathcal{M})_L = \max(0, 1 - E[N_a](\Pr(D_{(c,u)} < k))), \tag{2.24}$$

respectively, where u is an arbitrary node index in the active network. In Eq. (2.24), $E[N_a] = \lfloor N(1 - P_f) \rfloor$ is the expected number of active nodes in the network, where $\lfloor * \rfloor$ is the maximum integer less than $*$, P_f is the steady-state probability that a node is failed, and N denotes the total number of nodes. In Eq. (2.23), N_D is the number of points whose transmission ranges are mutually disjoint over the MANET area. Let A and r be the area of MANET and the node transmission radius, respectively. The number of disjoint points is given by $N_D = \lfloor N/(\lambda\pi r^2) \rfloor$, where $\lambda = N/A$ is the node density.

In this paper, we follow the same definition of network survivability as reference [12], but consider the expected network survivability instead of the low and upper bounds. Getting help from the graph theory, the expected network survivability is approximately given by the probability that expected active node in the network is k -connected:

$$NS_k(\mathcal{M})_E \approx \{1 - \Pr(D_{(c,u)} < k)\}^{E[N_a]}. \quad (2.25)$$

By the well-known total probability law, we have

$$\Pr(D_{(c,u)} < k) = \sum_{d=k}^{\infty} \Pr(D_{(c,u)} < k | D_{(u)} = d) \Pr(D_{(u)} = d), \quad (2.26)$$

so that we need to find the explicit forms of $\Pr(D_{(c,u)} < k | D_{(u)} = d)$ and $\Pr(D_{(u)} = d)$. From Eqs.(2.21) and (2.22), it is easy to obtain

$$\begin{aligned} & \Pr(D_{(c,u)} < k | D_{(u)} = d) \\ &= \Pr(D_{(c,u)} = 0 | D_{(u)} = d) + \sum_{m=1}^{k-1} \Pr(D_{(c,u)} = m | D_{(u)} = d) \\ &= 1 - (1 - P_b)^d + \sum_{m=0}^{k-1} \binom{d}{m} P_c^m (1 - P_c - P_b)^{d-m} \\ &= 1 - (1 - P_b)^d + \sum_{m=0}^{k-1} B_m(d, P_c, 1 - P_c - P_b), \end{aligned} \quad (2.27)$$

where B_m denotes the multinomial probability mass function. Replacing P_b and P_c by $P_{cb}(t)$ and $P_{cc}(t)$ respectively, we obtain the transient network survivability at an arbitrary time t . To derive $\Pr(D = d)$, Xing and Wang [12] used the Poissonization technique and presented the Poisson node degree model by using Poisson distribution. On the other hand, we know that binomial distribution can converge the Poisson distribution if the parameter of Poisson distribution μ

equals np and n tends to be infinite while the probability p approaches 0, where n and p are parameters of binomial distribution. Also, the negative binomial distribution can converge to Poisson distribution by other technique. Based on the above, we present the binomial and negative binomial node degree models.

(i) *Poisson Model* [11, 12]

Suppose that N nodes in a MANET are uniformly distributed over a 2-dimensional square with area A . The node transmission radius, denoted by r , is assumed to be identical for all nodes. To derive the node degree distribution $\Pr(D_{(u)} = d)$, we divide the area into N small grids virtually, so that the grid size has the same order as the physical size of a node. Consider the case where the network area is sufficiently larger than the physical node size. Then, the probability that a node occupies a specific grid, denoted by p , is very small. With large N and small p , the node distribution can be modeled by the Poisson distribution:

$$\Pr(D_{(u)} = d) = \frac{\mu^d}{d!} e^{-\mu}, \quad (2.28)$$

where $\mu = \rho\pi r^2$, and $\rho = E[N_a]/A$ is the node density depending on the underlying model. Finally, substituting Eqs.(2.26)-(2.28) into Eq. (2.25) yields

$$NS_k(\mathcal{M})_E^P \approx \left\{ e^{-\mu P_b} \left[1 - \frac{(k, \mu P_c)}{(k)} \right] \right\}^{E[N_a]}, \quad (2.29)$$

where $(x) = (x-1)!$ and $(h, x) = (h-1)! e^{-x} \sum_{l=0}^{h-1} x^l / l!$ are the complete and incomplete gamma functions, respectively.

(ii) *Binomial Model*

It is evident that the Poisson model just focuses on an ideal situation of node behavior. In other words, it is not always easy to measure the physical parameters such as r and A in practice. Let p denote the probability that each node is assigned into a communicate network area of a node. For the expected number of activated nodes $E[N_a]$, we describe the node distribution by the binomial distribution:

$$\begin{aligned} \Pr(D_{(u)} = d) &= \binom{E[N_a]}{d} p^d (1-p)^{E[N_a]-d} \\ &= B_d(E[N_a], p), \end{aligned} \quad (2.30)$$

where B_d is the binomial probability mass function. Substituting Eq. (2.30) into Eq. (2.25) yields an alternative formula of the network survivability:

$$NS_k(\mathcal{M})_E^B \approx \left\{ \sum_{k=0}^{E[N_a]} B_d(E[N_a], p) \left[(1 - P_b)^d \sum_{m=0}^{k-1} B_m(d, P_c, 1 - P_c - P_b) \right] \right\}^{E[N_a]} \quad (2.31)$$

Even though each node is assigned into a communication network area of a node with probability $p = \pi r^2/A$, then the corresponding binomial model results a different survivability measure from the Poisson model.

(iii) *Negative Binomial Model*

The negative binomial model comes from a mixed Poisson distribution instead of Poisson distribution. Let $f(\mu)$ be the distribution of parameter μ in the Poisson model. This implicitly assumes that the parameter μ includes uncertainty, and that the node distributions for all disjoint areas have different Poisson parameters. Then the node distribution can be represented by the following mixed Poisson distribution:

$$P(D_{(u)} = d) = \int_0^\infty e^{-\mu} \frac{\mu^d}{d!} f(\mu) d\mu. \quad (2.32)$$

For the sake of analytical simplicity, let $f(\mu)$ be the gamma probability density function with mean $\pi r^2 N(1 - P_f)/A$ and coefficient of variation c . Then we have

$$P(D_{(u)} = d) = \frac{(a+d)}{d!} \left(\frac{b}{a} \right)^a \left(\frac{1}{1+b} \right)^d = \lambda_d(a, b), \quad (2.33)$$

where $a = \lfloor 1/c^2 \rfloor$ and $b = \lfloor A/(\pi r^2 N(1 - P_f)c^2) \rfloor$. It should be noted that Eq. (2.33) corresponds to the negative binomial probability mass function with mean $\pi r^2 N(1 - P_f)/A$, and that the variance is greater than that in the Poisson model. In other words, it can represent the overdispersion or underdispersion property dissimilar to the Poisson model. From Eq. (2.33), we can obtain an alternative representation of the network survivability with an additional model parameter c .

$$NS_k(\mathcal{M})_E^{NB} \approx \left\{ \sum_{k=0}^{E[N_a]} \lambda_d(a, b) \left[(1 - P_b)^d \sum_{m=0}^{k-1} B_m(d, P_c, 1 - P_c - P_b) \right] \right\}^{E[N_a]} \quad (2.34)$$

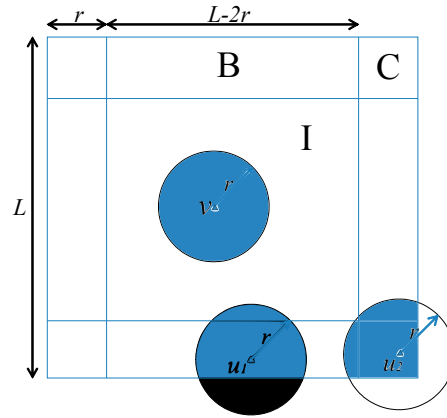


Figure 2.4: Border effects in square area.

2.3 Border Effects of Communication Network Area

The results on network survivability presented in Section 2.2 are based on the assumption that network area A has a node density $\rho = E[N_a]/A$. This strong assumption means that the expected number of neighbors of a node in the network has the exactly same value as $\rho\pi r^2$. In other words, such an assumption is not realistic in the real world communication network circumstance. It is well known that the border effect tends to decrease both the communication coverage and the node degree, which reflect the whole network availability. Laranjeira and Rodrigues [17] show that the relative average node degree for nodes in borders is independent of the node transmission range and of the overall network node density in a square communication network area. Bettsetetter [18] calculates the average node degree for nodes in borders for a circular communication network area. In the remaining part of this section, we consider the above two kinds of areas, and apply both results by Laranjeira and Rodrigues [17] and Bettsetetter [18] for the network survivability quantification.

2.3.1 Square Border Effect

Given a square area of side L in Fig. 2.4, the borders correspond to region B and C. We call the rectangular region B *the lateral border*, the square region C *the corne border*, and the square region I *the inner region*, respectively. In Fig. 2.4,

where $\alpha = \cos^{-1}(x/r)$. After a few algebraic manipulations, we get

$$EA_B(x, y) = r^2 \left[\left(\pi - \cos^{-1} \left(\frac{x}{r} \right) \right) + \frac{x}{r} \sqrt{1 - \left(\frac{x}{r} \right)^2} \right]. \quad (2.36)$$

Next we derive the average effective coverage area, ϕ_{lat} , for nodes in the lateral border B by integrating EA_B in Eq.(2.36) over the entire lateral border and dividing the result by its total area $r(L - 2r)$:

$$\phi_{lat} = \frac{1}{r(L - 2r)} \int_0^{L-2r} \left(\int_0^r EA_B(x, y) dx \right) dy. \quad (2.37)$$

Substituting Eq. (2.35) into Eq. (2.37), we get

$$\phi_{lat} = r^2 \left(\pi - \frac{2}{3} \right) \approx 0.787793\pi r^2. \quad (2.38)$$

Then, the expected effective node degree E_{lat} for nodes in the lateral border region B is given by

$$E_{lat} = \rho\phi_{lat} = 0.787793\rho\pi r^2. \quad (2.39)$$

In the similar way, the average effective coverage area ϕ_{cor} for nodes in the corner border C and the expected effective node degree E_{cor} for nodes in the lateral corner region C are obtained as [17]:

$$\phi_{cor} \approx 0.615336\pi r^2 \quad (2.40)$$

and

$$E_{cor} = \rho\phi_{cor} = 0.615336\rho\pi r^2. \quad (2.41)$$

Finally, the expected effective node degree μ_s for nodes in square communication network area is obtained as the weighted average with E_I , E_{lat} and E_{cor} :

$$\mu_s = \frac{E_I A_I + E_{lat} A_B + E_{cor} A_C}{A}, \quad (2.42)$$

where $A_I = (L - 2r)^2$, $A_B = 4r(L - 2r)$, $A_C = 4r^2$ and $A = L^2$. Substituting the area and expected node degree values in Eq. (2.42) and simplifying the resulting expression, we have

$$\mu = \mu_s = \frac{\rho\pi r^2 \sigma}{L^2}, \quad (2.43)$$

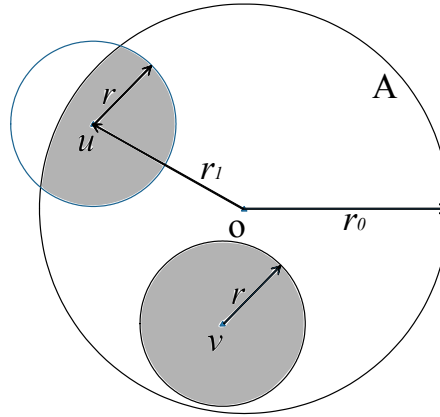


Figure 2.6: Border effects in circular area.

where $\sigma = (L - 2r)^2 + 3.07492r(L - 2r) + 2.461344r^2$.

For the binomial model, we need to find the probability that a node is assigned into the expected coverage of node in square communicate area (p_s). It can be obtained as

$$p = p_s = \frac{\pi r^2 \sigma}{L^4}. \quad (2.44)$$

On the other hand, the parameter b in the negative binomial model with square border effect, b_s , can be derived by

$$b = b_s = 1 / (\pi r^2 N_a c^2 \sigma) \quad (2.45)$$

for a given coefficient of variation c .

2.3.2 Circular Border Effect

For the circular area A with radius r_0 , define the origin O in A and use the coordinates r for a node in Fig. 2.6. Nodes in the circular communication network area that are located at least r away from the border, are called *the center nodes*, which are shown as a node v in Fig. 2.6. They have a coverage area equal to πr^2 and an expected node degree $E[N_a] \pi r^2 / A$. On the other hand, nodes located closer than r to the border are called *the border nodes* (node u in Fig. 2.6), which have a smaller coverage area, leading to a smaller expected node degree. The expected node degree of both center nodes and border nodes

can be obtained by

$$\mu = \begin{cases} N_a \hat{r}_1^2 & 0 \leq \hat{r} \leq 1 \quad \hat{r}_1 \\ \frac{n}{\pi} \left[\hat{r}_0^2 \arccos \frac{\hat{r}^2 + \hat{r}_1^2 - 1}{2\hat{r}\hat{r}_1} + \arccos \frac{\hat{r}^2 - \hat{r}_1^2 + 1}{2\hat{r}} \right] \frac{1}{2}\xi & 1 \quad \hat{r}_1 < \hat{r} \leq 1, \end{cases} \quad (2.46)$$

where $\xi = (\hat{r} + \hat{r}_1 + 1)(-\hat{r} + \hat{r}_1 + 1)(\hat{r} - \hat{r}_1 + 1)(\hat{r} + \hat{r}_1 - 1)$, $\hat{r} = r/r_0$ and $\hat{r}_1 = r_1/r_0$.

Bettsetttter [18] obtains the expected node degree of a node $\mu = \mu_c$ in circular communicate area:

$$\mu_c = \frac{N_a}{2\pi} \left[4(1 - \hat{r}^2) \arcsin \frac{\hat{r}}{2} + 2\hat{r}^2 \pi - (2\hat{r} + \hat{r}^3) \sqrt{1 - \frac{\hat{r}^2}{4}} \right], \quad (2.47)$$

which can be simplified by using Taylor series as

$$\mu_c \approx N_a \hat{r}^2 \left(1 - \frac{4\hat{r}}{3\pi} \right). \quad (2.48)$$

Then, $p = p_c$ for the binomial model and $b = b_c$ for the negative binomial model can be given in the following:

$$p_c = \frac{\tau}{2\pi}, \quad (2.49)$$

$$b_c = \frac{1}{2\pi \hat{r}^2 N_a c^2 \tau}, \quad (2.50)$$

where $\tau = 4(1 - \hat{r}^2) \arcsin(\hat{r}/2) + 2\hat{r}^2 \pi - (2\hat{r} + \hat{r}^3) \sqrt{1 - \hat{r}^2/4}$. By replacing the square border effect parameters μ , p and b in Eqs.(2.29), (2.31) and (2.34) by μ_s , p_s and b_s in Eqs.(2.43)-(2.45), we obtain the connectivity-based network survivability formulae with square border effects. Also, using μ_c , p_c and b_c in Eqs.(2.48)-(2.50), we calculate the connectivity-based network survivability in circular communication network area. We summarize refined network survivability formulae by taking account of border effects in Table 2.1.

2.4 Numerical Examples

2.4.1 Comparison of Steady-state Network Survivability

In this section, we investigate border effects in the connectivity-based network survivability quantification with three stochastic models. According to the connectivity analysis, given a network consisting of $N = 500$ nodes, we deploy all

Table 2.1: Summary of expected network survivability formulae with/without border effects.

Border Effects	Poisson	Binomial	Negative Binomial
Ignorance	$\left\{ e^{-\mu P_b} \left[1 - \frac{\Gamma(k, \mu P_c)}{\Gamma(k)} \right] \right\}^{E[N_a]}$	$\left\{ \sum_{k=0}^n B_d(n, p) \right\}^{E[N_a]}$	$\left\{ \sum_{k=0}^n \lambda_d(a, b) \right\}^{E[N_a]}$
Square	$\left\{ e^{-\mu_s P_b} \left[1 - \frac{\Gamma(k, \mu_s P_c)}{\Gamma(k)} \right] \right\}^{E[N_a]}$	$\left\{ \sum_{k=0}^n B_d(n, p_s) \right\}^{E[N_a]}$	$\left\{ \sum_{k=0}^n \lambda_d(a, b_s) \right\}^{E[N_a]}$
Circular	$\left\{ e^{-\mu_c P_b} \left[1 - \frac{\Gamma(k, \mu_c P_c)}{\Gamma(k)} \right] \right\}^{E[N_a]}$	$\left\{ \sum_{k=0}^n B_d(n, p_c) \right\}^{E[N_a]}$	$\left\{ \sum_{k=0}^n \lambda_d(a, b_c) \right\}^{E[N_a]}$
*	$(1 - P_b)^d \sum_{m=0}^{k-1} B_m(d, P_c, 1 - P_c - P_b)$		

the nodes in a square area of side $L = 1000(\text{m}^2)$. If the transmission radius of the nodes is greater than 83, i.e., $r > 83$, the probability that network is 1-connected is higher than 99%. From the simulation experiments, the result points out that a transmission radius of at least $r = 105(\text{m})$ is necessary to achieve a 1-connected network with probability higher than 99% [17]. However, the network survivability is more complicated. It does not depend on only the network parameters (A, r, N) , but also needs to determine the probability of each state of nodes. We set up the following model parameters [12]:

$$\begin{aligned}
 \lambda_{c,s} &= 1/240.0 \text{ [1/sec]}, & \lambda_{c,j} &= 3/2.0\text{e}+7 \text{ [1/sec]}, \\
 \lambda_{c,b} &= 1/6.0\text{e}+7 \text{ [1/sec]}, & \lambda_{c,f} &= 1/500.0 \text{ [1/sec]}, \\
 \lambda_{s,c} &= 1/60.0 \text{ [1/sec]}, & \lambda_{s,j} &= 3/2.0\text{e}+7 \text{ [1/sec]}, \\
 \lambda_{s,b} &= 1/6.0\text{e}+7 \text{ [1/sec]}, & \lambda_{s,f} &= 1/500.0 \text{ [1/sec]}, \\
 \lambda_{j,f} &= 1/50.0 \text{ [1/sec]}, & \lambda_{b,f} &= 1/50.0 \text{ [1/sec]}, \\
 \lambda_{j,s} &= 1/60.0 \text{ [1/sec]}, & &
 \end{aligned}$$

where λ_{ij} are transition rates from state i to state j in the exponential distributions. Under the above model parameters, the node probabilities in the steady state are given by

$$\begin{aligned}
 P_c &= 0.7299, & P_s &= 0.1629, & P_j &= 6.696\text{e}-6, \\
 P_b &= 7.44\text{e}-7, & P_f &= 0.1072.
 \end{aligned}$$

We also assume the network parameters as follows:

- $A = 1000 \text{ (m)} \times 1000 \text{ (m)}$: the area of MANET.
- $N = 500$: the number of mobile nodes.

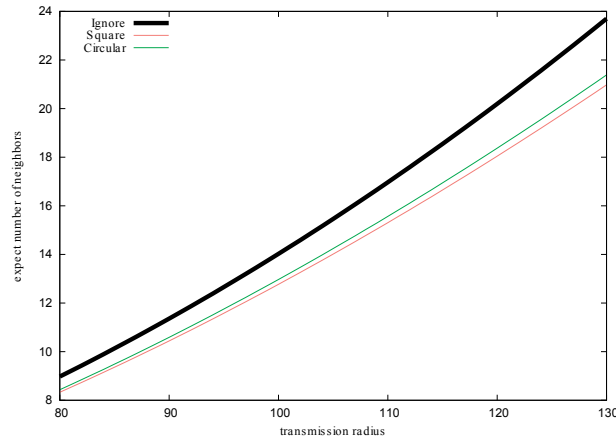


Figure 2.7: Effects of r on the expected node degree.

First, we compare the lower and upper bounds of connectivity-based network survivability [11, 12] with our expected network survivability in Eq.(2.29), (2.31) or (2.34). We set the transition radius r from 80 to 130, and connectivity requirement k from 1 to 3. The comparative results are shown in Table 2.2. From this table, we can see that the difference between lower and upper bounds of network survivability is very large for specific values of r and k . For example, when $r = 100$ and $k = 3$, the lower and upper bounds of network survivability in the Poisson model are equal to 0.0000 and 0.9296, respectively. On the other hand, the expected network survivability always takes a value between lower and upper bounds. This result shows us that our expected network survivability measure is more useful than the bounds for quantification of network survivability. Since it is known in [17, 18] that the number of neighbors of a node located in border areas is smaller than that located in the inner area, *i.e.*, the border effect is effective, we compare the expected number of neighbors in both types of network area in Fig. 2.7. From this result, it can be seen that as transmission radius increases, the gap between two cases with and without border effects becomes remarkable. Especially, it is found that the node in square area affects the border effect more than that in circular area.

To evaluate the accuracy of our analytical results on border effects, we conduct a Monte Carlo simulation, where two types of network communication areas; square area and circular area, are assumed identically to be $A = 1,000,000$

Table 2.2: Comparison of lower and upper bounds with expected network survivability.

r	k	Poisson			Binomial			Negative Binomial		
		SVB_L	SVB	SVB_U	SVB_L	SVB	SVB_U	SVB_L	SVB	SVB_U
80	1	0.3595	0.5268	0.9311	0.3807	0.5381	0.9333	0.3278	0.5103	0.927
	2	0.0000	0.0079	0.5830	0.0000	0.0088	0.5902	0.0000	0.0066	0.5716
	3	0.0000	0.0000	0.1219	0.0000	0.0088	0.1256	0.0000	0.0000	0.1154
90	1	0.8844	0.8908	0.9899	0.8908	0.8965	0.9904	0.8753	0.8827	0.9891
	2	0.0000	0.3519	0.9122	0.0020	0.3682	0.9158	0.0000	0.3295	0.9069
	3	0.0000	0.0073	0.6487	0.0000	0.0086	0.6576	0.0000	0.0058	0.6354
100	1	0.9793	0.9796	0.9985	0.9808	0.9810	0.9986	0.9773	0.9776	0.9984
	2	0.8156	0.8316	0.9869	0.8289	0.8427	0.9879	0.7971	0.8163	0.9856
	3	0.0000	0.3593	0.9296	0.0367	0.3812	0.9336	0.0000	0.3304	0.9241
110	1	0.9925	0.9925	0.9996	0.9928	0.9928	0.9996	0.9921	0.9922	0.9995
	2	0.9694	0.9699	0.9982	0.9723	0.9727	0.9984	0.9654	0.9660	0.9980
	3	0.8264	0.8406	0.9898	0.8426	0.8543	0.9908	0.8041	0.8220	0.9885
120	1	0.9931	0.9931	0.9997	0.9932	0.9932	0.9997	0.9931	0.9931	0.9997
	2	0.9905	0.9906	0.9995	0.9910	0.9910	0.9996	0.9898	0.9899	0.9995
	3	0.9713	0.9717	0.9986	0.9745	0.9748	0.9987	0.9667	0.9673	0.9984
130	1	0.9921	0.9921	0.9997	0.9921	0.9922	0.9997	0.9921	0.9921	0.9997
	2	0.9919	0.9919	0.9997	0.9920	0.9920	0.9997	0.9918	0.9918	0.9997
	3	0.9898	0.9899	0.9996	0.9903	0.9904	0.9996	0.9891	0.9892	0.9995

(m²). The expected active number of nodes, $E[N_a]$, is given by 446 with different communication radius r , which ranges from 80 to 130. We make r increase by 5. The random generation of active nodes is made 50 times for one radius. In each simulation, 20 nodes are randomly chosen, and the number of neighbors is counted for each node. Finally we get 1,000 values of number of neighbors for each r . From this result, we calculate the average number of neighbors for a node in both square and circular communication areas. Table 2.3 compares the simulation results with analytical ones in terms of the number of neighbors, where ‘ignorance’ denotes the case without border effects in [11, 12], ‘Square/a’ (‘Circular/a’) is the number of neighbors based on the analytical approach in Eq.(2.43) (Eq.(2.48)), and ‘Square/s’ (‘Circular/s’) is the simulation result in square (circular) area. In the comparison, we can see that the analytical results taking account of border effects get closer to the simulation results. However, the ignorance of border effects leads to an underestimation of the number of

Table 2.3: Simulation and analytical results on node degree.

r	Number of neighbors				
	Ignorance	Square/a	Square/s	Circular/a	Circular/s
80	8.9751	8.3288	8.1390	8.4350	8.5840
85	10.1321	9.3582	9.3510	9.4842	9.6990
90	11.3592	10.4421	10.5950	10.5901	10.6790
95	12.6563	11.5797	11.6510	11.7519	11.7150
100	14.0237	12.7700	12.8280	12.9687	13.0730
105	15.4611	14.0124	13.9660	14.2398	14.3040
110	16.9686	15.3059	15.2910	15.5645	15.6250
115	18.5463	16.6497	16.6480	16.9418	17.1330
120	20.1941	18.0429	17.9260	18.3711	18.3100
125	21.9120	19.4848	19.6190	19.8515	19.7780
130	23.7000	20.9746	21.1300	21.3823	21.2570

neighbors.

Table 2.4 presents the dependence of connectivity k and the number of nodes N on the steady-state network survivability among three stochastic models with and without border effects. Poisson model (Poisson), binomial model (Binomial) and negative binomial model (Negative Binomial) are compared in cases without border effects, which are denoted by Ignorance, Square and Circular in the table. From these results, it is shown that the network survivability is reduced fiercely as k increases when the number of nodes N is relatively small. The border effect is negligible in analysis if the network area is much larger than the transmission coverage area of a single node and the node density is not high. For example, the difference of survivability between with/without border effects for 1-connected network is less than 1%, when $N > 500$. The same results are shown in Table 2.4. We can ignore the border effects when $N > 700$ and $N > 900$ for 2-connected and 3-connected networks, respectively. In Fig. 2.8, we show the dependence of r and k on the steady-state network survivability in the Poisson model. From this figure, we find that the transition radius rather affects the steady-state network survivability, if each node has a relatively large r which is greater than 120(m). In this case even for the 3-connected network,

Table 2.4: Steady-state network survivability with three stochastic models.

N	k	Poisson			Binomial			Negative Binomial		
		Ignorance	Square	Circular	Ignorance	Square	Circular	Ignorance	Square	Circular
500	1	0.9787	0.9549	0.9602	0.9809	0.9594	0.9642	0.9780	0.9545	0.9592
	2	0.8249	0.6473	0.6824	0.8416	0.6735	0.7072	0.8193	0.6476	0.6780
	3	0.3435	0.1052	0.1350	0.3786	0.1257	0.1587	0.3373	0.1092	0.1351
600	1	0.9909	0.9865	0.9876	0.9912	0.9873	0.9883	0.9905	0.9856	0.9868
	2	0.9611	0.9078	0.9200	0.9643	0.9146	0.9260	0.9569	0.8986	0.9121
	3	0.7971	0.5700	0.6147	0.8120	0.5916	0.6355	0.7781	0.5415	0.5884
700	1	0.9905	0.9904	0.9905	0.9906	0.9905	0.9906	0.9905	0.9902	0.9903
	2	0.9853	0.9732	0.9762	0.9859	0.9749	0.9777	0.9843	0.9708	0.9743
	3	0.9482	0.8680	0.8866	0.9524	0.8772	0.8948	0.9421	0.8556	0.8761
800	1	0.9881	0.9890	0.9889	0.9881	0.9890	0.9889	0.9881	0.9889	0.9888
	2	0.9872	0.9855	0.9860	0.9874	0.9859	0.9864	0.9870	0.9849	0.9856
	3	0.9799	0.9597	0.9649	0.9809	0.9624	0.9672	0.9786	0.9561	0.9620
900	1	0.9850	0.9863	0.9861	0.9850	0.9863	0.9861	0.9850	0.9863	0.9861
	2	0.9849	0.9856	0.9856	0.9849	0.9857	0.9857	0.9848	0.9855	0.9855
	3	0.9835	0.9799	0.9810	0.9838	0.9807	0.9816	0.9832	0.9790	0.9802
1000	1	0.9815	0.9832	0.9829	0.9816	0.9832	0.9829	0.9815	0.9832	0.9829
	2	0.9815	0.9830	0.9828	0.9815	0.9831	0.9828	0.9815	0.9830	0.9828
	3	0.9813	0.9818	0.9819	0.9813	0.9820	0.9820	0.9812	0.9816	0.9817

the steady-state network survivability becomes 0.8 and tends to take a lower value. On the other hand, if n is sufficiently large and p is sufficiently small under $\mu = np$, from the small number's law, the binomial distribution can be well approximated by the Poisson distribution. This asymptotic inference can be confirmed in Fig. 2.9. So, three stochastic models provide almost similar performance in terms of connectivity-based network survivability in such a case.

2.4.2 Transient Analysis of Network Survivability

Next we concern the transient network survivability at arbitrary time t . For the numerical inversion of Laplace-Stieltjes transform, we apply the well-known Abate's algorithm [45]. Although we omit to show here for brevity, it can be numerically checked that the transient probability $P_{cc}(t)$ decreases in the first phase and approaches to the steady-state solution as time goes on. The other probability $P_{cs}(t)$, $P_{cj}(t)$, $P_{cb}(t)$ and $P_{cf}(t)$ increase in the first phase, but converge to their associated saturation levels asymptotically. Reminding these asymptotic properties on transition probabilities, we set $N = 500$ and $r = 100$, and consider the transient network survivability of three stochastic

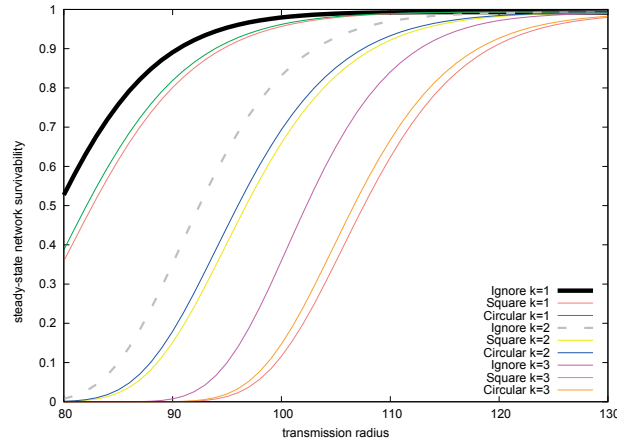


Figure 2.8: Effects of k on the steady-state network survivability.

models with and without border effects in Table 2.5. The network survivability with or without border effects has almost the similar initial values (0.9999), and the differences between them will be remarkable as time elapses.

Because three stochastic models show the quite similar tendency, hereafter we focus on only the Poisson model with k -connectivity ($k = 1, 2, 3, 4$) to investigate the impact on the transient network survivability. From Fig. 2.10, it is seen that the Poisson model has a higher transient network survivability when k is lower. Also, when the connectivity level becomes higher, the transient network survivability gets closer to 0 with time t elapsing. Finally we compare the Poisson model with and without border effects in terms of the transient network survivability. Figure 2.11 illustrates the transient network survivability when $k = 1$. It is shown that if the border effects are taken into consideration, the transient network survivability drops down as the operation time goes on. However, the transient solution without border effects still keeps higher levels in the same situation. This fact implies that the ignorance of border effects leads to an underestimation of network survivability. Since such an optimistic assessment of network survivability may result a risk through the network operation, it is recommended to take account of border effects in the connectivity-based network survivability assessment in MANETs.

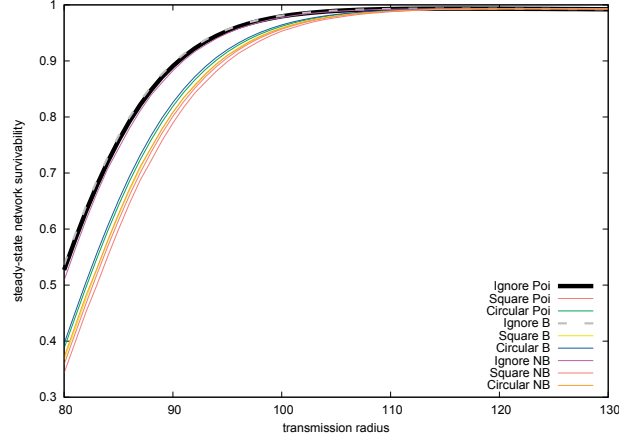


Figure 2.9: Comparison of three stochastic models with two types of border effect.

Table 2.5: Transient network survivability with three stochastic models.

t	k	Poisson			Binomial			Negative Binomial		
		Ignorance	Square	Circular	Ignorance	Square	Circular	Ignorance	Square	Circular
0	1	0.9999	0.9997	0.9998	0.9999	0.9997	0.9998	0.9999	0.9996	0.9997
	2	0.9987	0.9953	0.9962	0.9990	0.9960	0.9968	0.9984	0.9944	0.9954
	3	0.9895	0.9645	0.9707	0.9910	0.9688	0.9744	0.9871	0.9591	0.9653
40	1	0.9950	0.9915	0.9923	0.9953	0.9921	0.9929	0.9947	0.9906	0.9906
	2	0.9719	0.9289	0.9388	0.9746	0.9350	0.9442	0.9680	0.9204	0.9204
	3	0.8395	0.6425	0.6825	0.8527	0.6642	0.7032	0.8208	0.6131	0.6131
80	1	0.9893	0.9785	0.9810	0.9899	0.9799	0.9822	0.9883	0.9762	0.9791
	2	0.9186	0.8150	0.8371	0.9241	0.8252	0.8466	0.9091	0.7979	0.8220
	3	0.6076	0.3221	0.3696	0.6253	0.3397	0.3882	0.5768	0.2926	0.3401
120	1	0.9845	0.9678	0.9716	0.9855	0.9700	0.9735	0.9830	0.9646	0.9689
	2	0.8752	0.7336	0.7627	0.8834	0.7475	0.7758	0.8624	0.7130	0.7442
	3	0.4682	0.1919	0.2321	0.4888	0.2072	0.2492	0.4368	0.1699	0.2087
160	1	0.9819	0.9619	0.9664	0.9830	0.9643	0.9686	0.9800	0.9580	0.9631
	2	0.8515	0.6924	0.7245	0.8608	0.7073	0.7386	0.8368	0.6698	0.7040
	3	0.4057	0.1456	0.1809	0.4259	0.1586	0.1958	0.3742	0.1267	0.1602
200	1	0.9806	0.9590	0.9638	0.9820	0.9619	0.9665	0.9787	0.9553	0.9607
	2	0.8402	0.6735	0.7068	0.8512	0.6908	0.7233	0.8260	0.6523	0.6876
	3	0.3788	0.1278	0.1608	0.4016	0.1417	0.1769	0.3505	0.1121	0.1434

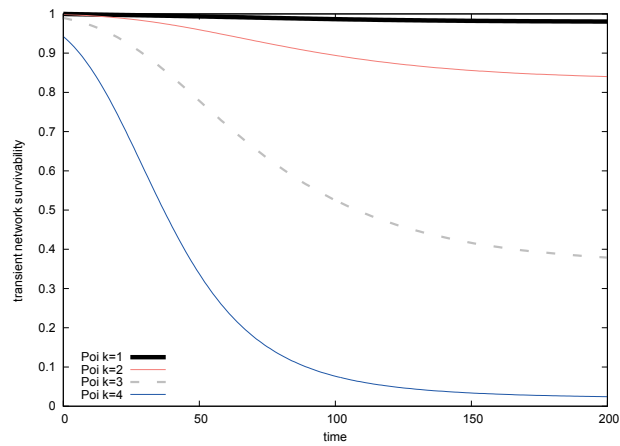
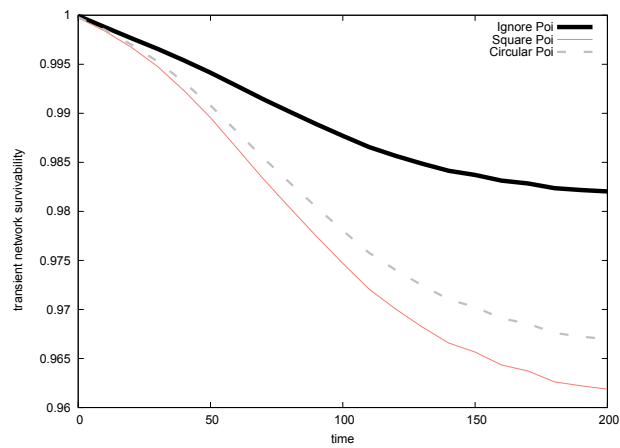
Figure 2.10: Transient network survivability with varying k .

Figure 2.11: Transient network survivability with border effects.

Chapter 3

Survivability Analysis for Power-Aware MANETs

This chapter presents the quantitative network survivability analysis for a power-aware MANET based on MRGPs. The MRGP is one of the widest class of stochastic point processes which are mathematically tractable. In the past literature, the model for a power-aware MANET was described by a CTMC. However, in the sense of representation ability, CTMC modeling is not sufficient to analyze the relationship between battery state and node behavior in the power-aware MANET. In particular, such problem seriously arises when we treat the transient behavior of the power-aware MANET. In this chapter, we revisit a power-aware MANET model by using MRGP, and present both stationary and transient analyses for the MRGP-based model.

3.1 Model Description

3.1.1 State of Node

In MANETs, nodes cooperate for the routing processes to maintain network connectivity [2]. Every node in MANET is designed as it behaves autonomously, and thus the behavior of requiring, sending and receiving route information should be decided as a strict protocol. Moreover, we find that it is also important to determine the protocol to prevent propagation of erroneous route information that is caused by malicious attacks. Xing and Wang [11, 12] discuss such a MANET that is suffered by a malicious attack, and present the following node states with represent to the wellness of a node:

- Cooperative state (C): an initialized state of a node which responds to route discoveries and forward data packets for others.
- Selfish state (S): a node may not forward control or data packets for others, and only responds to route discoveries for its own purpose by reason of low power.
- Malicious state (M): a node launches Jellyfish or Black hole DoS attack.
 - Jellyfish state (J): a node launches Jellyfish DoS attack, i.e., a node delays and fails to forward data packets maliciously.
 - Black hole state (B): a node launches Black hole DoS attack, i.e., a node broadcasts fake routes to disrupt legitimate path selections.
- Failed state (F): a node can no longer perform basic functions such as initiate or response route discoveries.

Jellyfish and Black hole attacks are typical DoS attacks in MANETs [25, 26]. The node in Jellyfish state can respond to route requests and route replies, but delays and fails to forward data packets without any reason. The node in Black hole state sends a fake message when a node requires the route information immediately, and spoofs the node on the optimal path. Both attacks cause the node isolation problem for neighbors.

Moreover, a node may be classified into the following states with respect to the battery:

- Fully charged battery state: The battery is fully charged.
- Low battery state: The battery is low and may cause a failure due to out of battery.

Based on the above node classification, we consider a CTMC model to describe the stochastic behavior of a node by combining the states with respect to the wellness and the battery. Concretely, we suppose that a node may change its behavior as follows:

- A cooperative node may become a failed node due to energy exhaustion and misconfiguration. It is apt to become a Malicious node when it launches DoS attack.

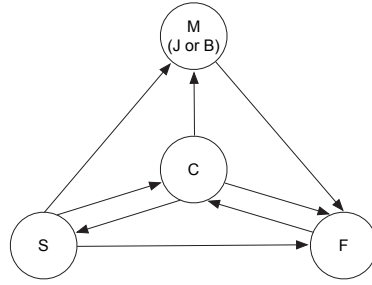


Figure 3.1: DoS attack model [12].

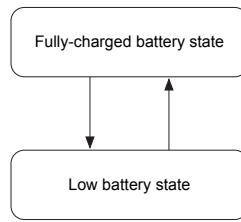


Figure 3.2: Power (battery) model.

- A malicious node cannot become a cooperative node again, but may become a failed node.
- A node in failed state may become a cooperative node again after it repairs and responds to routing requests for others.
- The node may become the low battery state as time passes.
- A node becomes the fully-charged battery state from the low battery state again by the battery charge.

Figure 3.1 depicts the state transition diagram of DoS attack behavior. The state cannot visit the cooperative state from neither Jellyfish and Black whole states. Figure 3.2 shows the state transition diagram of a battery.

3.1.2 MRGP modeling

Based on two CTMC models, we consider a composite model by combining two models with the following model assumptions:

- DoS attack behavior and battery state are independent with each other.

- All state transitions are occurred by exponential distributions.

However, for the first assumption, it is evident that the node failure depends on the state of battery, i.e., the failure rate in the empty battery state should be greater than that in the fully-charged battery state. Also, though the second assumption is useful to simplify the model analysis because the assumption gives a CTMC model, the battery life time is not exponentially distributed in general. Thus it is natural that the changes of the battery state are represented by non-exponential distributions such as deterministic, uniform and normal distributions. On the other hand, although Xing and Wang [11, 12] considered the non-exponential state transitions between DoS attack states, they did not discuss the effect of the state of battery.

This chapter presents a more general state-based model describing a node behavior. Concretely, we extend a CTMC modeling to an MRGP based modeling. MRGP is a stochastic point process which has both regenerative and non-regenerative time points [27, 28]. Generally, we consider a stochastic process $\{\mathcal{M}(t); t \geq 0\}$ with discrete state space. If $\mathcal{M}(t)$ has time points at which the process stochastically restarts itself, the process is called regenerative, and the time points are called regeneration points. Otherwise, the time points when $\mathcal{M}(t)$ does not restart are called non-regeneration points. Specifically, when state transition at the regeneration points is governed by a discrete-Time Markov chain (DTMC), the process $\mathcal{M}(t)$ is an MRGP.

In this chapter, we consider the following three battery states:

- Fully charged battery state: The battery is fully charged.
- Low battery state: The battery is low.
- Out of battery: The battery is out and the maintenance is required.

Also, in this chapter, the failed state F is caused by out of battery or exploit detection. Figure 3.3 illustrates the state transition diagram of our MRGP model. Three DoS attack states C , S and M are grouped by each battery state; fully-charged battery and low battery states, while the failed state F is grouped by an out of battery state. The state transition timings between fully-charged battery, low battery and out of battery states are defined by general

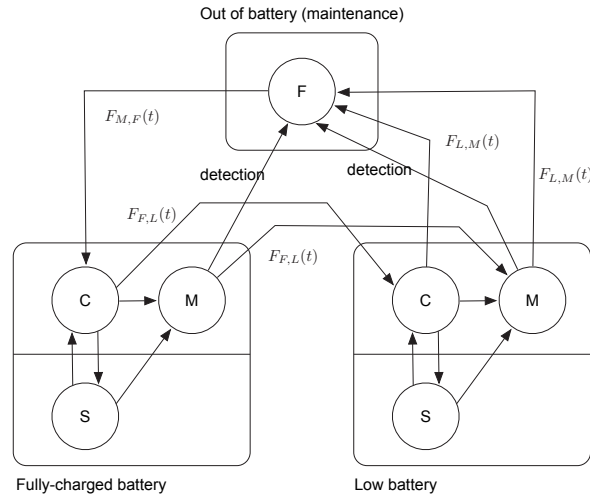


Figure 3.3: State transition diagram of MRGP model.

distributions. Let $F_{F,L}(t)$, $F_{L,M}(t)$ and $F_{M,L}(t)$ be cumulative distribution functions (c.d.f.'s) of the state transition distributions from fully-charged battery state to low battery state, from low battery state to out of battery state and from out of battery state to fully-charged battery state, respectively, and they are all regenerative transitions (dotted lines). On the other hand, the state transitions among C , S and M are non-regenerative (solid lines), whose transition rates are denoted by $\lambda_{x,y}^{(z)}$, $x, y \in \{C, S, M\}$, $z \in \{Full, Low\}$. In addition, in the malicious state, the exploit detection rates are $\lambda_{M,F}^{(z)}$, $z \in \{Full, Low\}$. This chapter assumes that a simultaneous transition in which both DoS attack and battery states change does not occur, except for transitions to out of battery state due to exploit detection and $F_{L,M}(t)$. Also, in Selfish state, the drain on battery power is reduced, i.e., the clocks of $F_{F,L}(t)$ and $F_{L,M}(t)$ are stopped by the preemptive resume [28, 30]. In the figure, the states of preemptive resume are located on the lower part of square representing a group of states.

3.2 Survivability Analysis

3.2.1 Definition

In [11, 12], the network survivability is defined as the probability that the MANET is a k -vertex-connected graph, which is the property that the net-

work is connected even if fewer than k vertices are deleted. In general, it is difficult to validate the vertex-connectivity in the graph whose configuration is dynamically changed such as MANETs. Therefore, Xing and Wang [11, 12] derived the approximate network survivability measure when the number of nodes is sufficient large by considering the connectivity of a node in the MANET.

Consider a MANET \mathcal{M} consisting of $|\mathcal{M}| = N$ mobile nodes and define the node degree $D(i)$ of node i , which means the number of neighbors of node i . Let $D_x(i)$ be the number of neighbors whose DoS attack states are $x \in \{C, S, J, B, F\}$. Then the node isolation condition can be described: If $D_S(i) + D_J(i) + D_F(i) = D(i)$ or $D_B(i) \geq 1$, then the node i is isolated from the network [11, 12]. Suppose that the DoS attack states of neighbors are mutually independent, and let the probability of DoS attack states of a neighbor be P_x ($x \in \{C, S, J, B, F\}$). The node isolation probability can be obtained as follows.

$$\begin{aligned} P(D_C(i) = 0 | D(i) = d) \\ = (1 - P_C - P_B)^d + 1 - (1 - P_B)^d. \end{aligned} \quad (3.1)$$

Furthermore, a node being k -connected to a network means that it has k -cooperative degree which is given by $D_C(i) = k$. Then the k -connected probability of node i is written by

$$\begin{aligned} P(D_C(i) = k | D(i) = d) \\ = \binom{d}{k} P_C^k (1 - P_C - P_B)^{d-k}, \quad k \geq 1. \end{aligned} \quad (3.2)$$

According to the network theory, Xing and Wang [11, 12] derived the approximate network survivability as the probability that every node in the active network has k -connected, namely,

$$NS_k(\mathcal{M}) \approx P(\theta(\mathcal{N}_a) \geq k), \quad (3.3)$$

where $\mathcal{N}_a \subseteq \mathcal{M}$ is the active network consisting of only cooperative nodes, and $\theta(\mathcal{N}_a) = \min\{D_C(i), i \in \mathcal{N}_a\}$. Moreover, the upper bound of the probability of Eq. (3.3) is given by

$$NS_k(\mathcal{M})_U = P(D_C(i) \geq k)^{N_D}, \quad (3.4)$$

and the lower bound:

$$NS_k(\mathcal{M})_L = \max(0, 1 - |\mathcal{N}_a|(1 - P(D_C(i) \geq k))), \quad (3.5)$$

where i is an arbitrary node index in the active network and $|\mathcal{N}_a| = N(1 - P_F)$ is the number of nodes in the active network \mathcal{N}_a . Also N_D is the number of points whose transmission ranges are mutually disjoint over the MANET area. Let A and r are the area of MANET and the node transmission radius. The number of disjoint points is given by $N_D = N/(\lambda\pi r^2)$ where λ is the node density, i.e., $\lambda = N/A$.

The probability $P(D_C(i) \geq k)$ in Eq. (3.5) can be rewritten in the form:

$$\begin{aligned}
P(D_C(i) \geq k) &= \sum_{d=k}^{\infty} P(D_C(i) \geq k | D(i) = d) P(D(i) = d) \\
&= \sum_{d=k}^{\infty} \sum_{n=k}^d P(D_C(i) = n | D(i) = d) P(D(i) = d) \\
&= \sum_{n=k}^{\infty} \sum_{d=n}^{\infty} P(D_C(i) = n | D(i) = d) P(D(i) = d). \tag{3.6}
\end{aligned}$$

Since $P(D_C(i) = n | D(i) = d)$ has already discussed in Eq. (3.1), this chapter considers two models to derive a closed form of $P(D(i) = d)$.

(i) Poisson Model [11, 12]

The Poisson model is based on the situation where N mobile nodes are uniformly placed in the area. The node distribution is assumed to be

$$P(D(i) = d) = \frac{\mu^d}{d!} e^{-\mu}, \tag{3.7}$$

where $\mu = \pi r^2 N(1 - P_F)/A$. Hence the probability $P(D_C(i) \geq k)$ is given by

$$P(D_C(i) \geq k) = \sum_{n=k}^{\infty} e^{-\mu(P_C+P_B)} \frac{(\mu P_C)^n}{n!}, \quad k \geq 1. \tag{3.8}$$

Substituting Eq. (3.8) into Eq. (3.5) yields the upper and lower bounds of network survivability.

(ii) Negative Binomial Model

The negative binomial model utilizes a mixed Poisson distribution instead of Poisson distribution. Let $f(\mu)$ be the distribution of parameter μ in the Poisson model. This implies that the parameter μ includes the uncertainty, and that the node distributions for all disjoint areas have different Poisson parameters. The

node distribution can be rewritten by the following mixed Poisson distribution:

$$P(D(i) = d) = \int_0^\infty e^{-\mu} \frac{\mu^d}{d!} f(\mu) d\mu. \quad (3.9)$$

For the sake of analytical simplicity, $f(\mu)$ is assumed to be the gamma distribution with mean $\pi r^2 N(1 - P_F)/A$ and coefficient of variation c . Then we have

$$P(D(i) = d) = \frac{(a+d)}{d!} \frac{1}{(a)} \left(\frac{b}{1+b} \right)^a \left(\frac{1}{1+b} \right)^d, \quad (3.10)$$

where $a = 1/c^2$ and $b = A/(\pi r^2 N(1 - P_F)c^2)$. It should be noted that Eq. (3.10) corresponds to the negative binomial p.m.f. with mean $\pi r^2 N(1 - P_F)/A$, and the variance is greater than the node distribution in the Poisson model. Based on Eq. (3.10), the probability $P(D_C(i) \geq k)$ is given by

$$\begin{aligned} & P(D_C(i) \geq k) \\ &= \sum_{n=k}^{\infty} \frac{(a+n)}{n!} \frac{1}{(a)} \left(\frac{b}{P_C + P_B + b} \right)^a \left(\frac{P_C}{P_C + P_B + b} \right)^d. \\ & k \geq 1. \end{aligned} \quad (3.11)$$

3.3 MRGP Analysis

To evaluate the network survivabilities in Eqs. (3.8) and (3.11), DoS attack state probabilities P_C and P_B should be computed from the MRGP model described in Section 3.1. In particular, we discuss the stationary analysis and transient analysis of MRGP model.

3.3.1 Stationary Analysis

In general, we define a regeneration time sequence $T_1 < T_2 < \dots$ and their time intervals $\Delta T_i = T_i - T_{i-1}$, $i = 1, 2, \dots$ in an MRGP model. Then the time interval behaves a Markov renewal sequence [31]. Suppose that the time sequence is time-homogeneous, i.e.,

$$\begin{aligned} & P(\mathcal{M}(T_n) = j, \Delta T_n < t \mid \mathcal{M}(T_{n-1}) = i) \\ &= P(\mathcal{M}(T_1) = j, \Delta T_1 < t \mid \mathcal{M}(T_0) = i) \\ &\equiv K_{i,j}(t). \end{aligned} \quad (3.12)$$

The state probability of MRGP is given by

$$\begin{aligned}
V_{i,j}(t) &= P(\mathcal{M}(t) = j \mid \mathcal{M}(0) = i) \\
&= P(\mathcal{M}(t) = j, \Delta T_1 \leq t \mid \mathcal{M}(0) = i) \\
&\quad + P(\mathcal{M}(t) = j, \Delta T_1 > t \mid \mathcal{M}(0) = i) \\
&= \sum_l \int_0^t P(\mathcal{M}(t-u) = j \mid \mathcal{M}(0) = l) dK_{i,l}(u) \\
&\quad + P(\mathcal{M}(t) = j, \Delta T_1 > t \mid \mathcal{M}(0) = i). \tag{3.13}
\end{aligned}$$

Let $\mathbf{K}(t)$, $\mathbf{V}(t)$ and $\mathbf{E}(t)$ denote matrices whose elements are $K_{i,j}(t)$, $V_{i,j}(t)$ and $P(\mathcal{M}(t) = j, \Delta T_1 > t \mid \mathcal{M}(0) = i)$, respectively. We have the Markov renewal equation for MRGP [27, 32];

$$\mathbf{V}(t) = \mathbf{E}(t) + \int_0^t d\mathbf{K}(u)\mathbf{V}(t-u), \tag{3.14}$$

where $\mathbf{E}(t)$ and $\mathbf{K}(t)$ are called local and global kernels.

MRGP is one of the widest stochastic processes which contain renewal structures, and can represent a variety of stochastic processes by choosing appropriate local and global kernels. According to the MRGP modeling in Section 3.1, we divide the state space into the subspaces \mathcal{S}_F^G , $\mathcal{S}_{F'}^G$, \mathcal{S}_L^G , $\mathcal{S}_{L'}^G$ and \mathcal{S}_M^G . The subspaces \mathcal{S}_F^G , \mathcal{S}_L^G and \mathcal{S}_M^G consist of the states which are categorized to fully-charged battery, low battery and out of battery states without preemptive resume, respectively. The subspaces $\mathcal{S}_{F'}^G$ and $\mathcal{S}_{L'}^G$ correspond to the states with preemptive resume in the fully-charged battery and low battery states. Also, the CTMC generators caused by non-regenerative transitions are partitioned by $\mathbf{Q}_{x,y}$, $x, y \in \{F, F', L, L', M\}$ which correspond to the non-regenerative transition kernel from the subspace \mathcal{S}_x^G to \mathcal{S}_y^G . The row vector $\mathbf{A}_{M,F}$ determines the DoS attack state in \mathcal{S}_F^G when the state transition of $F_{M,F}(t)$ occurs in \mathcal{S}_M^G .

Then we have the following Markov renewal equations:

$$\begin{aligned}
& \mathbf{V}_{F,F}(t) \\
&= \exp(\mathbf{S}_F t) \bar{\mathbf{F}}_{F,L}(t) \\
&+ \int_0^t \exp(\mathbf{S}_F u) \mathbf{V}_{L,F}(t-u) dF_{F,L}(u) \\
&+ \int_0^t \exp(\mathbf{S}_F u) \mathbf{Q}_{F,M} \mathbf{V}_{M,F}(t-u) \bar{\mathbf{F}}_{F,L}(u) du, \tag{3.15}
\end{aligned}$$

$$\begin{aligned}
& \mathbf{V}_{F,L}(t) \\
&= \int_0^t \exp(\mathbf{S}_F u) \mathbf{V}_{L,L}(t-u) dF_{F,L}(u) \\
&+ \int_0^t \exp(\mathbf{S}_F u) \mathbf{Q}_{F,M} \mathbf{V}_{M,L}(t-u) \bar{\mathbf{F}}_{F,L}(u) du, \tag{3.16}
\end{aligned}$$

$$\begin{aligned}
& \mathbf{V}_{F,M}(t) \\
&= \int_0^t \exp(\mathbf{S}_F u) \mathbf{V}_{L,M}(t-u) dF_{F,L}(u) \\
&+ \int_0^t \exp(\mathbf{S}_F u) \mathbf{Q}_{F,M} \mathbf{V}_{M,M}(t-u) \bar{\mathbf{F}}_{F,L}(u) du, \tag{3.17}
\end{aligned}$$

$$\begin{aligned}
& \mathbf{V}_{L,F}(t) \\
&= \int_0^t \exp(\mathbf{S}_L u) \mathbf{V}_{M,F}(t-u) dF_{L,M}(u) \\
&+ \int_0^t \exp(\mathbf{S}_L u) \mathbf{Q}_{L,M} \mathbf{V}_{M,F}(t-u) \bar{\mathbf{F}}_{L,M}(u) du, \tag{3.18}
\end{aligned}$$

$$\begin{aligned}
& \mathbf{V}_{L,L}(t) \\
&= \exp(\mathbf{S}_L t) \bar{\mathbf{F}}_{L,M}(t) \\
&+ \int_0^t \exp(\mathbf{S}_L u) \mathbf{V}_{M,L}(t-u) dF_{L,M}(u) \\
&+ \int_0^t \exp(\mathbf{S}_L u) \mathbf{Q}_{L,M} \mathbf{V}_{M,L}(t-u) \bar{\mathbf{F}}_{L,M}(u) du, \tag{3.19}
\end{aligned}$$

$$\begin{aligned}
& \mathbf{V}_{L,M}(t) \\
&= \int_0^t \exp(\mathbf{S}_L u) \mathbf{V}_{M,M}(t-u) dF_{L,M}(u) \\
&+ \int_0^t \exp(\mathbf{S}_L u) \mathbf{Q}_{L,M} \mathbf{V}_{M,M}(t-u) \bar{\mathbf{F}}_{L,M}(u) du, \tag{3.20}
\end{aligned}$$

$$\mathbf{V}_{M,F}(t) = \int_0^t \mathbf{A}_{M,F} \mathbf{V}_{F,F}(t-u) dF_{M,F}(u), \tag{3.21}$$

$$\mathbf{V}_{M,L}(t) = \int_0^t \mathbf{A}_{M,F} \mathbf{V}_{F,L}(t-u) dF_{M,F}(u), \tag{3.22}$$

$$\mathbf{V}_{M,M}(t) = \bar{\mathbf{F}}_{M,F}(t) + \int_0^t \mathbf{A}_{M,F} \mathbf{V}_{F,M}(t-u) dF_{M,F}(u), \tag{3.23}$$

where in general $\bar{F}(t) = 1 - F(t)$,

$$\mathbf{S}_F = \mathbf{Q}_{F,F} + \mathbf{Q}_{F,F'}(\mathbf{Q}_{F',F'})^{-1}\mathbf{Q}_{F',F}, \quad (3.24)$$

$$\mathbf{S}_L = \mathbf{Q}_{L,L} + \mathbf{Q}_{L,L'}(\mathbf{Q}_{L',L'})^{-1}\mathbf{Q}_{L',L} \quad (3.25)$$

and

$$\mathbf{V}(t) = \begin{pmatrix} \mathbf{V}_{F,F}(t) & \mathbf{V}_{F,L}(t) & \mathbf{V}_{F,M} \\ \mathbf{V}_{L,F}(t) & \mathbf{V}_{L,L}(t) & \mathbf{V}_{L,M} \\ \mathbf{V}_{M,F}(t) & \mathbf{V}_{M,L}(t) & \mathbf{V}_{M,M} \end{pmatrix}. \quad (3.26)$$

Note that the local kernel $\mathbf{E}(t)$ is a zero matrix in our model, because there are no state that has non-regenerative transition only.

The commonly used technique to compute stationary probability in MRGPs is an embedded Markov chain (EMC) approach [28]. The EMC approach consists of two steps; the steady-state probability on regeneration points and the computation of cumulative probabilities between two successive regeneration points.

Define the following matrices:

$$\mathbf{P}_{F,L} = \int_0^\infty \exp(\mathbf{S}_F u) dF_{F,L}(u), \quad (3.27)$$

$$\mathbf{P}_{F,M} = \int_0^\infty \int_0^u \exp(\mathbf{S}_F t) dt dF_{F,L}(u) \mathbf{Q}_{F,M}, \quad (3.28)$$

$$\begin{aligned} \mathbf{P}_{L,M} &= \int_0^\infty \exp(\mathbf{S}_L u) dF_{L,M}(u) \mathbf{A}_{L,M} \\ &\quad + \int_0^\infty \int_0^u \exp(\mathbf{S}_L t) dt dF_{L,M}(u) \mathbf{Q}_{L,M}, \end{aligned} \quad (3.29)$$

$$\mathbf{P}_{M,F} = \mathbf{A}_{M,F}. \quad (3.30)$$

These are submatrices for the probability transition matrix at time points when regenerative transitions occur. Let π_F^{EMC} , π_L^{EMC} and π_M^{EMC} be the stationary state probability vectors over \mathcal{S}_F^G , \mathcal{S}_L^G and \mathcal{S}_M^G . Thus we solve the following balance equation by a numerical technique [29].

$$\pi_F^{EMC} = \pi_M^{EMC} \mathbf{P}_{M,F}, \quad (3.31)$$

$$\pi_L^{EMC} = \pi_F^{EMC} \mathbf{P}_{F,L}, \quad (3.32)$$

$$\pi_M^{EMC} = \pi_F^{EMC} \mathbf{P}_{F,M} + \pi_L^{EMC} \mathbf{P}_{L,M}. \quad (3.33)$$

Next, we compute cumulative probabilities, i.e., expected sojourn time of each state between two successive regeneration points. Using the steady-state probability vectors $\boldsymbol{\pi}_F^{EMC}$, $\boldsymbol{\pi}_L^{EMC}$ and $\boldsymbol{\pi}_M^{EMC}$, the expected sojourn time are derived as follows.

$$\mathbf{s}_F = \boldsymbol{\pi}_F^{EMC} \int_0^\infty \int_0^u \exp(\mathbf{S}_F t) dt dF_{F,L}(u), \quad (3.34)$$

$$s_{F'} = \mathbf{s}_F \mathbf{Q}_{F,F'} (\mathbf{Q}_{F',F'})^{-1}, \quad (3.35)$$

$$\mathbf{s}_L = \boldsymbol{\pi}_L^{EMC} \int_0^\infty \int_0^u \exp(\mathbf{S}_L t) dt dF_{L,M}(u), \quad (3.36)$$

$$s_{L'} = \mathbf{s}_L \mathbf{Q}_{L,L'} (\mathbf{Q}_{L',L'})^{-1}, \quad (3.37)$$

$$\mathbf{s}_L = \boldsymbol{\pi}_L^{EMC} \int_0^\infty \int_0^u \exp(\mathbf{S}_L t) dt dF_{L,M}(u), \quad (3.38)$$

$$s_M = \boldsymbol{\pi}_M^{EMC} \int_0^\infty u dF_{M,F}(u). \quad (3.39)$$

The Markov renewal reward theory [31] gives the steady-state probability of MRGP as a fraction of the expected sojourn time for each state over the total time;

$$\boldsymbol{\pi}_F = \frac{\mathbf{s}_F}{\mathbf{s}_F \mathbf{1} + s_{F'} + \mathbf{s}_L \mathbf{1} + s_{L'} + s_M}, \quad (3.40)$$

$$\pi_{F'} = \frac{s_{F'}}{\mathbf{s}_F \mathbf{1} + s_{F'} + \mathbf{s}_L \mathbf{1} + s_{L'} + s_M}, \quad (3.41)$$

$$\boldsymbol{\pi}_L = \frac{\mathbf{s}_L}{\mathbf{s}_F \mathbf{1} + s_{F'} + \mathbf{s}_L \mathbf{1} + s_{L'} + s_M}, \quad (3.42)$$

$$\pi_{L'} = \frac{s_{L'}}{\mathbf{s}_F \mathbf{1} + s_{F'} + \mathbf{s}_L \mathbf{1} + s_{L'} + s_M}, \quad (3.43)$$

$$\pi_M = \frac{s_M}{\mathbf{s}_F \mathbf{1} + s_{F'} + \mathbf{s}_L \mathbf{1} + s_{L'} + s_M}, \quad (3.44)$$

where $\mathbf{1}$ is a column vector that every element is 1. The matrix exponential forms of Eqs. (3.34) through (3.39) can be computed by uniformization technique (see Appendix 1). Finally, we can obtain the state probabilities P_B and P_C by summing the corresponding elements in $\boldsymbol{\pi}_F$ and $\boldsymbol{\pi}_L$.

3.3.2 Transient Analysis

PH (phase-type) expansion is one of the most popular methods for the transient analysis of MRGP. The idea of PH expansion is to replace general distributions in MRGP with approximate PH distributions, and it can reduce the original MRGP to an approximate CTMC.

The PH distribution is defined as the time to absorption in a finite Markov chain with one absorbing state. Strictly speaking, the PH distribution is clas-

sified into continuous and discrete PH distributions. This chapter deals with continuous PH distribution. If we let \mathbf{T} be the transition rates between transient states and $\boldsymbol{\xi}$ be the exit rates from transient states to the absorbing state, without loss of generality, the infinitesimal generator \mathbf{D} of continuous-time Markov chain is assumed to be partitioned as follows:

$$\mathbf{D} = \left(\begin{array}{c|c} \mathbf{T} & \boldsymbol{\xi} \\ \hline \mathbf{0} & 0 \end{array} \right), \quad (3.45)$$

For the transient states, we set $\boldsymbol{\alpha}$ be an initial probability vector. The cumulative distribution function (c.d.f.) and the probability density function (p.d.f.) of PH distribution are defined by

$$F_{PH}(t) = 1 - \boldsymbol{\alpha} \exp(\mathbf{T}t)\mathbf{1}, \quad f_{PH}(t) = \boldsymbol{\alpha} \exp(\mathbf{T}t)\boldsymbol{\xi}, \quad (3.46)$$

where $\mathbf{1}$ is a column vector that every element is 1. Note that the exit rate vector is given by $\boldsymbol{\xi} = -\mathbf{T}\mathbf{1}$. We call the transient states *phases*.

The PH distribution has several sub-classes according to the structure of \mathbf{T} (see e.g. [33]). In particular, the acyclic PH distribution (APH) is the widest class among mathematically tractable PH distributions. Cumani [34] derived the canonical forms (CFs) as the minimal representation of APH, which has the smallest number of free parameters. The CF1 (canonical form 1) is defined by

$$\boldsymbol{\alpha} = \left(\alpha_1 \quad \alpha_2 \quad \cdots \quad \alpha_m \right), \quad (3.47)$$

$$\mathbf{T} = \begin{pmatrix} \nu_1 & \nu_1 & & & & \\ & \nu_2 & \nu_2 & & & \\ & & \ddots & \ddots & & \\ & & & \nu_{m-1} & \nu_{m-1} & \\ & & & & \nu_m & \end{pmatrix}, \quad \boldsymbol{\xi} = \begin{pmatrix} 0 \\ \vdots \\ \nu_m \end{pmatrix}, \quad (3.48)$$

where $\alpha_i \geq 0$, $\sum_{i=1}^m \alpha_i = 1$ and $0 < \nu_1 \leq \cdots \leq \nu_m$.

The first step of PH expansion is to approximate general distributions with PH distributions. The commonly used techniques of PH approximation are moment match, least square method of the difference of p.d.f.'s and ML estimation.

The ML estimation is widely used for the parameter estimation of general distributions, and has useful properties like asymptotic consistency and normality. Some authors have been discussed the ML estimation of PH distribution

[35, 36, 37, 38]. The ML estimates of PH distribution are derived so that the mode matches the theoretical one. According to [37], this paper uses the PH fitting based on ML estimation. Roughly speaking, ML estimation uses the Kullback-Leibler (KL) divergence. Therefore we directly apply the KL divergence as a criterion of function fitting.

Given an arbitrary probability density function $f(t)$, the KL divergence $KL(f, g)$ between $f(t)$ and any probability density function $g(t)$ is defined by

$$\begin{aligned} KL(f, g) &= \int_0^\infty f(t) \log \frac{f(t)}{g(t)} dt \\ &= \int_0^\infty f(t) \log f(t) dt - \int_0^\infty f(t) \log g(t) dt. \end{aligned} \quad (3.49)$$

The problem is to find $g(t)$ maximizing $\int_0^\infty f(t) \log g(t) dt$. Applying a suitable numerical integration technique, we have

$$\int_0^\infty f(t) \log g(t) dt \approx \sum_{i=1}^K w_i \log g(t_i), \quad (3.50)$$

where w_i , including $f(t_i)$, is a weight. The discretized points and their associated weights are determined by the numerical quadrature. Eq. (3.50) indicates that ML estimation is one approximation form of the KL divergence. Thus we can obtain an approximate PH distribution by using the weighted samples $(t_1, w_1), \dots, (t_K, w_K)$ (see Appendix 2).

Finally we apply the EM algorithm to derive the ML estimates for PH distribution [37]. The EM algorithm proposed in [37] further improves the computation speed of the EM algorithm by Asmussen et al. [36] with respect to the number of phases, though both algorithms are based on forward-backward computation [39, 40]. Since this method utilizes sparsity of the generator \mathbf{T} , the computation speed is drastically reduced for estimating CF1.

This chapter utilizes PH expansion of MRGP based on the Kronecker representation, which is often used to represent a superposition of Markov models [41]. The general distributions $F_{F,L}(t)$, $F_{L,M}(t)$ and $F_{M,F}(t)$ are approximated

by

$$\begin{aligned} F_{F,L}(t) &\approx 1 - \alpha_F \exp(\mathbf{T}_F t) \mathbf{1}_F, \\ f_{F,L}(t) &\approx \alpha_F \exp(\mathbf{T}_F t) \boldsymbol{\xi}_F, \end{aligned} \quad (3.51)$$

$$\begin{aligned} F_{L,M}(t) &\approx 1 - \alpha_L \exp(\mathbf{T}_L t) \mathbf{1}_L, \\ f_{L,M}(t) &\approx \alpha_L \exp(\mathbf{T}_L t) \boldsymbol{\xi}_L, \end{aligned} \quad (3.52)$$

$$\begin{aligned} F_{M,F}(t) &\approx 1 - \alpha_M \exp(\mathbf{T}_M t) \mathbf{1}_M, \\ f_{M,F}(t) &\approx \alpha_M \exp(\mathbf{T}_M t) \boldsymbol{\xi}_M. \end{aligned} \quad (3.53)$$

Then the MRGP process $\mathcal{M}(t)$ can be approximated by the CTMC with the following infinitesimal generator:

$$\mathbf{V}^{PH} = \begin{pmatrix} \mathbf{Q}_{F,F} \oplus \mathbf{T}_F & \mathbf{Q}_{F,F'} \otimes \mathbf{I} & \mathbf{A}_{F,L} \otimes (\boldsymbol{\xi}_F \boldsymbol{\alpha}_L) & & \mathbf{Q}_{F,M} \otimes (\mathbf{1}_F \boldsymbol{\alpha}_M) \\ \mathbf{Q}_{F',F} \otimes \mathbf{I} & \mathbf{Q}_{F',F'} \otimes \mathbf{I} & & & \\ & & \mathbf{Q}_{L,L} \oplus \mathbf{T}_L & \mathbf{Q}_{L,L'} \otimes \mathbf{I} & \mathbf{A}_{L,M} \otimes (\boldsymbol{\xi}_L \boldsymbol{\alpha}_M) \\ & & \mathbf{Q}_{L',L} \otimes \mathbf{I} & \mathbf{Q}_{L',L'} \otimes \mathbf{I} & + \mathbf{Q}_{L,M} \otimes (\mathbf{1}_L \boldsymbol{\alpha}_M) \\ \mathbf{A}_{M,F} \otimes (\boldsymbol{\xi}_M \boldsymbol{\alpha}_F) & & & & \mathbf{T}_M \end{pmatrix} \quad (3.54)$$

where \otimes and \oplus are Kronecker product and sum, respectively. The approximate transient probability vector of $\mathcal{M}(t)$ can be derived by summing the corresponding elements of the following probability vector

$$\begin{aligned} &(\boldsymbol{\pi}_F(0) \otimes \mathbf{1}_F^T, \boldsymbol{\pi}_{F'}(0) \otimes \mathbf{1}_{F'}^T, \boldsymbol{\pi}_L(0) \otimes \mathbf{1}_L^T, \\ &\boldsymbol{\pi}_{L'}(0) \otimes \mathbf{1}_{L'}^T, \boldsymbol{\pi}_M(0) \otimes \mathbf{1}_M^T) \exp(\mathbf{V}^{PH} t), \end{aligned} \quad (3.55)$$

where $\mathbf{1}^T$ is the transpose of vector $\mathbf{1}$.

3.4 Numerical Examples

3.4.1 Stationary Analysis

In this section, we investigate the network survivability in the MRGP model. We set the following model parameters, which are based on the simulation results in [12]:

Fully-charged battery state:

$$\begin{aligned}\lambda_{C,S} &= 1/240.0 \text{ [1/sec]}, & \lambda_{S,C} &= 1/60.0 \text{ [1/sec]}, \\ \lambda_{M,F} &= 1/50.0 \text{ [1/sec]}, & \lambda_{C,M} &= 1/6.0e+6 \text{ [1/sec]}, \\ p_B &= 0.1, & p_J &= 0.9, \\ f_{F,L}(t) &= \text{Gamma}(t, 5.0, 5.0/24000).\end{aligned}$$

Low battery state:

$$\begin{aligned}\lambda_{C,S} &= 1/60.0 \text{ [1/sec]}, & \lambda_{S,C} &= 1/240.0 \text{ [1/sec]}, \\ \lambda_{M,F} &= 1/50.0 \text{ [1/sec]}, & \lambda_{C,M} &= 1/6.0e+6 \text{ [1/sec]}, \\ p_B &= 0.1, & p_J &= 0.9, \\ f_{L,M}(t) &= \text{Gamma}(t, 2.0, 2.0/1000).\end{aligned}$$

Out of battery (maintenance) state:

$$f_{M,F}(t) = \text{Uniform}(t, 30, 90),$$

where $\text{Gamma}(t, \cdot, \cdot)$ and $\text{Uniform}(t, \cdot, \cdot)$ are gamma and uniform p.d.f.'s:

$$\text{Gamma}(t, a, b) = \frac{b^a t^{a-1} e^{-bt}}{(a)}, \quad t \geq 0, \quad (3.56)$$

$$\text{Uniform}(t, \min, \max) = \frac{1}{\max - \min}, \quad \min \leq t \leq \max. \quad (3.57)$$

Also, p_B is the probability that a node launches Black hole DoS attack, and p_J is the probability that a node launches Jellyfish DoS attack when the node becomes the malicious state. Moreover, we determine the network parameters as follows.

- $A = 1000 \text{ (m)} \times 1000 \text{ (m)}$: the area of MANET.
- $N = 500$: the number of mobile nodes.
- $r = 100 \text{ (m)}$: transmission radius of a node.

Under the above model parameters, the node probabilities in steady state are given by

Fully-charged battery state:

$$P_C = 0.6847, \quad P_S = 0.1712, \quad P_B = 5.694\text{e-}7,$$

$$P_J = 5.125\text{e-}6.$$

Low battery state:

$$P_C = 2.848\text{e-}2, \quad P_S = 0.1139, \quad P_B = 2.373\text{e-}8,$$

$$P_J = 2.136\text{e-}7.$$

Out of battery state:

$$P_F = 1.716\text{e-}3.$$

Since we assume that the transition rate from cooperative state to selfish state in low battery state is higher than that in fully-charged battery state, the steady state probability of the selfish state in low battery state is also high. According to the above stationary state probabilities, the upper and lower bounds of 1-connected network survivability of Poisson model are given by $NS_k(\mathcal{M})_U^P = 0.9993$ and $NS_k(\mathcal{M})_L^P = 0.9884$. On the other hand, the upper and lower bounds of 1-connected network survivability of negative binomial model are $NS_k(\mathcal{M})_U^{NB} = 0.06545$ and $NS_k(\mathcal{M})_L^{NB} = 0$, where the coefficient of variation (CV) is set as $c = 1.0$. The essential difference between Poisson and negative binomial models is the bias of the number of mobile nodes in a local area. That is, the Poisson model means that the number of nodes in a local area is close to a constant, compared to that of negative binomial model. In fact, when $c = 0.01$, the upper and lower bounds of network survivability of negative binomial model are $NS_k(\mathcal{M})_U^{NB} = 0.9989$ and $NS_k(\mathcal{M})_L^{NB} = 0.9829$ which are close to those of Poisson model. To investigate the effect of CV of the number of nodes on the network survivability, we perform the sensitivity analysis of the network survivability on the CV c in the negative binomial model. Figure 3.4 illustrates the upper bound of network survivability in the negative binomial model with varying c , where x-axis and y-axis indicate the CV and the upper bound of network survivability, respectively. From this figure, it can be seen that the network survivability is sensitive to the CV of the number of neighbors

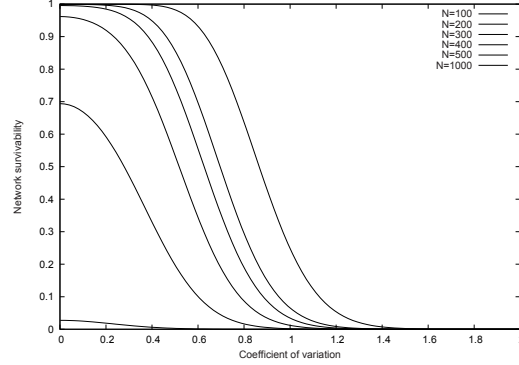


Figure 3.4: Upper bound of 1-connected network survivability in negative binomial model.

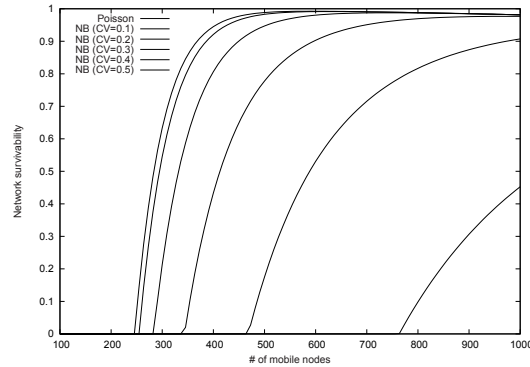


Figure 3.5: Upper bound of 1-connected network survivability with varying the number of nodes.

regardless of the number of total nodes. In all cases, the network survivability gets worse as CV increases. This implies that it is important to “uniformly” place mobile nodes to whole the MANET area in order to maintain high network survivability.

Next we investigate the relationship between the number of total nodes and the network survivability. Figure 3.5 shows the upper bounds of 1-connected network survivability with varying the number of mobile nodes in whole the MANET area. From the figure, we find that the number of nodes exponentially affects the network survivability, which is the same conclusion as [12], and that the curve rapidly increases when the CV is small. Similar to the previous

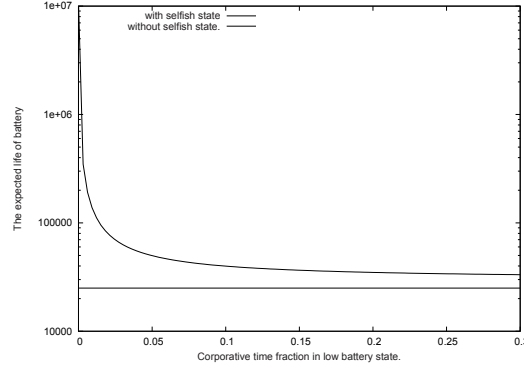


Figure 3.6: The expected life of battery.

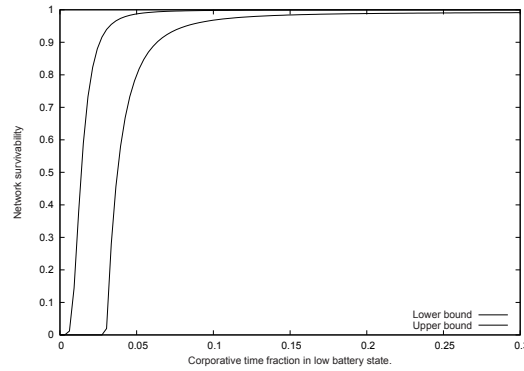


Figure 3.7: Bounds of 1-connected network survivability with varying the cooperative time fraction in low battery state.

insights, if mobile nodes are unevenly located to geographical areas, the network survivability becomes low even if a large number of mobile nodes are placed.

In our modeling, we can derive the expected life of battery by computing the expected cycle time from fully-charged battery state to out of battery state. Therefore, dissimilar to [19], we can examine the effect of selfish behavior on the battery life as well as the network survivability. Figures 3.6 and 3.7 show the expected life of battery and the upper and lower bounds of network survivability in Poisson model with varying the time fraction of sojourn time of cooperative state over that of selfish state in the low battery state. That is, the transition

rates in the low battery state are redefined as follows.

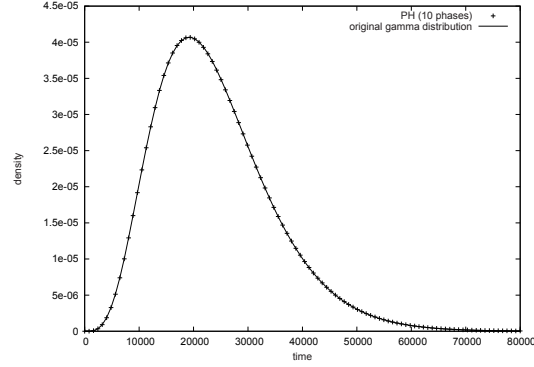
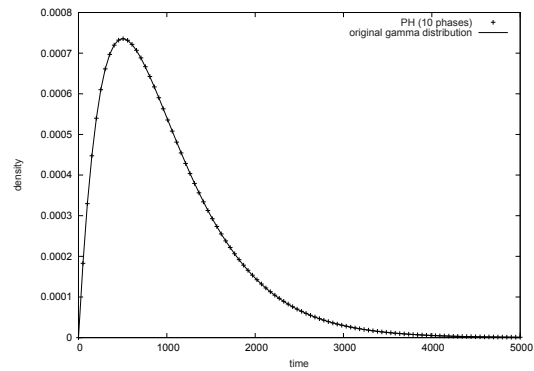
$$\lambda_{C,S} = \frac{1}{300.0f_a}, \quad \lambda_{S,C} = \frac{1}{300.0(1-f_a)}, \quad 0 < f_a < 1. \quad (3.58)$$

If f_a is close to 0, the node spends in selfish state for almost all time in low battery state. Also, in Fig. 3.6, we indicate the expected life of battery when nodes do not go to selfish state, which is labeled by ‘without selfish’. From Fig. 3.6, the expected life of battery exponentially grows as the cooperative time fraction is close to 0. However, the expected life of battery does not change around at 0.1 time fraction. On the other hand, from Fig. 3.7, it can be found that the network survivability becomes low as the cooperative time fraction decreases. In particular, when the cooperative time fraction is less than 0.1, the upper and lower bounds of network survivability rapidly decrease. This indicates that there is a tradeoff between the battery life and network survivability.

3.4.2 Transient Analysis

According to PH expansion described in Section 3.3, we examine the transient analysis of node state and derive the corresponding network survivability of MANET. We utilize the model parameters which are set in the stationary analysis.

First we describe the PH approximation for the distributions $F_{F,L}(t)$, $F_{L,M}(t)$ and $F_{M,L}$. In fact, since gamma distributions with integer shape parameters are a concrete class of PH distributions, $F_{F,L}(t)$ and $F_{L,M}(t)$ are originally represented by PH distributions. However, in order to examine the approximation performance of PH expansion, we apply the weighted sample-based PH approximation to all the distributions. Based on the weighted samples derived by DE formulas (see Appendix 2), we estimate PH parameters for $F_{F,L}(t)$, $F_{L,M}(t)$ and $F_{M,F}(t)$ with 10, 10 and 1000 phases, respectively. Figures 3.8 through 3.10 present the p.d.f.’s of original gamma and uniform distributions and the approximate PH distributions. In Figs. 3.8 and 3.9, the p.d.f.’s of approximate PH distributions are drawn by dots, because the p.d.f.’s of PH distributions are close to the original density functions so that they cannot be recognized. From Figs. 3.8 and 3.9, we see that the PH approximation for $F_{F,L}(t)$ and $F_{L,M}(t)$

Figure 3.8: PH approximation for $F_{F,L}(t)$.Figure 3.9: PH approximation for $F_{L,M}(t)$.

is accurate. This is because the gamma distributions with integer shape parameters are involved by acyclic PH distributions. Also, from Fig. 3.10, PH approximation works well for a uniform distribution by using a large number of phases.

Figures 3.11 through 3.13 illustrate the transient behavior of node probability which is approximated by PH distributions. In particular, we set the following state probability vectors as the initial probability vectors at $t = 0$:

Case 1: The probability vector just after the node becomes the cooperative state (Fig. 3.11).

Case 2: the probabilities of all the state, including phases of PH distributions

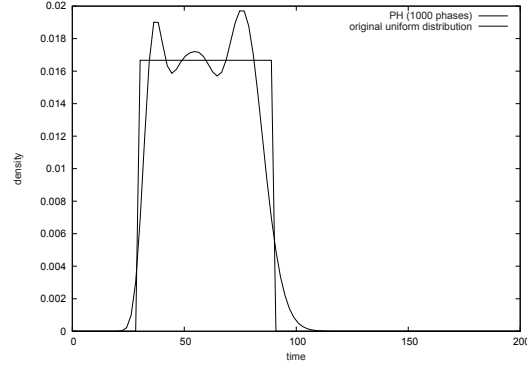
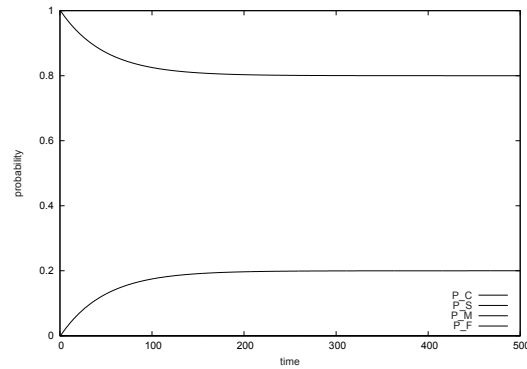
Figure 3.10: PH approximation for $F_{M,F}(t)$.

Figure 3.11: Transient state probabilities (Case 1).

the initial probability, are assigned to an equivalent value (Fig. 3.12).

Case 3: The probability vector just after the node becomes the failed state (Fig. 3.13).

The transient behavior of state probabilities strongly depends on the initial state probabilities. However, in all the results, the state probabilities converge to steady state probabilities after 200 to 300 seconds. Also, in Fig. 3.13, we find that the state suddenly changes in the range $t \in [30, 90]$. This is an evidence that the PH approximates the original uniform distribution very well.

Finally, Fig. 3.14 depicts the upper and lower bounds of network survivability in Poisson model by substituting the transient state probabilities in Case 1.

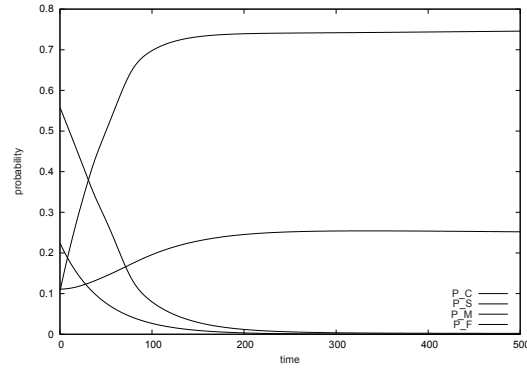


Figure 3.12: Transient state probabilities (Case 2).

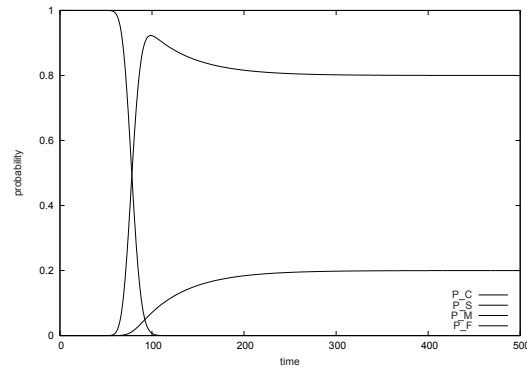


Figure 3.13: Transient state probabilities (Case 3).

Since the initial probability vector of Case 1 indicates that node is cooperative with probability 1, the network survivability also becomes high. However, the network survivability gradually decreases as time elapses, because the probability that the node is in selfish state increases. Similar to the node probability, the network survivability almost converges to the steady state after 200–300 seconds. This means that, even if any accident occurs in the network, the network connectivity becomes stable 200–300 seconds later after the recovery is finished. Such an analysis leads to another network survivability discussed in [5].

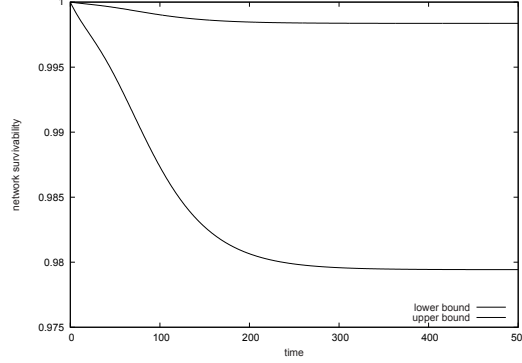


Figure 3.14: Transient 1-connected network survivability (Case 1).

3.5 APPENDIX 1

The uniformization approach is effective to compute the matrix exponential in the Markov analysis [42, 43]. Let $\gamma_{F,L}(v)$ and $\gamma_{L,F}(v)$ be the p.m.f.'s of mixed Poisson distribution with mixture probabilities $F_{F,L}(t)$ and $F_{L,F}(t)$, respectively:

$$\gamma_{F,L}(v) = \int_0^\infty e^{-q_F u} \frac{(q_F u)^v}{v!} dF_{F,L}(u), \quad (3.59)$$

$$\gamma_{L,F}(v) = \int_0^\infty e^{-q_L u} \frac{(q_L u)^v}{v!} dF_{L,F}(u), \quad (3.60)$$

where q_F and q_L are maximum values of absolute diagonal elements of \mathbf{Q}_F and \mathbf{Q}_L . Using the p.m.f.'s, the matrix exponential form can be rewritten by

$$\begin{aligned} \tilde{\mathbf{Q}}_F &= \sum_{v=0}^{\infty} \gamma_F(v) (\mathbf{I} + \mathbf{Q}_F/q_F)^v, \\ \tilde{\mathbf{Q}}_L &= \sum_{v=0}^{\infty} \gamma_L(v) (\mathbf{I} + \mathbf{Q}_L/q_L)^v, \end{aligned} \quad (3.61)$$

$$\boldsymbol{\xi}_F = \frac{1}{q_F} \sum_{v=0}^{\infty} \sum_{s=0}^v \gamma_F(v) \boldsymbol{\pi}_F^{EMC} (\mathbf{I} + \mathbf{Q}_F/q_F)^v, \quad (3.62)$$

$$\boldsymbol{\xi}_L = \frac{1}{q_L} \sum_{v=0}^{\infty} \sum_{s=0}^v \gamma_L(v) \boldsymbol{\pi}_L^{EMC} (\mathbf{I} + \mathbf{Q}_L/q_L)^v. \quad (3.63)$$

The infinite sums may be truncated by left truncation point L and right truncation point R such that

$$\sum_{v=L}^R \gamma_F(v) \geq 1 - \epsilon, \quad \sum_{v=L}^R \gamma_L(v) \geq 1 - \epsilon, \quad (3.64)$$

where ϵ is a tolerance error.

3.6 APPENDIX 2

This chapter utilizes the method to generate the weighted samples based on the double exponential (DE) formula [44]. This approach provides more accurate approximation to many types of integral functions, compared to trapezoidal rule, Simpson's rule, etc. The DE formula changes the original integration to an infinite integration of the function which decays according to double exponential function. Here we use the following function

$$\phi(x) = \exp\left(\frac{\pi}{2} \sinh(x)\right). \quad (3.65)$$

By substituting the above function to $\int_0^\infty f(t) \log g(t) dt$, the integration is transformed to

$$\int_0^\infty f(t) \log g(t) dt = \int_{-\infty}^\infty f(\phi(x)) \log g(\phi(x)) \phi'(x) dx, \quad (3.66)$$

where $\phi'(x)$ is the first derivative of $\phi(x)$. Applying the trapezoidal rule to the above integration, we have

$$\begin{aligned} & \int_{-\infty}^\infty f(\phi(x)) \log g(\phi(x)) \phi'(x) dx \\ & \approx \sum_{i=K^-}^{K^+} h \phi'(ih) f(\phi(ih)) \log g(\phi(ih)), \end{aligned} \quad (3.67)$$

where h is a step size and $K^+ (= -K^-)$ is a upper (lower) limit of discretization points. In fact, the accuracy of integration can be controlled by the parameters h and K^+ . That is, given h and K^+ , we generate the weighted samples $(t_1, w_1), \dots, (t_K, w_K)$ as follows

$$t_{i-K^-+1} = \phi(ih) \quad (3.68)$$

$$w_{i-K^-+1} = h \phi'(ih) f(\phi(ih)), \quad (3.69)$$

$$i = K^-, \dots, 0, \dots, K^+,$$

where $K = K^+ - K^- + 1$.

Chapter 4

Survivability Analysis for Power-Aware MANETs with Battery Charge

Network survivability is an attribute that network is continually available even if a communication failure occurs, and is regarded as one of the most important concepts to design dependable computer networks. In the existing work, a power-aware MANET is described by an MRGP, and takes account of the variability in power level, which is caused by the possible low-battery state in each communication node. However, it implicitly ignores effects by the so-called border effects, and lacks the reality in modeling. In this chapter, we revisit a power-aware MANET model taking account of border effects and quantify the network survivability more accurately.

4.1 Model Description

4.1.1 Node Classification

Since nodes in MANETs cooperate with the routing processes to maintain network connectivity, each of nodes is designed as it behaves autonomously, but its discipline to require, send and receive the route information, is defined as a strict protocol. At the same time, it is also important to define the protocol in order to prevent propagation of the erroneous route information caused by malicious attacks. Xing and Wang [12] consider a MANET that suffers such a malicious attack, whose node states are defined as follows:

- Cooperative state (C): a node complies with all routing and forwarding rules.
- Selfish state (S): a node may not forward control or data packets for others for the sake of power saving.
- Malicious state (M): a node launches Jellyfish or Black hole DoS attack.
 - Jellyfish state (J): a node being cooperative in the routing stage reluctant in forwarding data packets.
 - Blackhole state (B): a node disrupting legitimate path selections by broadcasting fakes route replies.
- Failed state (F): a node is unable to initiate or response route discoveries.

Moreover, each node may be classified into the following states in terms of the battery state:

- Fully charged battery state (H): the battery is fully charged.
- Low battery state (L): the battery level is low and may cause a failure due to out of power.

It is essential to characterize the power state in power-aware device. The modeling approach in Chapter 3 can be considered an incremental in technique but significant extension in reality. For common DoS attacks, the node in Jellyfish attack receives route requests and route replies. The main mechanism of Jellyfish state is to delay packets without any reason. On the other hand, the node in Blackhole attack can respond a node with a fake message immediately by declaring as it is in the optimal path or as it is only one-hop away to other nodes.

Suppose that each of states, $i = C, S, M$, has one of two sub-states; H and L . For instance, iH means a node in the state i with high energy level and iL means a node in the state i with low energy level. The failed state F also has one of two sub-states; energy exhaustion (EF) and DoS attack detection (DF).

4.1.2 Semi-Markov Node Model

Based on the above node classification, we consider a semi-Markov model to describe the stochastic behavior of a node by combining the network state and the battery state. We define the node behavior as follows:

- A Cooperative node (CH or CL) may become a Malicious node (MH or ML) when it launches DoS attack, and a low-battery Cooperative node (CL) may become a Failed node due to energy exhaustion (EF).
- A Cooperative node (CH or CL) may become a Selfish node (SH or SL) for saving the power.
- A Malicious (MH or ML) node cannot become a Cooperative node (CH or CL) again, but may become a Failed node by two reasons: energy exhaustion (EF) and DoS attack detection (DF).
- A node in Failed state (DF or EF) may become a Cooperative node (CH) again after it repairs and responds to routing requests for others.
- Each node may become the low battery state as operating time passes, but may become fully-charged battery state from the low battery state again by re-charge.

From above assumptions, we can define the state space $\mathcal{S} \in \{CH, CL, SH, SL, MH, ML, EF, DF\}$, and the time-dependent transition rates from state i to state j ($i, j \in \mathcal{S}$) by $\lambda_{i,j}(t)$.

Similar to the original idea by Xing and Wang [12], we describe the transition behavior of each node, by a stochastic process $\{Z(t), t \geq 0\}$, associated with the space \mathcal{S} . Let X_n denote the state at transition time t_n . Define

$$\begin{aligned} & \Pr(X_{n+1} = x_{n+1} | X_0 = x_0, \dots, X_n = x_n) \\ &= \Pr(X_{n+1} = x_{n+1} | X_n = x_n), \end{aligned} \quad (4.1)$$

where $x_i \in \mathcal{S}$ for $0 \leq i \leq n+1$. From Eq. (4.1), the stochastic process $\{X_n, n = 0, 1, 2, \dots\}$ constitutes a CTMC with state space \mathcal{S} , when all the transition times are exponentially distributed. However, since the transition time from one state to another state is subject to the time-inhomogeneous behavior of a node,

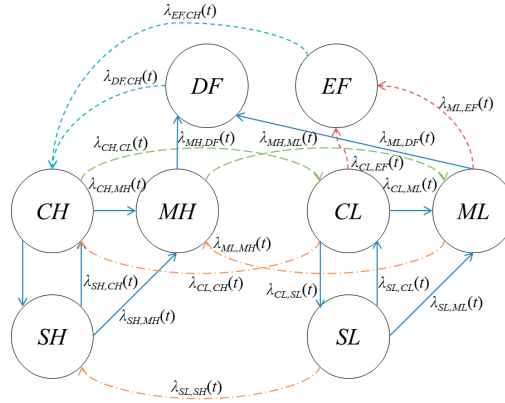


Figure 4.1: State transition diagram.

it is not realistic to characterize all the transition times by only exponentially distributed random variables. For instance, if a sensor node is more inclined to fail due to energy consumption as the operating time passes, and the less residual energy is left, then the more likely a sensor changes its behavior to selfish. This implies that the future action of a node may depend on how long it has been in the current state and that the transition time intervals should obey arbitrary probability distributions.

From the above reasons it is common to assume a SMP for $\{Z(t), t \geq 0\}$ to describe the node behavior transitions, which is defined by

$$Z(t) = X_n, \forall t_n \leq t \leq t_{n+1}. \quad (4.2)$$

Letting $T_n = t_{n+1} - t_n$ be the sojourn time between the n -th and $(n+1)$ -st transitions, we define the associated SMP kernel $\mathbf{Q} = (Q_{ij}(t))$ by

$$Q_{ij}(t) = \Pr(X_{n+1} = j, T_n \leq t | X_n = i) = p_{ij} F_{ij}(t), \quad (4.3)$$

where $p_{ij} = \lim_{t \rightarrow \infty} Q_{ij}(t)$ is the transition probability between state i and j ($i, j = ch, cl, sh, sl, mh, ml, ef, df$) corresponding to \mathcal{S} , and $F_{ij}(t) = \Pr(T_n < t | X_{n+1} = j, X_n = i)$ is the transition time distribution from state i to j . Figure 4.1 illustrates the transition diagram of the homogeneous SMP, $\{Z(t), t \geq 0\}$, under consideration, which is somewhat different from the MRGP in [16]. By using the Laplace-Stieltjes transform (LST) we can obtain analytically the steady-state probability of each node (see Appendix in this chapter).

4.2 Quantitative Network Survivability

4.2.1 Network Survivability Measures

In a MANET, the transmission of a packet from one node to another node must go through any path which is made by its neighbor nodes. Since the topology of a MANET keeps changing dynamically due to many reasons, such as node mobility, even when node failures or DoS attacks do not occur, it is difficult to clarify the connected topology for the MANET. Since the communication availability of a MANET depends on the existing paths between two nodes, it is intuitively understood that the network survivability strongly depends on the connectivity. In general, it is said that the MANET is *k-connected*, if there are at least k disjoint communication paths connecting one node to the other node. When $k = 1$, it means the probability that there is at least one communication path connecting one node to the other node, and is equivalent to the *network reliability*. Hence, thinking of higher network survivability is reduced to highly dependable MANET design.

Given a MANET \mathcal{M} , let $\kappa(\mathcal{M})$ denote the vertex-connectivity of \mathcal{M} . Based on the definition of connectivity, the network survivability of \mathcal{M} , denoted by $NS_k(\mathcal{M})$, is defined as the probability that all active (survived) nodes are k -connected [12], *i.e.*,

$$NS_k(\mathcal{M}) = \Pr(\kappa(\mathcal{M}_a) = k), \quad (4.4)$$

where \mathcal{M}_a is a sub-network of \mathcal{M} and includes all active nodes of \mathcal{M} . In the above definition, we need to find all the possible paths between arbitrary node pairs in a MANET. Unfortunately, it is very difficult to enumerate all the communication paths between arbitrary two nodes especially in a large-scaled MANET. For this state-explosion problem, we employ an approximate method to derive the network survivability. For a geometric graph \mathcal{G} with N vertices, define the minimum node degree as the minimum number of neighbor nodes of one node in \mathcal{G} by $\delta(\mathcal{G})$ and vertex-connectivity of \mathcal{G} by $\kappa(\mathcal{G})$, respectively. It turns out that $\kappa(\mathcal{G}) \leq \delta(\mathcal{G})$, *i.e.*, the network connectivity is no longer greater than the minimum number of neighbors of any node. When N is sufficiently large, the probability that \mathcal{G} is k -connected approximately equals to the probability

that every vertex has at least k neighbors. So, it is immediate to see that

$$\Pr(\kappa(\mathcal{G}) = k) \approx \Pr(\delta(\mathcal{G}) \geq k). \quad (4.5)$$

However, it should be noted that every neighbor does not always provide effective outgoing paths, because only the cooperative neighbor can transmit a packet for other node. Hence, a necessary condition for a MANET to be k -connected is that every node has at least k cooperative degree. Let $\theta(\mathcal{M})$ denote the minimum of the cooperative degree of all nodes in a MANET \mathcal{M} . Then, we have

$$\Pr(\kappa(\mathcal{M}) = k) \approx \Pr(\theta(\mathcal{M}) \geq k). \quad (4.6)$$

Remind that the network survivability is defined as the probability that all active nodes are k -connected to \mathcal{M} , so that the quantitative survivability of \mathcal{M} can be given by

$$NS_k(\mathcal{M}) \approx \Pr(\theta(\mathcal{M}_a) \geq k). \quad (4.7)$$

An immediate effect of node misbehaviors and failures in MANETs is the node isolation problem [12]. It is a direct cause for network partitioning, and eventually affects the network survivability. The node isolation problem is caused by four types of neighbor; Failed, Selfish, Jellyfish and Blackhole nodes. If all the neighbors of a node are Failed nodes, Selfish nodes or Jellyfish nodes, then it can no longer communicate with other nodes. On the other hand, if one of neighbors is Blackhole, it gives the other node a faked one-hope path, and can always shutdown the communication. In this case, it is said that the node is isolated by the Blackhole neighbor. Furthermore, if there exists a Blackhole node, then the minimum cooperative degree $\theta(\mathcal{M}_a)$ of network \mathcal{M}_a becomes 0, and the network survivability is always reduced to 0.

To formulate the above isolation problem, we define the node degree $D_{(u)}$ for node u by the maximum number of neighbors [13]. Let $D_{(i,u)}$ be the number of node u 's neighbors at state $i \in \{c, s, j, b, f\}$ corresponding to $\{C, S, J, B, F\}$. Then the isolation problem in our model can be formulated as follows: Given node u with degree d , *i.e.*, $D_{(u)} = d$, if $D_{(s,u)} + D_{(f,u)} + D_{(j,u)} = d$ or $D_{(b,u)} \geq 1$, the cooperative degree is zero, *i.e.*, $D_{(c,u)} = 0$, and u is isolated from the network,

so it holds that

$$\Pr(D_{(c,u)} = 0 | D_{(u)} = d) = 1 - (1 - P_b)^d + (1 - P_c - P_b)^d, \quad (4.8)$$

where P_c is the steady-state probability of a node in a Cooperative state and P_b is the steady-state probability of a node launching Blackhole attacks. In Appendix, we give the steady-state probability in our SMP model.

Hereafter, a node is said to be k -connected to a network if its associated cooperative degree is given by k (≥ 1). Given node u with degree d , *i.e.*, $D_{(u)} = d$, u is said to be k -connected to the network if the cooperative degree is k , *i.e.* $D_{(c,u)} = k$, which holds only if u has no Blackhole neighbor and has exactly k Cooperative neighbors, *i.e.*, $D_{(b,u)} = 0$ and $D_{(c,u)} = k$, respectively. Then it is straightforward to see that

$$\Pr(D_{(c,u)} = k | D_{(u)} = d) = \binom{d}{k} (P_c)^k (1 - P_c - P_b)^{d-k}. \quad (4.9)$$

Strictly speaking, it is still difficult to find the probability distribution of $\theta(\mathcal{M}_a) \geq k$ in Eq. (4.7). Xing and Wang [12] derive approximately the low and upper bounds of network survivability instead when the number of nodes is sufficiently large by considering the network connectivity of a node in a MANET. The upper and lower bounds of network survivability are given by

$$NS_k(\mathcal{M})_U = (\Pr(D_{(c,u)} \geq k))^{N_D}, \quad (4.10)$$

$$NS_k(\mathcal{M})_L = \max(0, 1 - E[N_a](\Pr(D_{(c,u)} < k))), \quad (4.11)$$

respectively, where u is an arbitrary node index in the active network \mathcal{M}_a . In Eq. (4.11), $E[N_a] = \lfloor N(1 - P_f) \rfloor$ is the expected number of active nodes in the network, where $\lfloor x \rfloor$ is the maximum integer less than x , P_f is the steady-state probability of a Failed node, and N denotes the total number of mobile nodes. In Eq. (4.10), N_D is the number of node points whose transmission ranges are mutually disjoint over the MANET area. Let A and r be the area of MANET and the node transmission radius, respectively. The number of disjoint points is given by $N_D = \lfloor N/(\lambda\pi r^2) \rfloor$, where $\lambda = N/A$ is the node density.

Next, we give an approximate form of the network survivability based on the expected number of active nodes [15]. Getting help from the graph theory, the expected network survivability is approximately given by the probability that

the active node in the network is k -connected:

$$NS_k(\mathcal{M})_E \approx \{1 - \Pr(D_{(c,u)} < k)\}^{E[N_a]}. \quad (4.12)$$

By the well-known total probability law, we have

$$\Pr(D_{(c,u)} < k) = \sum_{d=k}^N \Pr(D_{(c,u)} < k | D_{(u)} = d) \Pr(D_{(u)} = d), \quad (4.13)$$

so that we need to find the explicit forms of $\Pr(D_{(c,u)} < k | D_{(u)} = d)$ and $\Pr(D_{(u)} = d)$. From Eqs. (4.8) and (4.9), it is easy to obtain

$$\begin{aligned} & \Pr(D_{(c,u)} < k | D_{(u)} = d) \\ &= 1 - (1 - P_b)^d + \sum_{m=0}^{k-1} \binom{d}{m} P_c^m (1 - P_c - P_b)^{d-m} \\ &= 1 - (1 - P_b)^d + \sum_{m=0}^{k-1} B_m(d, P_c, 1 - P_c - P_b), \end{aligned} \quad (4.14)$$

where B_m denotes the multinomial probability mass function.

Since the node distribution $\Pr(D_{(u)} = d)$ strongly depends on the model property, we introduce three specific stochastic models [15] in the following:

(i) *Poisson Model* [12]

Suppose that N mobile nodes in a MANET are uniformly distributed over a 2-dimensional square with area A . The node transmission radius, denoted by r , is assumed to be identical for all nodes. To derive the node degree distribution $\Pr(D_{(u)} = d)$, we divide the area into N small grids virtually, so that the grid size has the same order as the physical size of a node. Consider the case where the network area is much larger than the physical node size. Then, the probability that a node occupies a specific grid, denoted by p , is very small. With large N and small p , the node distribution can be modeled by the Poisson distribution:

$$\Pr(D_{(u)} = d) = \frac{\mu^d}{d!} e^{-\mu}, \quad (4.15)$$

where $\mu = \rho\pi r^2$, and $\rho = E[N_a]/A$ is the node density depending on the underlying model. Finally, substituting Eqs. (4.13)-(4.15) into Eqs. (4.10)-(4.12)

yields

$$NS_k(\mathcal{M})_U^P = \left\{ e^{-\mu P_b} \left[1 - \frac{(k, \mu P_c)}{(k)} \right] \right\}^{N_D}, \quad (4.16)$$

$$NS_k(\mathcal{M})_L^P = 1 - E[N_a] \left(1 - \left\{ e^{-\mu P_b} \left[1 - \frac{(k, \mu P_c)}{(k)} \right] \right\} \right), \quad (4.17)$$

$$NS_k(\mathcal{M})_E^P = \left\{ e^{-\mu P_b} \left[1 - \frac{(k, \mu P_c)}{(k)} \right] \right\}^{E[N_a]}, \quad (4.18)$$

where $(x) = (x-1)!$ and $(h, x) = (h-1)! e^{-x} \sum_{l=0}^{h-1} x^l / l!$ are the complete and incomplete gamma functions, respectively.

(ii) *Binomial Model* [15]

It is evident that the Poisson model just focuses on an ideal situation of mobile nodes. In other words, it is not always easy to measure the physical parameters such as r and A in practice. Let p denote the probability that each node is assigned into a communicate network area of a node. For the expected number of activate nodes $E[N_a]$, we describe the node distribution by the binomial distribution:

$$\begin{aligned} \Pr(D_{(u)} = d) &= \binom{E[N_a]}{d} p^d (1-p)^{E[N_a]-d} \\ &= B_d(E[N_a], p), \end{aligned} \quad (4.19)$$

where B_d is the binomial probability mass function. Substituting Eq. (4.19) into Eqs. (4.10)-(4.12) yields alternative formulas of the network survivability:

$$NS_k(\mathcal{M})_U^B = \left\{ \sum_{k=0}^{E[N_a]} B_d(E[N_a], p) \left[(1-P_b)^d \sum_{m=0}^{k-1} B_m(d, P_c, 1-P_c, P_b) \right] \right\}^{E[N_D]}, \quad (4.20)$$

$$NS_k(\mathcal{M})_L^B = 1 - E[N_a] \left(1 - \left\{ \sum_{k=0}^{E[N_a]} B_d(E[N_a], p) \left[(1-P_b)^d \sum_{m=0}^{k-1} B_m(d, P_c, 1-P_c, P_b) \right] \right\} \right), \quad (4.21)$$

$$NS_k(\mathcal{M})_E^B = \left\{ \sum_{k=0}^{E[N_a]} B_d(E[N_a], p) \left[(1 - P_b)^d \sum_{m=0}^{k-1} B_m(d, P_c, 1 - P_c - P_b) \right] \right\}^{E[N_a]}. \quad (4.22)$$

If each node is assigned into a communication network area of a node with probability $p = \pi r^2/A$, then the corresponding binomial model results a different survivability measure.

(iii) *Negative Binomial Model* [15]

The negative binomial model comes from a mixed Poisson distribution instead of Poisson distribution. Let $f(\mu)$ be the distribution of parameter μ in the Poisson model. This implicitly assumes that the parameter μ includes uncertainty, and that the node distributions for all disjoint areas have different Poisson parameters. Then the node distribution can be represented by the following mixed Poisson distribution:

$$P(D_{(u)} = d) = \int_0^\infty e^{-\mu} \frac{\mu^d}{d!} f(\mu) d\mu. \quad (4.23)$$

For the sake of analytical simplicity, let $f(\mu)$ be the gamma probability density function with mean $\pi r^2 N(1 - P_f)/A$ and coefficient of variation c . Then we have

$$P(D_{(u)} = d) = \frac{(a+d)}{d!} \left(\frac{b}{a} \right)^a \left(\frac{1}{1+b} \right)^d = \lambda_d(a, b), \quad (4.24)$$

where $a = \lfloor 1/c^2 \rfloor$ and $b = \lfloor A/(\pi r^2 N(1 - P_f)c^2) \rfloor$. It should be noted that Eq. (4.24) corresponds to the negative binomial probability mass function with mean $\pi r^2 N(1 - P_f)/A$, and that the variance is greater than that in the Poisson model. From Eq. (4.24), we can obtain alternative representations of the

network survivability with an additional model parameter c .

$$NS_k(\mathcal{M})_U^{NB} = \left\{ \sum_{k=0}^{E[N_a]} \lambda_d(a, b) \left[(1 - P_b)^d \sum_{m=0}^{k-1} B_m(d, P_c, 1 - P_c - P_b) \right] \right\}^{E[N_D]}, \quad (4.25)$$

$$NS_k(\mathcal{M})_L^{NB} = 1 - E[N_a] \left(1 - \left\{ \sum_{k=0}^{E[N_a]} \lambda_d(a, b) \left[(1 - P_b)^d \sum_{m=0}^{k-1} B_m(d, P_c, 1 - P_c - P_b) \right] \right\} \right), \quad (4.26)$$

$$NS_k(\mathcal{M})_E^{NB} = \left\{ \sum_{k=0}^{E[N_a]} \lambda_d(a, b) \left[(1 - P_b)^d \sum_{m=0}^{k-1} B_m(d, P_c, 1 - P_c - P_b) \right] \right\}^{E[N_a]}. \quad (4.27)$$

4.3 Border Effects of Network Communication Area

The results on network survivability presented in Section 4.2 are based on a non-informative assumption that network area A has a node density $\rho = E[N_a]/A$. This means that the expected number of neighbors of a node in a MANET has the same value as $\rho\pi r^2$. In other words, such an assumption is not realistic in real world network communication circumstance. It is well recognized that the border effects tend to decrease both the communication coverage and the node degree of a node, which reflect the whole network availability. Laranjeira and Rodrigues [17] show that the relative average node degree for nodes in borders is independent of the node transmission range and of the overall network node density in a square communication area. Bettsetetter [18] calculates the average node degree for nodes in borders for a circular communication area. We apply their results directly to revisit the network survivability measures in Eqs. (4.10)-(4.12).

Given a square area of side L , the expected number of neighbors of a node in a MANET is given by [17]:

$$\mu_s = \frac{\rho\pi r^2\sigma}{L^2}, \quad (4.28)$$

where $\sigma = (L - 2r)^2 + 3.07492r(L - 2r) + 2.461344r^2$. For the circular area A with radius R , Bettsetttter [18] obtains the expected node degree of a node μ_c in a circular communicate area:

$$\mu_c = \frac{N_a}{2\pi} \left[4(1 - \hat{r}^2) \arcsin \frac{\hat{r}}{2} + 2\hat{r}^2\pi - (2\hat{r} + \hat{r}^3) \sqrt{1 - \frac{\hat{r}^2}{4}} \right], \quad (4.29)$$

where $\hat{r} = r/R$. The above formula can be further simplified by using Taylor series as

$$\mu_c \approx N_a \hat{r}^2 \left(1 - \frac{4\hat{r}}{3\pi} \right). \quad (4.30)$$

By replacing the square border effect parameter μ in Eqs. (4.16)-(4.18), (4.20)-(4.22), and (4.24)-(4.26) by μ_s in Eq. (4.28), we obtain the improved network survivability measures taking account of square border effects. Also, using μ_c in Eq. (4.30), we derive the network survivability measures in a circular communicate area as well.

4.4 Numerical Examples

4.4.1 Comparison of Network Survivability

In our numerical experiments, we set model parameters as follows:

$$\begin{aligned} \lambda_{CH,CL}(t) &= \lambda_{MH,ML} = \text{Gamma}(t, 5, 1/600), \\ \lambda_{CH,MH}(t) &= \lambda_{CL,ML}(t) = \lambda_{SH,MH}(t) = \text{Exp}(t, 1/6e+7), \\ \lambda_{CH,SH}(t) &= \text{Exp}(t, 1/720.0), \quad \lambda_{CL,EF}(t) = \text{Gamma}(t, 2, 1/900), \\ \lambda_{CL,SL}(t) &= \lambda_{SH,CH}(t) = \text{Exp}(t, 1/180), \\ \lambda_{MH,DF}(t) &= \lambda_{ML,DF}(t) = \text{Exp}(t, 1/480), \\ \lambda_{SL,CL}(t) &= \text{Exp}(t, 1/360), \quad \lambda_{SL,ML}(t) = \text{Exp}(t, 1/6e+7), \\ \lambda_{DF,CH}(t) &= \text{Uniform}(t, 30, 120), \lambda_{EF,CH}(t) = \text{Uniform}(t, 30, 90), \\ p_B &= 0.1, \quad p_J = 0.9, \end{aligned}$$

where p_B and p_J are the Blackhole attack ratio and the Jellyfish attack ratio of DoS attack. Exp, Gamma and Uniform are exponential, gamma and uniform

p.d.f.'s :

$$\text{Exp}(t, x) = xe^{-xt}, \quad t \geq 0, \quad (4.31)$$

$$\text{Gamma}(t, a, b) = \frac{b^a t^{a-1} e^{-bt}}{(a)}, \quad t \geq 0, \quad (4.32)$$

$$\text{Uniform}(t, \min, \max) = \frac{1}{\max - \min}, \quad \min \leq t \leq \max. \quad (4.33)$$

To analyze the effect of battery re-charge, we consider three cases of transition time from low battery states (CL, SL, ML) to fully charged battery states (CH, SH, MH):

$$\text{Case (1)} : \lambda_{(iL),(iH)}(t) = \text{Gamma}(t, 2, 1/2400),$$

$$\text{Case (2)} : \lambda_{(iL),(iH)}(t) = \text{Exp}(t, 1/4800),$$

$$\text{Case (3)} : \lambda_{(iL),(iH)}(t) = 0, \quad i \in \{C, S, M\},$$

where $\lambda_{(iL),(iH)}(t) = 0$ in Case (3) denotes that there is no battery re-charge in the MANET.

Suppose the following network parameter:

- $A = 1000 \text{ (m)} \times 1000 \text{ (m)}$.

To compare several stochastic models with different combination; three node degree models (Poisson, binomial and negative binomial), the lower and upper bounds versus an approximate network survivability, existence of border effects, we consider Case 1, and change the transition radius from $r = 80$ to $r = 130$ and connectivity requirement from $k = 1$ to $k = 3$. The comparative results are shown in Table 4.1. From this table, we can see that the difference between three node degree models of network survivability is very small for the specific values of r and k . For example, when $r = 120$ and $k = 1$, the difference among three models are less than 0.0003 for the lower and upper bounds and the approximate network survivability. Then, we attempt to understand the differences among three node degree models with three battery charge cases. The results are shown in Table 4.2. From the table, we can see that these are the similar results to Table 4.1. The difference among three models is small and the battery charge case in Exp is higher than others when r is small.

Table 4.3 presents effects of communication range of a node r on k -connected ($k = 1, 2, 3$) network survivability in three cases in the approximate model

Table 4.1: Comparison of lower and upper bounds with approximate network survivability.

r	k	Poisson			Binomial			Negative Binomial		
		Lower	Appro	Upper	Lower	Appro	Upper	Lower	Appro	Upper
80	1	0.0000	0.2325	0.8648	0.0000	0.2402	0.8676	0.0000	0.2209	0.8604
	2	0.0000	0.0000	0.3679	0.0000	0.0001	0.3732	0.0000	0.0000	0.3588
	3	0.0000	0.0000	0.0278	0.0000	0.0000	0.0286	0.0000	0.0000	0.0261
90	1	0.6872	0.7313	0.9757	0.6994	0.7403	0.9766	0.6696	0.7186	0.9743
	2	0.0000	0.0746	0.8152	0.0000	0.0803	0.8200	0.0000	0.0667	0.8081
	3	0.0000	0.0000	0.4167	0.0000	0.0000	0.4239	0.0000	0.0000	0.4053
100	1	0.9397	0.9415	0.9962	0.9432	0.9448	0.9964	0.9349	0.9369	0.9959
	2	0.4433	0.5729	0.9651	0.4708	0.5889	0.9668	0.4044	0.5511	0.9627
	3	0.0000	0.0590	0.8350	0.0000	0.0657	0.8407	0.0000	0.0506	0.8268
110	1	0.9848	0.9850	0.9992	0.9856	0.9857	0.9992	0.9838	0.9839	0.9991
	2	0.8965	0.9016	0.9946	0.9041	0.9086	0.9950	0.8859	0.8921	0.9940
	3	0.4085	0.5533	0.9693	0.4459	0.5744	0.9712	0.3564	0.5252	0.9666
120	1	0.9905	0.9906	0.9996	0.9907	0.9907	0.9996	0.9903	0.9904	0.9996
	2	0.9776	0.9779	0.9990	0.9793	0.9795	0.9991	0.9753	0.9756	0.9989
	3	0.8929	0.8984	0.9953	0.9028	0.9073	0.9957	0.8793	0.8863	0.9947
130	1	0.9899	0.9900	0.9996	0.9900	0.9900	0.9996	0.9899	0.9899	0.9996
	2	0.9884	0.9884	0.9996	0.9887	0.9887	0.9996	0.9880	0.9880	0.9995
	3	0.9764	0.9767	0.9991	0.9785	0.9787	0.9992	0.9736	0.9740	0.9990

for a given $N = 500$, where “NONE” indicates $\lambda_{(iL),(iH)}(t) = 0$. We find that the network survivability increases as the communication range of a node r increases, and that the MANET with battery re-charge is more survivable. More specifically, when r is small (*e.g.* $r = 80$), the network survivability for Exp is higher than 68%, and the case with “NONE” is less than 16%. On the other hand, even when the mean transition time for Gamma is equal to that for Exp, there exists large difference on the network survivability for small r . However, when r is sufficiently large, the difference among Exp, Gamma and “NONE” is very small. Moreover, as connectivity requirement k increases, the survivability takes a lower level when r is small. This result means that the network survivability is more sensitive to battery re-charge with small r . In Table 4.4, we investigate the sensitivity of the total number of nodes N on the network survivability measures, where the transmission range r is fixed as 100. Note once again that $k = 1$ corresponds the network reliability. From this

Table 4.2: Comparison of three battery charge cases with approximate network survivability.

r	k	Poisson			Binomial			Negative Binomial		
		Gamma	EXP	NONE	Gamma	EXP	NONE	Gamma	EXP	NONE
80	1	0.2325	0.6869	0.1592	0.2402	0.6964	0.1653	0.2209	0.6732	0.1500
	2	0.0000	0.0468	0.0000	0.0001	0.0508	0.0000	0.0000	0.0413	0.0000
	3	0.0000	0.0000	0.0000	0.0000	0.0000	0.0000	0.0000	0.0000	0.0000
90	1	0.7313	0.9419	0.6587	0.7403	0.9453	0.6686	0.7186	0.9374	0.6445
	2	0.0746	0.5712	0.0348	0.0803	0.5872	0.0380	0.0667	0.5495	0.0305
	3	0.0000	0.0580	0.0000	0.0000	0.0646	0.0000	0.0000	0.0497	0.0000
100	1	0.9415	0.9875	0.9195	0.9448	0.9881	0.9237	0.9369	0.9866	0.9137
	2	0.5729	0.9182	0.4637	0.5889	0.9243	0.4799	0.5511	0.9100	0.4415
	3	0.0590	0.6098	0.0228	0.0657	0.6301	0.0259	0.0506	0.5827	0.0189
110	1	0.9850	0.9920	0.9807	0.9857	0.9921	0.9818	0.9839	0.9919	0.9792
	2	0.9016	0.9838	0.8599	0.9086	0.9850	0.8689	0.8921	0.9823	0.8477
	3	0.5533	0.9299	0.4282	0.5744	0.9366	0.4494	0.5252	0.9209	0.4001
120	1	0.9906	0.9911	0.9900	0.9907	0.9912	0.9902	0.9904	0.9911	0.9897
	2	0.9779	0.9904	0.9695	0.9795	0.9906	0.9719	0.9756	0.9902	0.9663
	3	0.8984	0.9845	0.8501	0.9073	0.9856	0.8620	0.8863	0.9829	0.8339
130	1	0.9900	0.9897	0.9900	0.9900	0.9897	0.9900	0.9899	0.9897	0.9899
	2	0.9884	0.9896	0.9873	0.9887	0.9896	0.9877	0.9880	0.9896	0.9866
	3	0.9767	0.9891	0.9675	0.9787	0.9893	0.9705	0.9740	0.9889	0.9633

result, it can be seen that when the number of nodes is greater than 500, the network reliability is higher than 90%. However, once the reliability attains the maximum value with $N = 700$, it decreases gradually as the number of nodes increases. Because of increasing number of nodes, it turns out that the network connectivity increases. However, from Table 4.4 with $k = 2, 3$, we come to know that the network survivability does not show the monotone tendency on N , similar to the network reliability. This is because the number of Blackhole nodes increases as the total number of nodes in the whole network increases.

In Table 4.5, we focus on the network reliability ($k = 1$) and compare the upper and lower bounds of network survivability in Eqs. (4.10) and (4.11) with our approximate formula in Eq. (4.12), where the number of nodes is $N = 500$ and the transmission range changes from $r = 80$ to $r = 130$. In this table, the values in ‘‘Square’’ and ‘‘Circular’’ are calculated based on Eqs. (4.28) and (4.30), respectively. From the result, we can see that the difference between lower and upper bounds of network reliability is rather remarkable for some

Table 4.3: Steady-state network survivability for varying node transmission radius r .

r	$k = 1$			$k = 2$			$k = 3$		
	Gamma	EXP	NONE	Gamma	EXP	NONE	Gamma	EXP	NONE
80	0.2328	0.6867	0.1595	0.0000	0.0467	0.0000	0.0000	0.0000	0.0000
85	0.5023	0.8596	0.4096	0.0054	0.2599	0.0014	0.0000	0.0019	0.0000
90	0.7315	0.9419	0.6589	0.0747	0.5711	0.0349	0.0000	0.0580	0.0000
95	0.8714	0.9754	0.8281	0.2927	0.8012	0.1938	0.0032	0.2946	0.0006
100	0.9415	0.9875	0.9196	0.5732	0.9182	0.4640	0.0592	0.6096	0.0229
105	0.9725	0.9912	0.9625	0.7847	0.9665	0.7081	0.2662	0.8261	0.1603
110	0.9850	0.9920	0.9807	0.9017	0.9838	0.8600	0.5536	0.9299	0.4285
115	0.9894	0.9917	0.9877	0.9558	0.9892	0.9362	0.7757	0.9706	0.6864
120	0.9906	0.9911	0.9900	0.9779	0.9904	0.9696	0.8985	0.9845	0.8502
125	0.9905	0.9904	0.9903	0.9860	0.9902	0.9827	0.9544	0.9885	0.9321
130	0.9900	0.9897	0.9900	0.9885	0.9896	0.9873	0.9767	0.9891	0.9675

specific values on r . For example, when $r = 80$, the difference between the lower and upper bounds with/without border effects are 0.8648 (Ignorance), 0.8016 (Square) and 0.8135 (Circular). On the other hand, the approximate network reliability always takes a value between lower and upper bounds. This result tells us that the approximate network reliability in Eq. (4.12) is more useful than the bounds for quantification of network reliability. Table 4.6 presents the dependence of the number of nodes N on the steady-state network reliability among three situations with/without border effects. From these results, it is shown that the network reliability without border effects (Ignorance) is higher than those with border effects (Square and Circular).

4.4.2 Transient Analysis of Network Survivability

Next we calculate the transient network survivability with the limiting probabilities $P_{ch,j}(t)$ ($j \in \{ch, cl, sh, sl, mh, ml, ef, df\}$) corresponding to \mathcal{S} , by taking the Laplace inversion of Eqs. (4.56)-(4.63) in Appendix. We apply the well-known Abate's algorithm [45] for the numerical inversion of Laplace transforms. Reminding these properties on transition probabilities, we set $N = 500$ and $r = 100$, and consider the transient network survivability at time t of three node degree models with lower and upper bounds and an approximate form. From Table 4.7, the transient network survivability has almost the same initial

Table 4.4: Steady-state network survivability for varying number of node N .

N	$k = 1$			$k = 2$			$k = 3$		
	Gamma	EXP	NONE	Gamma	EXP	NONE	Gamma	EXP	NONE
500	0.9415	0.9875	0.9196	0.5732	0.9182	0.4640	0.0592	0.6096	0.0229
550	0.9693	0.9903	0.9581	0.7617	0.9624	0.6789	0.2268	0.8065	0.1287
600	0.9812	0.9904	0.9756	0.8744	0.9795	0.8226	0.4652	0.9092	0.3351
650	0.9856	0.9894	0.9829	0.9335	0.9852	0.9043	0.6764	0.9554	0.5623
700	0.9865	0.9879	0.9853	0.9619	0.9864	0.9465	0.8185	0.9742	0.7393
750	0.9860	0.9862	0.9855	0.9745	0.9856	0.9667	0.8998	0.9808	0.8519
800	0.9846	0.9844	0.9845	0.9794	0.9842	0.9755	0.9421	0.9822	0.9152
850	0.9829	0.9824	0.9829	0.9806	0.9823	0.9787	0.9624	0.9816	0.9480
900	0.9810	0.9803	0.9811	0.9799	0.9802	0.9791	0.9712	0.9800	0.9638
950	0.9789	0.9780	0.9790	0.9784	0.9780	0.9781	0.9743	0.9779	0.9706
1000	0.9766	0.9757	0.9768	0.9764	0.9757	0.9764	0.9745	0.9757	0.9727

values, and the difference between them will be remarkable as time elapses.

Figure 4.2 illustrates the transient probability of cooperate state at time t . We can see that three cases have the similar values in the first 500 seconds and become different after that. Because three node degree models show the similar tendency, we focus on only the Poisson model to investigate the impact on transient network survivability here. We set the total number of nodes $N = 500$ and transmission radius $r = 100$. Then, we plot the transient network survivability of three battery charge cases; Gamma, Exp and No charge, with lower/upper bounds and approximate solution based on the behavior of the limiting probabilities at arbitrary time t , in Fig. 4.3, Fig. 4.4 and Fig. 4.5, respectively. From these figures, it can be seen clearly that the lower/upper bounds and approximate solution of network survivability have almost the same initial values, and the differences among them also becomes remarkable as time elapses. All three battery charge cases have a higher transient network survivability when connectivity requirement k is lower. When the k becomes higher ($k = 3$), the transient network survivability gets closer to 0.0624 (Gamma)/ 0.6096 (Exp)/ 0.026 (No Charge) with time t elapsing. Finally we compare the approximate solution of three battery charge cases in terms of the transient network survivability. Figure 4.6 depicts the transient network survivability by varying the connectivity requirement k . It is shown that if there is no battery charge, the transient

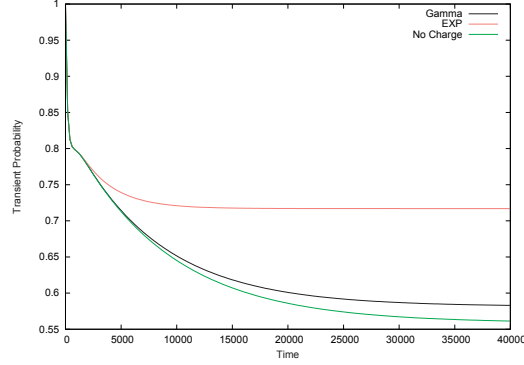


Figure 4.2: Transient probability of Cooperative state in three cases.

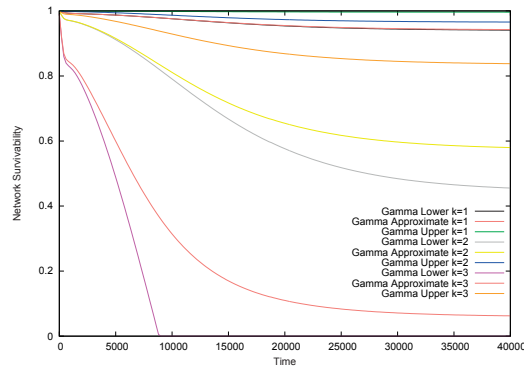


Figure 4.3: Transient network survivability of Gamma case.

network survivability drops down as the operation time goes on. However, the transient solution with battery charge (Exp) still keeps higher levels in the same situation. This fact implies that the battery charge of node leads to an better performance of MANETs.

4.5 Appendix

In this Appendix, we derive the steady-state probability of our SMP model. Let $1/\lambda_{ij}$ denote the mean transition time from state i to state j . Define the Laplace-Stieltjes transform (LST) by $q_{ij}(s) = \int_0^\infty \exp\{-st\}dQ_{ij}(t)$. From the

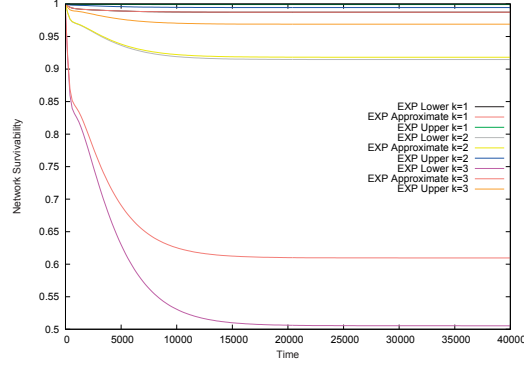


Figure 4.4: Transient network survivability of EXP case.

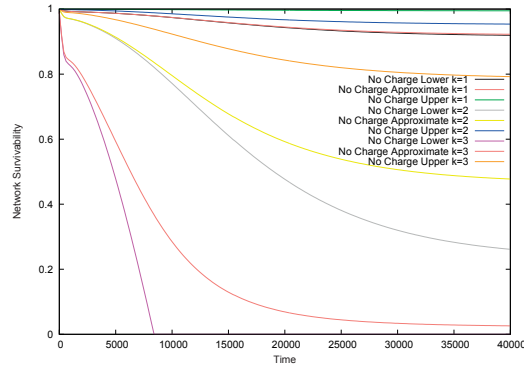


Figure 4.5: Transient network survivability of No Charge case.

familiar SMP analysis technique, it is immediate to see that

$$q_{ch,cl}(s) = \int_0^{\infty} \exp\{-st\} \bar{F}_{ch,mh}(t) \bar{F}_{ch,sg}(t) dF_{ch,cl}(t) \quad (4.34)$$

$$q_{ch,mh}(s) = \int_0^{\infty} \exp\{-st\} \bar{F}_{ch,cl}(t) \bar{F}_{ch,sh}(t) dF_{ch,mh}(t) \quad (4.35)$$

$$q_{ch,sh}(s) = \int_0^{\infty} \exp\{-st\} \bar{F}_{ch,cl}(t) \bar{F}_{ch,mh}(t) dF_{ch,sh}(t) \quad (4.36)$$

$$q_{cl,ch}(s) = \int_0^{\infty} \exp\{-st\} \bar{F}_{cl,mi}(t) \bar{F}_{cl,sl}(t) \bar{F}_{cl,ef}(t) dF_{cl,ch}(t) \quad (4.37)$$

$$q_{cl,mi}(s) = \int_0^{\infty} \exp\{-st\} \bar{F}_{cl,ch}(t) \bar{F}_{cl,sl}(t) \bar{F}_{cl,ef}(t) dF_{cl,mi}(t) \quad (4.38)$$

$$q_{cl,sl}(s) = \int_0^{\infty} \exp\{-st\} \bar{F}_{cl,ch}(t) \bar{F}_{cl,mi}(t) \bar{F}_{cl,ef}(t) dF_{cl,sl}(t) \quad (4.39)$$

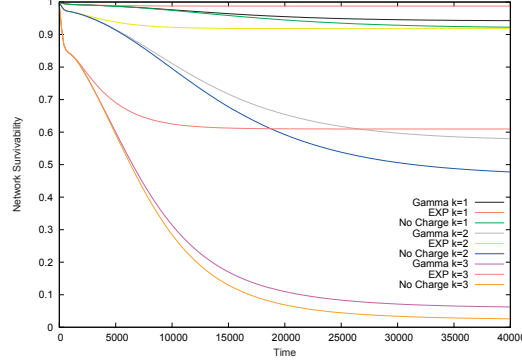


Figure 4.6: Comparison of Approximate transient network survivability.

$$q_{cl,ef}(s) = \int_0^{\infty} \exp\{ -st \} \bar{F}_{cl,ch}(t) \bar{F}_{cl,ml}(t) \bar{F}_{cl,sl}(t) dF_{cl,ef}(t) \quad (4.40)$$

$$q_{mh,ml}(s) = \int_0^{\infty} \exp\{ -st \} \bar{F}_{mh,df}(t) dF_{mh,ml}(t) \quad (4.41)$$

$$q_{mh,df}(s) = \int_0^{\infty} \exp\{ -st \} \bar{F}_{mh,ml}(t) dF_{mh,df}(t) \quad (4.42)$$

$$q_{ml,mh}(s) = \int_0^{\infty} \exp\{ -st \} \bar{F}_{ml,df}(t) \bar{F}_{ml,ef}(t) dF_{ml,mh}(t) \quad (4.43)$$

$$q_{ml,df}(s) = \int_0^{\infty} \exp\{ -st \} \bar{F}_{ml,mh}(t) \bar{F}_{ml,ef}(t) dF_{ml,df}(t) \quad (4.44)$$

$$q_{ml,ef}(s) = \int_0^{\infty} \exp\{ -st \} \bar{F}_{ml,mh}(t) \bar{F}_{ml,df}(t) dF_{ml,ef}(t) \quad (4.45)$$

$$q_{sh,ch}(s) = \int_0^{\infty} \exp\{ -st \} \bar{F}_{sh,mh}(t) dF_{sh,ch}(t) \quad (4.46)$$

$$q_{sh,mh}(s) = \int_0^{\infty} \exp\{ -st \} \bar{F}_{sh,ch}(t) dF_{sh,mh}(t) \quad (4.47)$$

$$q_{sl,sh}(s) = \int_0^{\infty} \exp\{ -st \} \bar{F}_{sl,cf}(t) \bar{F}_{sl,ml}(t) dF_{sl,sh}(t) \quad (4.48)$$

$$q_{sl,cl}(s) = \int_0^{\infty} \exp\{ -st \} \bar{F}_{sl,sh}(t) \bar{F}_{sl,ml}(t) dF_{sl,cl}(t) \quad (4.49)$$

$$q_{sl,ml}(s) = \int_0^{\infty} \exp\{ -st \} \bar{F}_{sl,sh}(t) \bar{F}_{sl,cl}(t) dF_{sl,ml}(t) \quad (4.50)$$

$$q_{df,ch}(s) = \int_0^{\infty} \exp\{ -st \} dF_{df,ch}(t) \quad (4.51)$$

$$q_{ef,ch}(s) = \int_0^{\infty} \exp\{ -st \} dF_{ef,ch}(t), \quad (4.52)$$

where in general $\bar{\psi}(\cdot) = 1 - \psi(\cdot)$. We also define the recurrent time distribution from state CH to state CH and its LST by $H_{ch,ch}(t)$ and $h_{ch,ch}(s)$, respectively.

Then, from the one-step transition probabilities from Eqs. (4.34)-(4.52), we have

$$\begin{aligned}
h_{ch,ch}(s) &= \int_0^\infty \exp\{-st\} dH_{ch,ch}(t) \\
&= q_{ch,cl}(s)[q_{cl,ch}(s) + q_{cl,ml}(s)(q_{ml,mh}(s)q_{mh,df}(s) \\
&\quad \times q_{df,ch}(s) + q_{ml,df}(s)q_{df,ch}(s) + q_{ml,ef}(s) \\
&\quad \times q_{ef,ch}(s))/k(s)] + q_{cl,sl}(s)[q_{sl,sh}(s)(q_{sh,ch}(s) \\
&\quad + q_{sh,mh}(s)(q_{mh,df}(s)q_{df,ch}(s) + q_{mh,ml}(s) \\
&\quad \times (q_{ml,df}(s)q_{df,ch}(s) + q_{ml,ef}(s)q_{ef,ch}(s)))/k(s)] \\
&\quad + q_{sl,ml}(s)(q_{ml,mh}(s)q_{mh,df}(s)q_{df,ch}(s) \\
&\quad + q_{ml,df}(s)q_{df,ch}(s) + q_{ml,ef}(s)q_{ef,ch}(s))/k(s)] \\
&\quad + q_{cl,ef}(s)q_{ef,ch}(s)/l(s) + q_{ch,mh}(s)[q_{mh,ml}(s) \\
&\quad \times (q_{ml,df}(s)q_{df,ch}(s) + q_{ml,ef}(s)q_{ef,ch}(s)) \\
&\quad + q_{mh,df}(s)q_{df,ch}(s)]/k(s) + q_{ch,sh}(s)[q_{sh,ch}(s) \\
&\quad + q_{sh,mh}(s)(q_{mh,ml}(s)(q_{ml,df}(s)q_{df,ch}(s) \\
&\quad + q_{ml,ef}(s)q_{ef,ch}(s)) + q_{mh,df}(s)q_{df,ch}(s)]/k(s)],
\end{aligned} \tag{4.53}$$

where

$$l(s) = 1 - q_{cl,sl}(s)q_{sl,cl}(s) \tag{4.54}$$

$$k(s) = 1 - q_{mh,ml}(s)q_{ml,mh}(s). \tag{4.55}$$

Let $P_{ch,i}(t)$ denote the transition probability from the initial state CH to respective states $i \in \{ch, cl, sh, sl, mh, ml, ef, df\}$ corresponding to \mathcal{S} . Then, the LSTs of the transition probability, $p_{ch,i} = \int_0^\infty \exp\{-st\} dP_{ch,i}(t)$, are given by

$$p_{ch,ch}(s) = \left\{ \bar{q}_{ch,mh}(s) \quad q_{ch,sh}(s) \quad q_{ch,cl}(s) \right\} / \bar{h}_{ch,ch}(s) \tag{4.56}$$

$$\begin{aligned}
p_{ch,cl}(s) &= q_{ch,cl}(s) \left\{ \bar{q}_{cl,ch}(s) \quad q_{cl,ml}(s) \quad q_{cl,sl}(s) \right. \\
&\quad \left. q_{cl,ef}(s) \right\} / \left\{ \bar{h}_{ch,ch}(s) k(s) \right\}
\end{aligned} \tag{4.57}$$

$$\begin{aligned}
p_{ch,sh}(s) &= \left\{ q_{ch,sh}(s) + q_{ch,cl}(s)q_{cl,sl}(s)q_{sl,sh}(s)/l(s) \right\} \\
&\quad \times \left\{ \bar{q}_{sh,mh}(s) \quad q_{sh,ch}(s) \right\} / \bar{h}_{ch,ch}(s)
\end{aligned} \tag{4.58}$$

$$p_{ch,sl}(s) = \left\{ q_{ch,cl}(s)q_{cl,sl}(s)/l(s) \right\} \left\{ \bar{q}_{sl,cl}(s) \quad q_{sl,sh}(s) \quad q_{sl,ml}(s) \right\} / \bar{h}_{ch,ch}(s) \quad (4.59)$$

$$p_{ch,ml}(s) = \left\{ q_{ch,mh}(s)q_{mh,ml}(s) + q_{ch,sh}(s)q_{sh,mh}(s) \right. \\ \times q_{mh,ml}(s) + q_{ch,cl}(s) [q_{cl,ml}(s) + q_{cl,sl}(s) \\ \times [q_{sl,ml}(s) + q_{sl,sh}(s)q_{sh,mh}(s)q_{mh,ml}(s)]] \\ \left. / l(s) \right\} \left\{ \bar{q}_{ml,mh}(s) \quad q_{ml,df}(s) \quad q_{ml,ef}(s) \right\} / \left\{ \bar{h}_{ch,ch}(s)k(s) \right\} \quad (4.60)$$

$$p_{ch,mh}(s) = \left\{ q_{ch,mh}(s) + q_{ch,sh}(s)q_{sh,mh}(s) + q_{ch,cl}(s) \right. \\ \times [q_{cl,ml}(s)q_{ml,mh}(s) + q_{cl,sl}(s)[q_{sl,ml}(s) \\ \times q_{ml,mh}(s) + q_{sl,sh}(s)q_{sh,mh}(s)]] / l(s) \left. \right\} \\ \times \left\{ \bar{q}_{mh,ml}(s) \quad q_{mh,df}(s) \right\} / \left\{ \bar{h}_{ch,ch}(s)k(s) \right\}. \quad (4.61)$$

$$p_{ch,df}(s) = \left\{ q_{ch,cl}(s) [q_{cl,ml}(s)(q_{ml,mh}(s)q_{mh,df}(s) \right. \\ + q_{ml,df}(s)) + q_{cl,sl}(s)[q_{sl,sh}(s)q_{sh,mh}(s) \\ \times [q_{mh,df}(s) + q_{mh,ml}(s)q_{ml,df}(s)] + q_{sl,ml}(s) \\ \times (q_{ml,mh}(s)q_{mh,df}(s) + q_{ml,df}(s))] / l(s) \\ + q_{ch,sh}(s)q_{sh,mh}(s) [q_{mh,ml}(s)q_{ml,df}(s) \\ + q_{mh,df}(s)] + q_{ch,mh}(s) [q_{mh,ml}(s)q_{ml,df}(s) \\ + q_{mh,df}(s)] \left. \right\} \bar{q}_{df,ch}(s) / \left\{ \bar{h}_{ch,ch}(s)k(s) \right\} \quad (4.62)$$

$$p_{ch,ef}(s) = \left\{ q_{ch,mh}(s)q_{mh,ml}(s)q_{ml,ef}(s)/k(s) + q_{ch,sh}(s) \right. \\ \times q_{sh,mh}(s)q_{mh,ml}(s)q_{ml,ef}(s)/k(s) + q_{ch,cl}(s) \\ \times [q_{cl,ml}(s)q_{ml,ef}(s)/k(s) + q_{cl,sl}(s)[q_{sl,ml}(s) \\ \times q_{ml,ef}(s) + q_{sl,sh}(s)q_{sh,mh}(s)q_{mh,ml}(s) \\ \times q_{ml,ef}(s)] / k(s) + q_{cl,ef}(s) / l(s) \left. \right\} \bar{q}_{ef,ch}(s) / \bar{h}_{ch,ch}(s). \quad (4.63)$$

From Eqs. (4.56)-(4.63), the transient solutions, $P_{ch,i}(t)$, $i \in \{ch, cl, sh, sl, mh, ml, ef, df\}$, which mean the probability that the state travels in another state i at time t , can be derived numerically, by means of the Laplace inversion technique (*e.g.* see [45]). As a special case, it is easy to derive the steady-state probability $P_i = \lim_{t \rightarrow \infty} P_{ch,i}(t)$, $i \in \{ch, cl, sh, sl, mh, ml, ef, df\}$ corresponding to \mathcal{S} . Based on the LSTs, $p_{ch,i}(s)$, we can obtain $P_i = \lim_{t \rightarrow \infty} P_{ch,i}(t) = \lim_{s \rightarrow 0} p_{ch,i}(s)$ from Eqs. (4.56)-(4.63).

Table 4.5: Steady-state network reliability for node transmission radius r with/without border effects in case(1).

Ignorance			
r	Approximate	Lower Bound	Upper Bound
80	0.2328	0.0000	0.8648
85	0.5023	0.3114	0.9410
90	0.7315	0.6872	0.9757
95	0.8714	0.8622	0.9903
100	0.9415	0.9397	0.9962
105	0.9725	0.9721	0.9984
110	0.9850	0.9848	0.9992
115	0.9894	0.9893	0.9995
120	0.9906	0.9905	0.9996
125	0.9905	0.9905	0.9996
130	0.9900	0.9899	0.9996
Square			
r	Approximate	Lower Bound	Upper Bound
80	0.1087	0.0000	0.8016
85	0.3209	0.0000	0.9045
90	0.5692	0.4362	0.9566
95	0.7622	0.7283	0.9810
100	0.8796	0.8716	0.9919
105	0.9412	0.9393	0.9965
110	0.9704	0.9699	0.9984
115	0.9833	0.9831	0.9992
120	0.9885	0.9884	0.9995
125	0.9903	0.9902	0.9996
130	0.9906	0.9906	0.9996
Circular			
r	Approximate	Lower Bound	Upper Bound
80	0.1261	0.0000	0.8135
85	0.3509	0.0000	0.9117
90	0.5991	0.4875	0.9605
95	0.7840	0.7565	0.9829
100	0.8928	0.8865	0.9928
105	0.9482	0.9467	0.9969
110	0.9739	0.9735	0.9986
115	0.9848	0.9847	0.9993
120	0.9891	0.9890	0.9995
125	0.9905	0.9904	0.9996
130	0.9906	0.9905	0.9996

Table 4.6: Steady-state network reliability for varying number of node N with/without border effects in case(1).

Ignorance			
N	Approximate	Lower Bound	Upper Bound
500	0.9415	0.9397	0.9962
550	0.9693	0.9688	0.9982
600	0.9812	0.9810	0.9990
650	0.9856	0.9854	0.9993
700	0.9865	0.9864	0.9994
750	0.9860	0.9859	0.9994
800	0.9846	0.9845	0.9994
850	0.9829	0.9828	0.9994
900	0.9810	0.9808	0.9993
950	0.9789	0.9787	0.9993
1000	0.9766	0.9764	0.9992
Square			
N	Approximate	Lower Bound	Upper Bound
500	0.8796	0.8716	0.9919
550	0.9367	0.9346	0.9962
600	0.9649	0.9642	0.9981
650	0.9779	0.9777	0.9989
700	0.9834	0.9833	0.9992
750	0.9851	0.9850	0.9994
800	0.9850	0.9849	0.9994
850	0.9840	0.9838	0.9994
900	0.9824	0.9823	0.9994
950	0.9806	0.9805	0.9993
1000	0.9787	0.9784	0.9993
Circular			
N	Approximate	Lower Bound	Upper Bound
500	0.8928	0.8865	0.9928
550	0.9439	0.9423	0.9967
600	0.9687	0.9682	0.9983
650	0.9798	0.9796	0.9990
700	0.9843	0.9841	0.9993
750	0.9854	0.9853	0.9994
800	0.9850	0.9849	0.9994
850	0.9839	0.9837	0.9994
900	0.9822	0.9821	0.9994
950	0.9804	0.9802	0.9993
1000	0.9783	0.9781	0.9993

Table 4.7: Transient network survivability with three stochastic models.

t	k	Poisson			Binomial			Negative Binomial		
		Lower	Appro	Upper	Lower	Appro	Upper	Lower	Appro	Upper
0	1	0.9999	0.9999	1.0000	0.9999	0.9999	1.0000	0.9999	0.9999	1.0000
	2	0.9987	0.9987	0.9999	0.9990	0.9990	0.9999	0.9984	0.9984	0.9999
	3	0.9894	0.9895	0.9993	0.9911	0.9911	0.9994	0.9872	0.9873	0.9992
4000	1	0.9888	0.9888	0.9993	0.9893	0.9894	0.9993	0.9880	0.9881	0.9992
	2	0.9307	0.9330	0.9956	0.9362	0.9382	0.9959	0.9231	0.9260	0.9951
	3	0.5965	0.6679	0.9746	0.6248	0.6871	0.9764	0.5577	0.6424	0.9722
8000	1	0.9808	0.9810	0.9988	0.9820	0.9821	0.9989	0.9792	0.9795	0.9987
	2	0.8425	0.8542	0.9900	0.8533	0.8635	0.9907	0.8276	0.8416	0.9891
	3	0.1129	0.4115	0.9450	0.1627	0.4326	0.9480	0.0434	0.3838	0.9408
12000	1	0.9708	0.9712	0.9981	0.9726	0.9730	0.9983	0.9683	0.9688	0.9980
	2	0.7392	0.7704	0.9835	0.7550	0.7827	0.9845	0.7171	0.7536	0.9821
	3	0.0000	0.2422	0.9136	0.0000	0.2593	0.9176	0.0000	0.2198	0.9080
16000	1	0.9614	0.9621	0.9975	0.9637	0.9644	0.9977	0.9581	0.9590	0.9973
	2	0.6466	0.7022	0.9777	0.6664	0.7163	0.9790	0.6188	0.6829	0.9760
	3	0.0000	0.1536	0.8875	0.0000	0.1667	0.8921	0.0000	0.1365	0.8808
20000	1	0.9540	0.9550	0.9971	0.9567	0.9577	0.9972	0.9502	0.9514	0.9968
	2	0.5759	0.6542	0.9733	0.5986	0.6692	0.9747	0.5441	0.6337	0.9714
	3	0.0000	0.1095	0.8685	0.0000	0.1200	0.8736	0.0000	0.0960	0.8613

Chapter 5

A Simulation Approach to Quantify Network Survivability for MANETs

The network survivability is an emerging requirement for highly reliable communication services in MANETs and is defined as the probability that the network can keep to be connected even under node failures and DoS attacks. Although some analytical formulas on the quantitative network survivability have been proposed, they have not been validated yet by comparing with the exact value of network survivability in a comprehensive way. In this chapter, we revisit the existing lower and upper bounds of network survivability by taking account of border effects in a network communication area and develop a simulation model. It is shown through simulation experiments that the analytical solutions often fail in the exact network survivability measurement.

5.1 Simulation Algorithms

For our SMP modulated network survivability model in Chapter 2, it is needed to quantify the network survivability throughout Monte Carlo simulation, because the analytical solutions (upper and lower bounds) may not be validated without knowing the exact solution. Unfortunately, the simulation approach mentioned in Xing and Wang [12] is oversimplified and does not seem to catch up impacts of both node misbehavior and node failure accurately. Once the shape of communication area, such as a square area, is given, a fixed number of

```

Set Node and Nodei to empty;
Set N to the total number of node in the MANET;
Set L to the side length of square area;
For (i = 0; i ≤ N; i++) {
Set x and y to 0;
Randomly generate (x, y) (x, y ∈ [0, L])
for Nodei (i ∈ [0, N]);
Add Nodei to Node;}
/*Nodei is the i-th element of Node*/

```

Figure 5.1: A node location algorithm for square areas.

nodes are uniformly distributed to the area. A commonly used technique for a square communication area is to locate points randomly with abscissa x and ordinate y for each node (x, y) in a Cartesian coordinate system. We generate the random numbers for x and y , which are sampled from the continuous uniform distribution with lower and upper endpoints at 0 and 1, respectively, where the side length of communication area is given by L . In our simulation, we never take account of effects of the speed and destination of moving nodes, to simplify the simulation procedure, although this is because we employ the SMP modulated network survivability model. Figure 5.1 presents a pseudo code to give the node location for a square area. Here, we suppose that a circle area can be approximated by the sum of infinitesimal triangles, BCD, where the point C is at the origin, and the points B and D are located on the circumference. Since the sum of two triangles BCD is equivalent to the area of a parallelogram BCDE, then we can apply the similar algorithm to Fig. 5.1. Figure 5.2 is a pseudo code to give the node location for circular areas. For a circular communication area with radius R , we randomly choose two points on BC and CD. Let a and b be the distances between origin and these chosen points on BC and CD. Then let z equal to $2R - (a + b)$ if $a + b > R$, otherwise $a + b$. We can select one of triangles BCD by picking an angle $\alpha \in [0, 2\pi)$, so the random points in a circular area with abscissa x and ordinate y can be calculated as $(x, y) = (z \cos \alpha, z \sin \alpha)$.

In this way, when each node is located over a 2-dimensional area, the next step is to modulate each node state by an SMP. If we focus on the steady-state behavior of MANETs, then the steady-state probability P_i , $i \in \{c, s, b, j, f\}$ can be used. In our simulation experiments, we generate the node state with probability P_i uniformly, where the unit length, $\sum_{i=1}^5 P_i = 1$, is divided by 5

```

Set Node and Nodei to empty;
Set N to the total number of node in the MANET;
Set R to the radius of circular area;
For (i = 0; i ≤ N; i++) {
Set α, a, b, z, x and y to 0;
Randomly generate α (α ∈ [0, 2π));
Randomly generate a and b (a, b ∈ [0, R]);
if a + b > R then z = 2R - (a + b),
otherwise z = a + b;
calculate (x, y) by:
x = z cos α;
y = z sin α;
for Nodei (i ∈ [0, N]);
Add Nodei to Node; }
/*Nodei is the i-th element of Node*/

```

Figure 5.2: A node location algorithm for circular areas.

portions proportional to P_i . Let N_i , $i \in \{c, s, j, s, f\}$ be the number of nodes in state i in the network. If $N_B \neq 0$, then the minimum cooperative degree of network \mathcal{M} , is given by $\theta(\mathcal{M}) = 0$, otherwise, divide the active nodes into two state groups; Cooperative nodes and Selfish/Jellyfish nodes, and calculate the $\theta(\mathcal{M})$ of an arbitrary node in a MANET \mathcal{M} . For a given transmission radius r and the number of node N , we generate the node location 100 times and make 100 state transitions for each node. Finally, we execute 10,000 simulation runs to represent the node location and state for a fixed size of networks, say, N . Then the connectivity-based network survivability in our simulation experiments is calculated by

$$SVB_k(\mathcal{M}) = \frac{\sum_{i=1}^{10,000} I_{\{A_i\}}}{10,000}, \quad (5.1)$$

where A_i indicates the event $\theta(\mathcal{M}) \geq k$ at i -th simulation and $I_{\{A\}}$ is the indicator function to output 1 or 0 for occurrence of the event A .

Figures 5.3 and 5.4 illustrate simulated examples of network topology in square and circular areas, respectively, where small points denote Cooperative nodes and can be used to transmission, and larger points denote Jellyfish and Selfish nodes which initiate the transmission. Counting the number of cooperative neighbors for all active nodes, we can find the minimum cooperative degree $\theta(\mathcal{M})$. An algorithm to change the state of each node and to find the minimum cooperative degree is given in Fig. 5.5. Let $Node$ and $Node_i$ be the sequence of node in a MANET and i -th element of $Node$. Also let $NodeC$, $NodeSJ$

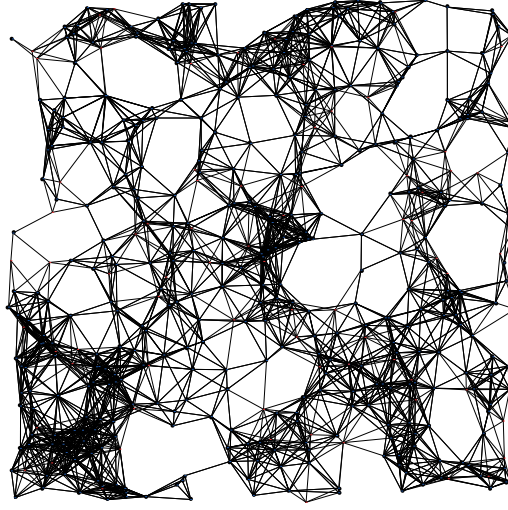


Figure 5.3: Network topology used in simulation (square area).

and $NodeB$ denote the subsets of sequence $Node$ with Cooperative node, Selfish/Jellfish node and Blackhole node, respectively. For each $Node_i$, we choose a value v randomly from 0 to 1, and identify the state $j (\in C, S, J, B, F)$. If the subset $NodeB$ is not empty, then the minimum cooperative degree $\theta(\mathcal{M})$ equals to 0, otherwise, we need to count the number of cooperative neighbors of each node in subsets $NodeC$ and $NodeSJ$. For a given transmission radius r , we calculate the distance of each element between $NodeSJ$ and $NodeC$. Besides, we also calculate the distance of each element in $NodeC$. If the distance of a node pair is not greater than r , then they are considered as neighbors. After counting the number of cooperative neighbors for all node in $NodeC$ and $NodeSJ$, we can find the minimum cooperative degree $\theta(\mathcal{M})$.

To our best knowledge, the simulator developed here is a unique tool to quantify the connectivity-based network survivability with higher accuracy. However, as well known, the computation cost to seek the survivability measure is troublesome and very expensive. In other words, it is quite hard to simulate the node behavior and calculate the network survivability in on-line procedure. Hence, the analytical solution is still valuable to measure the connectivity-based network survivability in real MANETs.

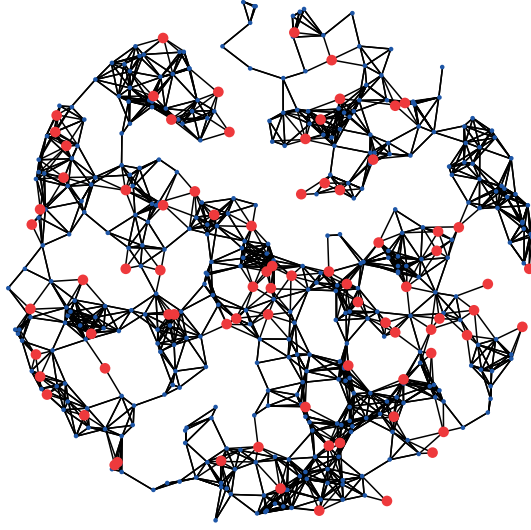


Figure 5.4: Network topology used in simulation (circular area).

5.2 Numerical Examples

In the numerical experiments, we set up the following model parameters [12]:

$$\begin{aligned}
 \lambda_{c,s} &= 1/240.0 \text{ [1/sec]}, & \lambda_{c,j} &= 3/2.0e+7 \text{ [1/sec]}, \\
 \lambda_{c,b} &= 1/6.0e+7 \text{ [1/sec]}, & \lambda_{c,f} &= 1/500.0 \text{ [1/sec]}, \\
 \lambda_{s,c} &= 1/60.0 \text{ [1/sec]}, & \lambda_{s,j} &= 3/2.0e+7 \text{ [1/sec]}, \\
 \lambda_{s,b} &= 1/6.0e+7 \text{ [1/sec]}, & \lambda_{s,f} &= 1/500.0 \text{ [1/sec]}, \\
 \lambda_{j,f} &= 1/50.0 \text{ [1/sec]}, & \lambda_{b,f} &= 1/50.0 \text{ [1/sec]}, \\
 \lambda_{j,s} &= 1/60.0 \text{ [1/sec]}, & &
 \end{aligned}$$

where λ_{ij} are transition rates from state i to state j in the exponential distributions. Under the above model parameters, the node probabilities in the steady state are given by

$$\begin{aligned}
 P_c &= 0.7299, & P_s &= 0.1629, & P_j &= 6.696e-6, \\
 P_b &= 7.44e-7, & P_f &= 0.1072.
 \end{aligned}$$

We also assume the network parameters as follows:

- $A = 1000 \text{ (m)} \times 1000 \text{ (m)}$: the area of MANET.

```

Set  $P_C, P_S, P_J, P_B, P_F$  to the steady state
probability of each state;
Set  $NodeC, NodeSJ, NodeB, \theta(\mathcal{M}_a)$  to empty;
For ( $i = 0; i \leq N; i++$ ){
Set  $v$  to 0;
Randomly generate  $j$  ( $j \in [0, 1]$ );
if  $0 \leq v < P_C$  then add  $Node_i$  to  $NodeC$ ;
if  $P_C \leq v < P_C + P_S + P_J$ 
then add  $Node_i$  to  $NodeSJ$ ;
if  $P_C + P_S + P_J \leq v < P_C + P_S + P_J + P_B$ 
then add  $Node_i$  to  $NodeB$ ;}
/* $NodeC, NodeSJ, NodeB$  are the set of nodes
in the states  $C, S$  and  $J, B$ , respectively*/
if  $NodeB$  is not empty then add 0 to  $\theta(\mathcal{M}_a)$ ,
else Set  $NoC, NoSJ$  to the number of elements
of  $NodeC$  and  $NodeSJ$ , respectively;
Set  $r$  to the transmission radius;
Set  $degree$  to empty;
For ( $i = 0; i \leq NoSJ; i++$ ){
Set  $count = 0$ ; /*count the number of
cooperative neighbor*/
For ( $j = 0; j \leq NoC; j++$ ){
if distance between  $NodeSJ_i$  and
 $NodeC_j$  is no greater than  $r$ ,
 $count++$ ;}
Add  $count$  to  $degree$ ;}
For ( $i = 0; i \leq NoC; i++$ ){
Set  $count = 0$ ;
For ( $j = 0; j \leq NoC; j++$ ){
if  $i \neq j$  and distance between  $NodeC_i$  and
 $NodeC_j$  is no greater than  $r$ ,
 $count++$ ;}
Add  $count$  to  $degree$ ;}
Add  $\min\{degree\}$  to  $\theta(\mathcal{M}_a)$ ; /* $\min\{degree\}$ 
is the smallest element of  $degree$ */
}

```

Figure 5.5: An algorithm to find the minimum cooperative degree.

- $N = 500$: the number of mobile nodes.

We have already shown in Table 2.3 that our analytical models with border effects provide relatively nice performance comparing with the simulation solutions in terms of the number of neighbors. Here, we compare the network survivability in analytical models with the simulation results. As analytical solutions, we calculate the expected network survivability and its associated bounds in two cases with/without border effects. Suppose that the number of nodes N equals to 500 for varying transition radius r from 80 to 130 by 5.

Since the network survivability depends on the connectivity level k , we set $k = 1, 2, 3$ in the simulation experiments. In Tables 5.1 and 5.2 the steady-state network survivability for varying node transmission radius r in square and cir-

cular areas are calculated. It can be seen that the simulation result is two-sided bounded in a few cases with $(k, r) = (1, 125), (1, 130), (2, 80), (2, 85), (2, 90), (3, 80), (3, 85), (3, 90), (3, 95), (3, 100)$.

Looking at the expected network survivability, it takes rather different values from the simulation results. In Tables 5.3 and 5.4, we compare our analytical solutions with the simulated ones for varying N . In the combination of $(k, N) = (1, 800), (1, 900), (1, 1000), (2, 1000), (3, 500)$, it is shown that the simulation result is two-sided bounded, but the expected network survivability does not always take the closed values to simulation results. When ‘Ignorance’ is compared with ‘Square’ or ‘Circular’, the latter can take the closer value than the former, but fails to get the satisfactory approximate performance. In other words, our analytical models taking account of border effects still fail to evaluate the accurate network survivability except in very few cases. This negative observation implies that there is no satisfactory analytical model to assess the connectivity-based network survivability and that it is a challenging issue to develop a more sophisticated stochastic model to evaluate it. The lesson learned from the comparative study in this chapter will motivate to investigate the other stochastic modeling approach for the purpose.

Table 5.1: Steady-state network survivability for varying node transmission radius r in square area.

$k = 1$		Ignorance		Square	
r	Simulation	Expected	Bounds	Expected	Bounds
80	0.3522	0.5268	[0.3595, 0.9311]	0.3557	[0.0000, 0.8920]
85	0.5365	0.7459	[0.7227, 0.9730]	0.6054	[0.5149, 0.9532]
90	0.7071	0.8908	[0.8844, 0.9899]	0.7891	[0.7780, 0.9806]
95	0.7964	0.9547	[0.9524, 0.9962]	0.8952	[0.9009, 0.9922]
100	0.8867	0.9796	[0.9793, 0.9985]	0.9481	[0.9558, 0.9969]
105	0.9451	0.9928	[0.9893, 0.9993]	0.9721	[0.9792, 0.9987]
110	0.9532	0.9925	[0.9925, 0.9996]	0.9821	[0.9886, 0.9993]
115	0.9632	0.9973	[0.9933, 0.9996]	0.9859	[0.9921, 0.9996]
120	0.9854	0.9931	[0.9931, 0.9997]	0.9872	[0.9932, 0.9997]
125	0.9943	0.9931	[0.9927, 0.9997]	0.9873	[0.9932, 0.9997]
130	0.9963	0.9921	[0.9921, 0.9997]	0.9871	[0.9929, 0.9997]
$k = 2$		Ignorance		Square	
r	Simulation	Expected	Bounds	Expected	Bounds
80	0.0019	0.0079	[0.0000, 0.5830]	0.0014	[0.0000, 0.4436]
85	0.0279	0.1073	[0.0000, 0.7962]	0.0283	[0.0000, 0.6877]
90	0.1335	0.3519	[0.0000, 0.9122]	0.1577	[0.0000, 0.8466]
95	0.2744	0.6249	[0.5515, 0.9652]	0.3997	[0.0959, 0.9310]
100	0.4286	0.8316	[0.8156, 0.9869]	0.6453	[0.5835, 0.9707]
105	0.6579	0.9271	[0.9260, 0.9952]	0.8158	[0.8143, 0.9881]
110	0.7492	0.9699	[0.9694, 0.9982]	0.9098	[0.9185, 0.9952]
115	0.8078	0.9882	[0.9853, 0.9992]	0.9549	[0.9635, 0.9980]
120	0.8767	0.9906	[0.9905, 0.9995]	0.9745	[0.9820, 0.9991]
125	0.9378	0.9958	[0.9919, 0.9996]	0.9824	[0.9890, 0.9995]
130	0.9606	0.9919	[0.9919, 0.9997]	0.9852	[0.9914, 0.9996]
$k = 3$		Ignorance		Square	
r	Simulation	Expected	Bounds	Expected	Bounds
80	0.0000	0.0000	[0.0000, 0.1219]	0.0000	[0.0000, 0.0498]
85	0.0000	0.0002	[0.0000, 0.3762]	0.0000	[0.0000, 0.2213]
90	0.0012	0.0073	[0.0000, 0.6487]	0.0008	[0.0000, 0.4811]
95	0.0121	0.1108	[0.0000, 0.8334]	0.0195	[0.0000, 0.7104]
100	0.0538	0.3593	[0.0000, 0.9296]	0.1265	[0.0000, 0.8574]
105	0.2062	0.6336	[0.5693, 0.9725]	0.3545	[0.0000, 0.9355]
110	0.3367	0.8406	[0.8264, 0.9898]	0.6074	[0.5270, 0.9725]
115	0.4664	0.9408	[0.9313, 0.9963]	0.7927	[0.7898, 0.9887]
120	0.5940	0.9717	[0.9713, 0.9986]	0.8981	[0.9082, 0.9955]
125	0.7363	0.9882	[0.9854, 0.9993]	0.9492	[0.9590, 0.9981]
130	0.8174	0.9899	[0.9898, 0.9996]	0.9717	[0.9797, 0.9991]

Table 5.2: Steady-state network survivability for varying node transmission radius r in circular area.

$k = 1$		Ignorance		Circular	
r	Simulation	Expected	Bounds	Expected	Bounds
80	0.3852	0.5268	[0.3595, 0.9311]	0.3831	[0.0516, 0.8996]
85	0.6175	0.7459	[0.7227, 0.9730]	0.6315	[0.5572, 0.9572]
90	0.7735	0.8908	[0.8844, 0.9899]	0.8072	[0.8004, 0.9826]
95	0.8437	0.9547	[0.9524, 0.9962]	0.9057	[0.9121, 0.9931]
100	0.9301	0.9796	[0.9793, 0.9985]	0.9535	[0.9611, 0.9972]
105	0.9542	0.9928	[0.9893, 0.9993]	0.9746	[0.9816, 0.9988]
110	0.9793	0.9925	[0.9925, 0.9996]	0.9832	[0.9896, 0.9994]
115	0.9920	0.9973	[0.9933, 0.9996]	0.9863	[0.9925, 0.9996]
120	0.9937	0.9931	[0.9931, 0.9997]	0.9873	[0.9932, 0.9997]
125	0.9970	0.9931	[0.9927, 0.9997]	0.9873	[0.9932, 0.9997]
130	0.9989	0.9921	[0.9921, 0.9997]	0.9870	[0.9928, 0.9997]
$k = 2$		Ignorance		Circular	
r	Simulation	Expected	Bounds	Expected	Bounds
80	0.0052	0.0079	[0.0000, 0.5830]	0.0020	[0.0000, 0.4676]
85	0.0422	0.1073	[0.0000, 0.7962]	0.0367	[0.0000, 0.7079]
90	0.1755	0.3519	[0.0000, 0.9122]	0.1850	[0.0000, 0.8596]
95	0.3392	0.6249	[0.5515, 0.9652]	0.4385	[0.1916, 0.9381]
100	0.5507	0.8316	[0.8156, 0.9869]	0.6789	[0.6341, 0.9742]
105	0.6825	0.9271	[0.9260, 0.9952]	0.8375	[0.8396, 0.9897]
110	0.8191	0.9699	[0.9694, 0.9982]	0.9216	[0.9306, 0.9959]
115	0.9169	0.9882	[0.9853, 0.9992]	0.9606	[0.9690, 0.9983]
120	0.9497	0.9906	[0.9905, 0.9995]	0.9771	[0.9842, 0.9992]
125	0.9706	0.9858	[0.9919, 0.9996]	0.9834	[0.9899, 0.9995]
130	0.9824	0.9919	[0.9919, 0.9997]	0.9856	[0.9917, 0.9996]
$k = 3$		Ignorance		Circular	
r	Simulation	Expected	Bounds	Expected	Bounds
80	0.0000	0.0000	[0.0000, 0.1219]	0.0000	[0.0000, 0.0590]
85	0.0000	0.0002	[0.0000, 0.3762]	0.0000	[0.0000, 0.2451]
90	0.0019	0.0073	[0.0000, 0.6487]	0.0013	[0.0000, 0.5104]
95	0.0223	0.1108	[0.0000, 0.8334]	0.0276	[0.0000, 0.7339]
100	0.1035	0.3593	[0.0000, 0.9296]	0.1567	[0.0000, 0.8722]
105	0.2500	0.6336	[0.5693, 0.9725]	0.4016	[0.1016, 0.9435]
110	0.4206	0.8406	[0.8264, 0.9898]	0.6503	[0.5954, 0.9764]
115	0.6730	0.9408	[0.9313, 0.9963]	0.8212	[0.8236, 0.9905]
120	0.7696	0.9717	[0.9713, 0.9986]	0.9136	[0.9240, 0.9962]
125	0.8414	0.9882	[0.9854, 0.9993]	0.9568	[0.9660, 0.9985]
130	0.8967	0.9899	[0.9898, 0.9996]	0.9750	[0.9826, 0.9993]

Table 5.3: Steady-state network survivability for varying number of node N in square area.

$k = 1$		Ignorance		Square	
N	Simulation	Expected	Bounds	Expected	Bounds
500	0.9065	0.9787	[0.9793, 0.9985]	0.9549	[0.9611, 0.9972]
600	0.9715	0.9909	[0.9908, 0.9995]	0.9865	[0.9876, 0.9993]
700	0.9853	0.9905	[0.9905, 0.9995]	0.9904	[0.9905, 0.9995]
800	0.9960	0.9881	[0.9880, 0.9995]	0.9890	[0.9888, 0.9995]
900	0.9987	0.9850	[0.9849, 0.9994]	0.9863	[0.9860, 0.9994]
1000	0.9988	0.9815	[0.9814, 0.9993]	0.9832	[0.9828, 0.9994]
$k = 2$		Ignorance		Square	
N	Simulation	Expected	Bounds	Expected	Bounds
500	0.5231	0.8249	[0.8156, 0.9869]	0.6473	[0.6341, 0.9742]
600	0.8055	0.9611	[0.9604, 0.9976]	0.9078	[0.9166, 0.9951]
700	0.9027	0.9853	[0.9851, 0.9992]	0.9732	[0.9759, 0.9988]
800	0.9569	0.9872	[0.9871, 0.9994]	0.9855	[0.9859, 0.9994]
900	0.9872	0.9849	[0.9848, 0.9994]	0.9856	[0.9855, 0.9994]
1000	0.9960	0.9815	[0.9813, 0.9993]	0.9830	[0.9827, 0.9994]
$k = 3$		Ignorance		Square	
N	Simulation	Expected	Bounds	Expected	Bounds
500	0.0910	0.3435	[0.0000, 0.9296]	0.1052	[0.0000, 0.8722]
600	0.4031	0.7971	[0.7734, 0.9866]	0.5700	[0.5138, 0.9715]
700	0.6545	0.9482	[0.9468, 0.9973]	0.8680	[0.8796, 0.9939]
800	0.8189	0.9799	[0.9797, 0.9991]	0.9597	[0.9643, 0.9984]
900	0.9351	0.9835	[0.9834, 0.9993]	0.9799	[0.9808, 0.9992]
1000	0.9758	0.9813	[0.9811, 0.9993]	0.9818	[0.9817, 0.9993]

Table 5.4: Steady-state network survivability for varying number of node N in circular area.

$k = 1$		Ignorance		Circular	
N	Simulation	Expected	Bounds	Expected	Bounds
500	0.8599	0.9787	[0.9793, 0.9985]	0.9602	[0.9558, 0.9969]
600	0.9536	0.9909	[0.9908, 0.9995]	0.9876	[0.9865, 0.9992]
700	0.9775	0.9905	[0.9905, 0.9995]	0.9905	[0.9903, 0.9995]
800	0.9912	0.9881	[0.9880, 0.9995]	0.9889	[0.9889, 0.9995]
900	0.9974	0.9850	[0.9849, 0.9994]	0.9861	[0.9862, 0.9995]
1000	0.9988	0.9815	[0.9814, 0.9993]	0.9829	[0.9830, 0.9994]
$k = 2$		Ignorance		Circular	
N	Simulation	Expected	Bounds	Expected	Bounds
500	0.3888	0.8249	[0.8156, 0.9869]	0.6824	[0.5835, 0.9707]
600	0.7211	0.9611	[0.9604, 0.9976]	0.9200	[0.9034, 0.9943]
700	0.8404	0.9853	[0.9851, 0.9992]	0.9762	[0.9728, 0.9986]
800	0.9148	0.9872	[0.9871, 0.9994]	0.9860	[0.9854, 0.9993]
900	0.9739	0.9849	[0.9848, 0.9994]	0.9856	[0.9855, 0.9994]
1000	0.9862	0.9815	[0.9813, 0.9993]	0.9828	[0.9829, 0.9994]
$k = 3$		Ignorance		Circular	
N	Simulation	Expected	Bounds	Expected	Bounds
500	0.0464	0.3435	[0.0000, 0.9296]	0.1350	[0.0000, 0.8574]
600	0.3154	0.7971	[0.7734, 0.9866]	0.6147	[0.4386, 0.9672]
700	0.5176	0.9482	[0.9468, 0.9973]	0.8866	[0.8584, 0.9928]
800	0.6979	0.9799	[0.9797, 0.9991]	0.9649	[0.9589, 0.9982]
900	0.8770	0.9835	[0.9834, 0.9993]	0.9810	[0.9797, 0.9992]
1000	0.9263	0.9813	[0.9811, 0.9993]	0.9819	[0.9817, 0.9993]

Chapter 6

Conclusions

6.1 Summary and Remarks

In Chapter 2, we have refined the network survivability models by taking account of border effects in both square and circular areas. Based on the definition of border effects in communication areas, we have calculated the expected coverage of node in MANETs which resulted the expected node degree, and have formulated the network survivability with border effects. In numerical experiments, we have calculated the expected node degree and the connectivity-based network survivability measures in both analytical and simulation models, and shown that the border effects were significant to evaluate the number of neighbors accurately. We have also compared the steady-state network survivability and the transient network survivability in three stochastic models, and shown numerically that the network survivability was reduced fiercely as k increased when N was small and that the connectivity-based network survivability without border effects was higher than that without border effects.

In Chapter 3, We have pointed out that the CTMC model for the node behavior in past was too simple to describe the effect of energy consumption on the network survivability. Therefore, we have revisited the network survivability modeling for the power-aware MANET by using MRGP modeling. By modeling the battery life as non-exponential distributions, the MRGP model can describe the detailed behavior of a node, compared to the simple CTMC model in [19]. Also, by applying PH expansion technique, we have performed the transient analysis of network survivability. However, the model presented in Chapter 3

was not compared with simulation results to validate it. This will be done as a future work.

In Chapter 4, we have revisited the network survivability models in MANETs by taking account of the battery re-charge and border effects in both square and circular communication areas. Getting idea from the network connectivity, we have presented the approximate network survivability formulae by calculating the probability that all expected number of active nodes in the MANET is k . In numerical experiments, we have considered two cases where the transition time from lower battery states to fully charged battery states were given by the gamma and exponential distributions. We have also compared the steady-state network survivability with/without battery re-charge. It has been shown numerically that the network survivability with battery re-charge was higher than that with no battery charge, when r was small, and that the approximate network reliability always took a middle value between the lower and upper bounds.

In Chapter 5, we have developed a simulation model to quantify the network survivability. In numerical experiments, we have shown that in the comparison of connectivity-based network survivability, both the analytical bounds and the expected network survivability did poorly worked except in a few cases, although it has been shown that the border effects were still significant to evaluate the number of neighbors accurately when the transmission radius r changed.

6.2 Future Works

In this study, the network survivability has been defined by the minimum cooperative degree, but it is worth mentioning that it can be considered as an approximate measure. In future, we will develop a comprehensive network survivability model and investigate whether the approximate method for network survivability itself can work well in several random network environments. Also, the simulation model to calculate the exact network survivability dependent of all the possible number of communication paths should be developed.

Bibliography

- [1] R. Ellison, D. Fisher, R. Linger, H. Lipson, T. Longstaff and N. Mead, “Survival network systems: an emerging discipline,” *Technical Report of SEI/CMU*, CMU/SEI-97-TR-013 (1997).
- [2] J. C. Knight and K. J. Sullivan, “On the definition of survivability,” *Technical Report of Dept. of Computer Science/University of Virginia*, CS-TR-33-00 (2000).
- [3] S. C. Liew and K. W. Lu, “A framework for characterizing disaster-based network survivability,” *IEEE Transactions on Selected Areas in Communications*, vol. 12, no. 1, pp. 52–58 (1994).
- [4] A. Zolfaghari and F. J. Kaudel, “Framework for network survivability performance,” *IEEE Transactions on Selected Areas in Communications*, vol. 12, no. 1, pp. 46–51 (1994).
- [5] D. Chen, S. Garg and K. S. Trivedi, “Network survivability performance evaluation: a quantitative approach with applications in wireless ad-hoc networks,” *Proceeding of ACM International Conference on Modeling, Analysis and Simulation of Wireless and Mobile Systems (MSWiM-2002)*, pp. 61–68, ACM (2002).
- [6] L. Cloth and B. R. Haverkort, “Model checking for survivability,” *Proceeding of the 2nd IEEE Conference on Quantitative Evaluation of Systems (QEST-2005)*, pp. 145–154, IEEE CPS (2005).
- [7] P. E. Heegaard and K. S. Trivedi, “Network survivability modeling,” *Computer Networks*, vol. 53, pp. 1215–1234 (2009).

- [8] Y. Liu, V. B. Mendiratta and K. S. Trivedi, "Survivability analysis of telephone access network," *Proceeding of the 15th IEEE International Symposium on Software Reliability Engineering (ISSRE-2004)*, pp. 367–378, IEEE CPS (2004).
- [9] Y. Liu and K. S. Trivedi, "Survivability quantification: the analytical modeling approach," *International Journal of Performability Engineering*, vol. 2, no. 1, pp.29-44 (2006).
- [10] J. Zheng, H. Okamura and T. Dohi, "Survivability analysis of VM-based intrusion tolerant systems," *IEICE Transactions on Information & Systems (D)*, in press (2015).
- [11] F. Xing and W. Wang, "Modeling and analysis of connectivity in mobile ad hoc networks with misbehaving nodes," *Proceeding of IEEE Conference on Communications (ICC-2006)*, pp. 1879–1884, IEEE CPS (2006).
- [12] F. Xing and W. Wang, "On the survivability of wireless ad hoc networks with node misbehaviors and failures," *IEEE Transactions on Dependable and Secure Computing*, vol. 7, no. 3, pp. 284–299 (2010).
- [13] C. Bettstetter, "On the minimum node degree and connectivity of a wireless multihop network," *Proceeding of ACM International Symposium on Mobile Ad Hoc Networking and Computing (MobiHoc-2002)*, pp. 80–91, ACM (2002).
- [14] C. Bettstetter, J. Klinglmayr and S. Lettner, "On the degree distribution of k-connected random networks," *Proceeding of IEEE Conference on Communications (ICC-2010)*, pp. 1–6, IEEE CPS (2010).
- [15] Z. Yi, T. Dohi, "Survivability analysis for a wireless ad hoc network based on semi-Markov model," *IEICE Transactions on Information & Systems*, vol. E95-D, no. 12, pp. 2844–2851 (2012).
- [16] H. Okamura, Z. Yi, T. Dohi: Network survivability modeling and analysis for a power-aware MANETs by Markov regenerative processes, *Telecommunication Systems Journal*, vol. 60, pp. 471–484 (2015).

- [17] L. Laranjeira and G. N. Rodrigues, “Border effect analysis for reliability assurance and continuous connectivity of wireless sensor networks in the presence of sensor failures,” *IEEE Transactions on Wireless Communications*, vol. 13, no. 8, pp. 4232–4246 (2014).
- [18] C. Bettstetter, “On the connectivity of ad hoc networks,” *The Computer Journal*, vol. 47, no. 4, pp. 432–447 (2004).
- [19] Z. Yi, T. Dohi and H. Okamura, “Survivability modeling and analysis for a power-aware wireless ad hoc network,” *Proceedings of 4th International Workshop on Reliable Networks Design and Modeling (RNDM 2012)*, pp. 832–838 (2012).
- [20] L. Cloth, B. R. Haverkort and M. R. Jongerden, “Computing battery lifetime distribution,” *Proceedings of the 37th Annual IEEE/IFIP International Conference on Dependable Systems and Networks*, pp. 780–789 (2007).
- [21] G. D. Caro, F. Ducatelle and L. M. Gambardella, “AntHocNet: An adaptive nature-inspired algorithm for routing in mobile ad hoc networks,” *European Transactions on Telecommunications*, vol. 16, no. 5, pp. 443–455 (2005).
- [22] L. Guo, “A new and improved algorithm for dynamic survivable routing in optical WDM networks,” *Computer Communications*, vol. 30, no. 6, pp. 1419–1423 (2007).
- [23] Z. Yi, T. Dohi and H. Okamura, “Survivability quantification of wireless ad hoc network taking account of border effects,” *Proceedings of The 21st IEEE Pacific Rim International Symposium on Dependable Computing (PRDC 2015)*, pp. 149–158 (2015).
- [24] Z. Yi and T. Dohi, “Quantitative comparison of survivability models for wireless ad hoc networks,” *Proceedings of 2nd International Conference on Networking and Computing (ICNC-2011)*, pp. 284–287 (2011).
- [25] V. Gupta, S. Krishnamurthy and M. Faloutsos, “Denial of service attacks at the MAC layer in wireless ad hoc networks,” *Proceedings of IEEE Conference on Military Communications*, pp. 1118–1123 (2002).

- [26] I Aad, J. P. Hubaux and E. W. Knightly, “Denial of service resilience in ad hoc networks,” *Proceedings of the 10th Annual International Conference on Mobile Computing and Networking*, pp. 202–215 (2004).
- [27] H. Choi, V. G. Kulkarni and K. S. Trivedi, “Markov regenerative stochastic Petri nets,” *Performance Evaluation*, vol.20, pp. 337–357 (1994).
- [28] M. Telek, A. Bobbio, L. Jereb, A. Puliafito and K. S. Trivedi, “Steady state analysis of Markov regenerative SPN with age memory policy,” *Quantitative Evaluation of Computing and Communication Systems (LNCS 977)*, pp. 165–179 (1995).
- [29] G. Bolch, S. Greiner, H. de Meer and K. S. Trivedi, “Queueing Networks and Markov Chains: Modeling and Performance Evaluation with Computer Science Applications, 2nd edition” *John Wiley & Sons*, New York (2006).
- [30] M. Telek and A. Horváth, “Transient analysis of Age-MRSPNs by the method of supplementary variables,” *Performance Evaluation*, vol.45, pp. 205–221 (2001).
- [31] E. Çinlar, “Markov renewal theory,” *Advances in Applied Probability*, vol.1, pp. 123–187 (1969).
- [32] R. Fricks, M. Telek, A. Puliafito and K. S. Trivedi, “Markov renewal theory applied to performability evaluation,” *State-of-the Art in Performance Modeling and Simulation. Modeling and Simulation of Advanced Computer Systems: Applications and Systems*, pp. 193–236 (1998).
- [33] A. Thümmler, P. Buchholz and M. Telek, “A novel approach for phase-type fitting with the EM algorithm,” *IEEE Transactions on Dependable and Secure Computing*, vol.3, no.3, pp. 245–258 (2006).
- [34] A. Cumani, “On the canonical representation of homogeneous Markov Processes modelling failure-time distributions,” *Microelectronics Reliability*, vol.22, pp. 583–602 (1982).
- [35] A. Bobbio and A. Cumani, “ML estimation of the parameters of a PH distribution in triangular canonical form,” *Computer Performance Evaluation*, pp. 33–46 (1992).

- [36] S. Asmussen, O. Nerman and M. Olsson, “Fitting phase-type distributions via the EM algorithm,” *Scandinavian Journal of Statistics*, vol.23, no.4, pp. 419–441 (1996).
- [37] H. Okamura, T. Dohi and K. S. Trivedi, “A refined EM algorithm for PH distributions,” *Performance Evaluation*, vol.68, no.10, pp. 938–954 (2011).
- [38] H. Okamura, H. Kishikawa and T. Dohi, “Application of deterministic annealing EM algorithm to MAP/PH parameter estimation,” *Telecommunication Systems*, vol.54, pp. 79–90 (2013).
- [39] L. E. Baum, T. Petrie, G. Soules and N. Weiss, “A maximization technique occurring in the statistical analysis of probabilistic function of Markov chains,” *The Annals of Mathematical Statistics*, vol.41, no.1, pp. 164–171 (1970).
- [40] L. Deng and J. Mark, “Parameter estimation for Markov modulated Poisson processes via the EM algorithm with time discretization,” *Telecommunication Systems*, vol.1, pp. 321–338 (1993).
- [41] T. Yoshihara, S. Kasahara and Y. Takahashi, “Practical time-scale fitting of self-similar traffic with Markov modulated Poisson process,” *Telecommunication Systems*, vol.17, no.1-2, pp. 185–211 (1993).
- [42] A. Reibman and K. S. Trivedi, “Numerical transient analysis of Markov models,” *Computers & Operations Research*, vol.15, pp. 19–36 (1988).
- [43] A. Reibman and K. S. Trivedi, “Transient analysis of cumulative measures of Markov model behavior,” *Stochastic Models*, vol.5, no.4, pp. 683–710 (1989).
- [44] H. Takahasi and M. Mori, “Double exponential formulas for numerical integration,” *Publications of RIMS, Kyoto University*, vol.9, pp. 721–741 (1974).
- [45] P. Valko and J. Abate, “Numerical inversion of Laplace transform with multiple precision using the complex domain,” <http://library.wolfram.com/MathSource/5026/>.

Publication List of the Author

- [1] Z. Yi and T. Dohi, Survivability analysis for a wireless ad hoc network based on semi-Markov model, *IEICE Transactions on Information and Systems*, vol. E95-D, no. 12, pp. 2844-2851, Dec. 2012.
- [2] H. Okamura, Z. Yi and T. Dohi, Network survivability modeling and analysis for power-aware MANETs by Markov regenerative processes, *Telecommunication Systems*, vol. 60, no. 4, pp. 471-484, Sep. 2015
- [3] Z. Yi and T. Dohi, Towards highly dependable power-aware mobile ad hoc network – survivability evaluation framework –, *IEEE Access* vol. 3, pp. 2665-2676, Dec. 2015.
- [4] Z. Yi and T. Dohi, Quantitative comparison of survivability models for wireless ad hoc networks, *Proc. of The 2nd International Workshop on Advances in Networking and Computing (WANC-2011), in conjunction with The Second International Conference on Networking and Computing (ICNC 2011)*, pp. 284-287, Osaka, Japan, Nov. 2011.
- [5] Z. Yi, T. Dohi and H. Okamura, Survivability modeling and analysis for a power-aware wireless ad hoc network, *Proc. of The 4th International Workshop on Reliable Networks Design and Modeling (RNDM 2012)* pp. 813-819, St. Petersburg, Russia, Oct. 2012.
- [6] Z. Yi and T. Dohi, A simulation approach to quantify network survivability on MANETs, *Proc. of The 5th IEEE International Workshop on Network Technologies and Security, Administration and Protection (NET-SAP 2015), in conjunction with The 39th Annual International Computer*

Software and Applications Conference (COMPSAC 2015), pp. 268–273.
Taichung, Taiwan, Jul. 2015.

- [7] Z. Yi and T. Dohi, Survivability analysis with border effects for power-aware mobile ad hoc network, *Proc. of The 12th IEEE International Conference on Advanced and Trusted Computing (ATC 2015)*, pp. 476–483, Beijing, China, Aug. 2015.
- [8] Z. Yi, T. Dohi and H. Okamura, Survivability quantification of wireless ad hoc network taking account of border effects, *Proc. of The 21st IEEE Pacific Rim International Symposium on Dependable Computing (PRDC 2015)*, pp. 149–158, Zhangjiajie, China, Nov. 2015.